Molecular characterization of glycolysis in *Pyrococcus furiosus*

Cornelis Hubertus Verhees

Promotor:	prof. dr. W.M. de Vos Hoogleraar Microbiologie Wageningen Universiteit
Co-promotor:	dr. J. van der Oost Universitair docent bij de leerstoelgroep Microbiologie Wageningen Universiteit
Leden van de promotie commissie:	prof. dr. A.J.M. Driessen Rijksuniversiteit Groningen
	prof. dr. M.A. Huynen Katholieke Universiteit Nijmegen
	prof. dr. W.J. Stiekema Wageningen Universiteit/ Plant Research International
	prof. dr. P. Schönheit Christian-Albrechts-Universität Kiel, Duitsland

Molecular characterization of glycolysis in *Pyrococcus furiosus*

Cornelis Hubertus Verhees

Proefschrift

ter verkrijging van de graad van doctor
op gezag van de rector magnificus
van Wageningen Universiteit,
prof. dr. ir. L. Speelman,
in het openbaar te verdedigen
op vrijdag 5 april 2002
des namiddags te vier uur in de Aula.

C.H. Verhees- Molecular characterization of glycolysis in *Pyrococcus furiosus* – 2002
Dutch: 'Moleculaire karakterisatie van de glycolyse in *Pyrococcus furiosus*'

PhD Thesis Wageningen University, Wageningen, The Netherlands – With summary in Dutch
ISBN: 90-5808-611-9

Stellingen

1. De toenemende hoeveelheid aan genoomsequenties is vaak niet direct bruikbaar als de annotatie niet betrouwbaar en deskundig is uitgevoerd.
   (**Himmelreich R, Hilbert H, Plagens H, Pirkl E, Li BC, Herrmann R.** 1996. *Nucleic Acids Res.* **15**:4420-4449; **Dandekar T, Huynen M, Regula JT, Ueberle B, Zimmermann CU, Andrade MA, Doerks T, Sanchez-Pulido L, Snel B, Suyama M, Yuan YP, Herrmann R, Bork P.** 2000. *Nucleic Acids Res.* **28**:3278-3288)

2. Unieke eiwitsequenties blijken vaak toch een minder unieke ruimtelijke structuur te bezitten.
   (**Ito, S., Fushinobu, S., Yoshioka, I., Koga, S., Matsuzawa, H., Wakagi, T.** 2001. *Structure* **9**: 205-214)

3. Door technieken als "directed evolution" worden eiwitten weer als een zwarte doos gezien.

4. Het verdient aanbeveling de samenwerking tussen bioinformatici en andere onderzoekers te bevorderen.

5. De uitkomsten van de biochemische karakterisatie van een enzym zeggen meer iets over de onderzoeker dan over het enzym.
   (dit proefschrift; **Hansen, T., Oehlmann, M, Schönheit, P.** 2001. *J. Bacteriol.* **183:** 3428-3435; **Hutchins, A.M., Holden, J.F., Adams, M.W.W.** 2001. *J. Bacteriol.* **183:** 709-715; **Sakuraba, H., Utsumi, E., Kujo, C., Ohshima, T.** 1999. *Arch. Biochem. Biophys.* **364:** 125-128)

6. De term 'modified Embden-Meyerhof pathway' is vanuit biochemisch oogpunt correct maar vanuit evolutionair oogpunt misleidend.
   (dit proefschrift)

7. De vermelding 'vers verpakt' op een product zonder bijvermelding van de verpakkingsdatum is volkomen zinloze informatie.

8. Onafhankelijke hypotheek- en verzekeringsadviseurs bestaan niet.

Stellingen behorende bij het proefschrift
'Molecular characterization of glycolysis in *Pyrococcus furiosus*'
Corné Verhees, Wageningen, 5 april 2002

pap en mam, dit is voor jullie

The research described in this thesis was financially supported in contract 805.33.353-P, by the Earth and Life Sciences Foundation (ALW), which is subsidized by the Netherlands Organization for Scientific Research (NWO).

Cover design and realization: Michielsen New Media (www.mnm.nl)
picture *Pyrococcus furiosus* (http://comb5-156.umbi.umd.edu)

Printing: Ponsen & Looijen B.V., Wageningen

Dankwoord

Dit is het dan.....

Als AIO (of OIO) kijk je al vanaf de eerste dag uit naar het schrijven van het dankwoord. Want als je eenmaal zover bent dan weet je dat al het zwoegen en zweten erop zit. Al die momenten waarop je denkt 'waar doe ik het eigenlijk voor', zijn overwonnen en als je dan je eigen boekje ziet denk je 'het was zeker de moeite waard' Zoals voor iedere promovendus geldt heb ook ik het nooit voor elkaar kunnen krijgen zonder de hulp van vele anderen.

Je stond erop, dus als eerste wil ik Ilse bedanken. Zonder jou was ik aan deze klus nooit begonnen en had de 'toekomst' er heel anders uitgezien. Je steun is van onschatbare waarde geweest waar ik me nog steeds elke dag bewust van ben. Heel blij ben ik je te hebben mogen leren kennen en hopelijk kunnen we nog lang van elkaar genieten.

Eveneens zeer belangrijk waren mijn promotor Willem M. de Vos en co-promotor John van der Oost voor het vertrouwen en de mogelijkheid die zij mij gaven om te kunnen promoveren. Willem, bedankt voor je kritische blik en je geduld. John, voor de manier waarop jij met je AIO's omgaat is gewoon fantastisch. Een hint, check nooit je labtop in als je gaat vliegen. Iedereen van de BacGen groep (John, Servé, Ronnie, Johan, Arjen, Pino, Krisztina, Hauke, Anna, Joyce, Leon, Thijs E., Thijs K. Stan, Wilfried, Ans, Ineke, Don, Valerie, Nina, Gaël en Ken) bedankt voor de leuke en gezellige tijd. De lunches waren apart en de kroegavonden subliem. Thijs K. bedankt voor de sportieve onderonsjes. Het afreageren op de tennisbaan deed soms goed. Kamergenoten van K1011, het moet voor jullie een enorme opoffering geweest zijn te blijven zitten na de vele gasexplosies. K1007, duidelijk het beste lab van Micro. Servé, dankbaar heb ik gebruik gemaakt van je *Pyrococcus* expertise. Judith, we zijn samen de *Pyrococcus* glycolyse ingedoken. Sorry als je soms het gevoel kreeg dat ik teveel in jouw vaarwater bezig was. Bedankt voor de prettige samenwerking. Ook de samenwerking met Groningen (Sonja K, Sonja A, Arnold en Wil) was inspirerend. Het werk van een reeks 'labslaven' heeft ervoor gezorgd dat het boekje dikker is geworden dan 6 pagina's. Dus, Arno, Thijs E., Bart, Denise en Jasper bedankt voor jullie inzet. Thijs E, ik zal je nooit meer om 5 uur 's morgens uit je bed bellen!! David, het was gezellig om ook iemand van 'vroeger' in het lab te hebben. Don, I will never forget the ethanol you spread into my face!! Ineke, 'de tattoo' blijft!! Bettina, thanks for the nice collaboration and discussions. The pub-crawl in Essen was great! Cor, de vele NMR plaatjes brachten niet hetgeen wat we wilden zien, maar gelukkig is het nog gedeeltelijk teruggekomen in een publicatie. Paranimfen Johan en Judith, ik ben blij dat jullie naast me staan.

Bewoners van Haarweg 19, Nieuwstraat 14, Grebbedijk 12 bedankt voor het fijne leefplezier en ontspanning. Wageningen-vrienden, bedankt voor het studentenleven. Ed, laten we de bartraditie

voort blijven zetten. Thuis-vrienden, bedankt voor de interesse en vooral de carnavalsdagen..... gaan jullie me toch nog een uur serieus zien. Pieter M. (http://www.mnm.nl), bedankt voor de voorkant. Met 3 tegen 2 verliezen is minimaal!! Familie, het was soms lastig om uit te leggen wat ik eigenlijk aan het doen was, daarom voor jullie hoofdstuk 11. Mariëlle, ik hoop dat je na 5 april gaat bevallen! Niek, Janne en Joep, een hele toekomst ligt nog voor jullie open, maak er wat van. Pieter van de W., bedankt voor de vele hulp tijdens alle verhuizingen. Alle klussers van Tuindorp 24, bedankt voor jullie inzet, waardoor ik zonder teveel stress dit boekje kon afmaken.

Pap en mam, bedankt dat ik heb mogen en kunnen studeren. Dit boekje is voor jullie.

Table of contents

Chapter 1

Aim and outline of the thesis

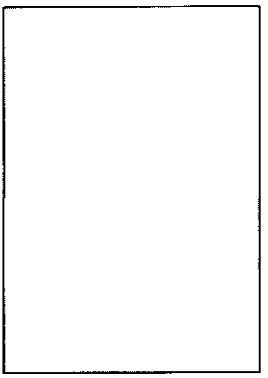

Hyperthermophilic microbes that grow optimally at or above the boiling temperature of water all belong to the archaea, the third domain of life. Archaea have been found to contain unique lipids, enzymes and metabolites that are involved in novel processes. The research presented in this thesis is focused on novel metabolic processes and aims to unravel the catabolism of glycosides in the hyperthermophilic archaeon *Pyrococcus furiosus*. This is accomplished by an integrated multidisciplinary approach involving laboratories with complementary expertise focusing on the analysis of the enzymology, kinetics, bioenergetics of key proteins involved in uptake and metabolism of glycosides. This research involves three partners, *i.e.* Molecular Microbiology, University of Groningen; Microbial Physiology, Wageningen University; Bacterial Genetics, Wageningen University. The research of the latter is presented in this thesis and focuses on the molecular and biochemical characterization of notably the non-canonical enzymes of sugar utilization pathways in *P. furiosus*. Using different approaches the genes coding for these enzymes have been identified, cloned and characterized at the sequence level in order to reveal their primary structure and signature motifs that allowed a further characterization of their molecular properties. Selected glycolytic genes have been overexpressed in heterologous systems and their biochemical and physical properties have been revealed. Structure-function analysis has been performed by means of site-directed mutagenesis and structure prediction, or crystallization of the proteins in close collaboration with the group of Prof. David Rice (Sheffield, UK). Finally, promoter elements of the selected genes have been analyzed to reveal specific motifs that might be involved in the transcription regulation.

Chapter 2 introduces various aspects of archaeal sugar metabolism. Latest results are incorporated and speculations on the evolution of archaeal sugar metabolic pathways are discussed.

The first identified unusual glycolytic enzyme is the ADP-dependent phosphofructokinase (ADP-PFK) that is described in **Chapter 3**. The biochemical and molecular properties of this novel enzyme from *P. furiosus* are investigated and compared to those of canonical counterparts. The orthologous ADP-PFK from *Methanococcus jannaschii* is studied in **Chapter 4**. Variations in the properties of the ADP-PFKs from organisms with either a chemolithoautotrophic or a heterotrophic life-style are compared, and the distribution of these enzymes is investigated by biochemical and molecular analyses.

Chapter 5 describes the biochemical properties of the canonical ATP-dependent galactokinase, and the novel ADP-dependent glucokinase from *P. furiosus*, with special emphasis on adaptations of these enzymes to the extreme conditions encountered by *P. furiosus*.

A novel phosphoglucose isomerase is purified from *P. furiosus* cell extracts and its characteristics are described in **Chapter 6**. Molecular analysis indicates that the enzyme is unrelated to canonical glycolytic isomerases, but rather related to a broad family of proteins with different functions.

In collaboration with Bettina Siebers (Essen University, Germany) the fructose-1,6-bisphosphate aldolases from the euryachaeon *P. furiosus* and the crenarchaeaon *Thermoproteus tenax* are studied (**Chapter 7**). The mechanism of the enzymes is investigated and a catalytic site residue has been identified by site-directed mutagenesis. Phylogenetic analysis is performed and evolutionary aspects of these enzymes are discussed.

The novel gluconeogenic enzyme fructose-1,6-bisphosphatase from *P. furiosus* contains sequence motifs that are present in inositol monophosphatases as well, as described in **Chapter 8**. Its biochemical properties and the effects of inhibitory compounds differ from those of the orthologous enzyme from *M. jannaschii*. As a consequence, the classification of fructose-1,6-bisphophatases is re-evaluated.

The promoter architecture of genes that encode glycolytic enzymes in *P. furiosus* is investigated and described in **Chapter 9**. Transcription initiation sites are mapped and consensus sequences for the *P. furiosus* BRE site and TATA box are proposed. An inverted repeat is identified in several promoters of glycolytic genes. The presence and location of this inverted repeat is investigated in the complete genomic sequence of *P. furiosus* and its putative function is discussed.

Chapter 10 summarizes the obtained results and a laymen version is presented in **Chapter 11** in the Dutch language.

Chapter 2

Unraveling glycolytic pathways in archaea-unique features in central metabolic routes

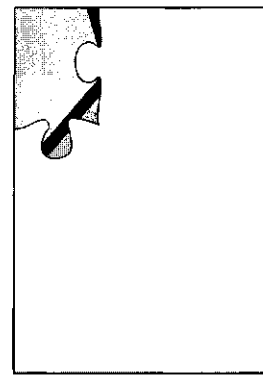

Corné H. Verhees, Willem M. de Vos and John van der Oost

A modified version of this chapter will be submitted for publication

Abstract

An early divergence in evolution has resulted in two prokaryotic domains, the bacteria and the archaea. Whereas the central metabolic routes of bacteria and eucarya are generally well conserved, variant pathways involving several novel enzymes with unique control have developed in archaea. A spectacular example of convergent evolution concerns the glucose-degrading pathways of saccharolytic archaea. The identification, characterization and comparison of the glycolytic enzymes of a variety of phylogenetic lineages has revealed a mosaic of canonical and unique enzymes in the archaeal variants of the Embden-Meyerhof and the Entner-Doudoroff pathways. Current structural and functional insights of the archaeal glycolytic routes are reviewed and evolutionary scenarios are discussed.

Introduction

Carbohydrates are the main carbon source for heterotrophic life-style in the three domains of life, bacteria, archaea, and eucarya. Saccharolytic growth involves extracellular hydrolysis of polysaccharides, uptake of oligosaccharides by specific transporters, and a range of catabolic pathways to generate monosaccharides and degrade them. Extensive research during several decades has resulted in detailed information on the composition of sugar metabolic pathways and the regulation thereof in bacteria and eucarya (1) (2). Of archaeal sugar metabolism relatively little is known.

The isolation of microbial life from boiling geysers, geothermally heated sediments, acid mudholes, hypersaline inland lakes and below Antarctic ice-floors, has vastly expanded our conceptions of which environments are able to sustain microbial life. Most of these exotic microbes belong to the domain of the archaea. The archaeal isolates from marine and terrestrial environments that share the capacity to grow at temperatures around the boiling point of water are called hyperthermophiles, and by definition exhibit optimal growth temperatures above 80 °C (3). Since the early 1990s, insight is emerging in the sugar metabolism of archaea in general and that of hyperthermophiles in particular. Several modified sugar degradation pathways that are operational under these extremely high temperatures have been identified in some of these hyperthermophiles. The constitution of these pathways has established by combining enzyme activities with ^{13}C-labeling experiments (4) (5). Comparative genomics and recent discoveries of novel sequences have resulted in better understanding of these metabolic networks. In this review, the main features of sugar metabolism of archaea is discussed, and by integrating different molecular and biochemical approaches potential evolutionary scenarios are discussed.

Table 2.1 Carbohydrate metabolizing archaea.

Organism	T-opt. (°C)	(an)aerobe	environment[1]	carbohydrates	pathway[2]	reference
Sulfolobales						
Sulfolobus solfataricus	80	a	t	starch, dextrin, xyloglucan, maltose, sucrose, lactose, glucose, xylose	ED*	(5) (17)
Sulfolobus shibatae	81	a	t	starch, glucose, galactose, arabinose		(5)
Sulfolobus acidocaldaricus	75	a	t	sucrose, lactose, glucose, galactose		(5)
Thermoproteales						
Thermoproteus tenax	88	an	t	starch, glycogen, glucose	EM*/ED*	(5)
Desulfurococcales						
Desulfurococcus amylolyticus	90	an	t	starch, glycogen	EM*	(5) (4)
Desulfurococcus saccharovorans	85	an	t	glucose		(5)
Desulfurococcus mucosus	88	an	t	starch		(5)
Pyrodictium abyssi	97	an	m	starch, glycogen, raffinose, lactose		(5)
Thermococcales						
Pyrococcus furiosus	100	an	m	starch, pullulanan,glycogen,maltose, cellobiose, glucose, lactose, melibiose[3]	EM*	(5) C. Verhees unpublished (10)
Pyrococcus woesei	100	an	m	starch, glycogen, maltose, cellobiose	EM*	(5)
Pyrococcus abyssi	96	an	m	starch, maltose	EM*	(5) (81)
Pyrococcus glycovorans	95	an	m	starch, maltose, cellobiose, glucose		(82)
Thermococcus celer	88	an	m	sucrose		(83)
Thermococcus stetteri	75	an	m	starch	EM*	(5)
Thermococcus zilligii	75	an	t	maltose	EM*	(84) (85)
Thermococcus litoralis	88	an	m	starch, maltose	EM*	(5) (86)
Thermococcus profundus	80	an	m	starch, maltose		(5)
Thermococcus hydrothermalis	90	an	m	cellobiose, maltose		(87)
Thermococcus aggregans	88	an	m	starch, maltose		(88)
Thermococcus guaymasensis	88	an	m	starch, maltose		(88)
Thermococcus pacificus	85	an	m	starch		(89)
Thermococcus fumicolans	85	an	m	maltose		(90)
Thermococcus profundus	80	an	m	starch, maltose		(91)
Archaeoglobales						
Archaeoglobus fulgidus strain 7324	83	an	m	starch	EM*	(41)
Thermoplasmales						
Thermopasma acidophilum	59	a	t	glucose	ED*	(48)
Halobacteriales[4]						
Halococcus saccharolyticus	37	a	h	arabinose, lactose, fructose, glucose	EM/ED*	(92), (29)
Haloferax mediteranei	35	a	h	starch, lactose, sucrose, fructose, glucose	EM/ED*	(93) (94) (95)
Haloarcula vallismortis	37	a	h	fructose, glucose	EM/ED*	(95)
Halobacterium saccharovorum	37	a	h	glucose	ED*	(96)

[1] t, terrestrial; m, marine; high salts, i.e. > 12% (2 M) NaCl.

[2] EM, Embden-Meyerhof pathway; ED, Entner-Doudoroff pathway; *, modifications in these pathways.

[3] *P.furiosus* degrades the glucose moiety of lactose and melibiose. Galactose is mainly secreted in the medium.

[4] Halophiles use an EM-like pathway for the degradation of fructose and a modified ED pathway for the degradation of glucose.

Saccharolytic archaea

A variety of archaea share the capacity to grow on carbohydrates under extreme conditions. A growing number of saccharolytic archaeal species has been identified, and efficient growth was observed on a variety of substrates ranging from poly- to monosaccharides (Table 2.1). Detailed studied hyperthermophilic saccharolytic archaea are representatives of euryarchaeota, *e.g. Pyrococcus furiosus* (6) and crenarchaeota, *e.g. Sulfolobus solfataricus* (7). Both of these hyperthermophilic archaea are able to grow on a variety of α- and β-linked glucose saccharides and glucose (6) (8) (9) (10) (11) (12). Polysaccharides are degraded by extracellular glycosyl hydrolases to oligosaccharides (13) (14) (15) (16) (9) (10) (17), which are subsequently transported into the cell by high-affinity ABC-transporters (18) (12) (19) (20). Active transport of glucose has also been described for archaea and involves either ABC or secondary transporters (21) (22) (23). Sugar transport via the phospho*enol*pyruvate (PEP)-dependent phosphotransferase system (PTS) is very common in bacteria but apparently absent in archaea and eucarya. Interestingly, genomic analyses reveal that PTS is also missing in the thermophilic bacteria *Thermotoga maritima* and *Aquifex aeolicus*. Transported oligosaccharides are further hydrolyzed to glucose by specific intracellular glycosyl hydrolases (8) (24) (25) (26) (27) (17). It has been shown that, at least *in vitro*, intra- and extracellular glycosyl hydrolases synergistically degrade polysaccharides to monosaccharides (9) (10).

Archaeal sugar metabolic pathways

Two major pathways are involved in the degradation of glucose to pyruvate in bacteria, eucarya and archaea, the Embden-Meyerhof (EM) and Entner-Doudoroff (ED) pathway. The co-existence of both EM- and ED-pathways has been observed in several mesophilic bacteria, but also in a hyperthermophilic bacterium (*Thermotoga maritima*) and a hyperthermophilic archaeon (*Thermoproteus tenax*) (28) (4). It has recently been demonstrated that the archaeon *Halococcus saccharolyticus* discriminates between an ED-like pathway and an EM-like pathway for growth on glucose and fructose, respectively (29). A third route, the pentose phosphate pathway, is present in bacteria and eucarya, and is needed for growth on pentoses, like xylulose and arabinose. Apart from pentose degradation, the pentose phosphate pathway is involved in the synthesis of RNA/DNA building blocks and the reduction of NADP to NADPH.

The two main glucose catabolic pathways, *i.e.* EM-pathway and ED-pathway differ in the key enzymes acting on glucose or glucose-6-phosphate and subsequently, in several of the following steps that lead to the formation and aldolytic cleavage of the intermediates fructose-1,6-bisphosphate (EM) and 2-keto-3-deoxy-6-phosphogluconate (ED) (Fig. 2.1). A major energetic difference in both canonical pathways is that in the ED-pathway only 1 mol ATP is formed per mol

glucose, instead of 2 mol ATP in the EM-pathway. It appears that the less efficient ED-pathway is often found in micro-organisms that possess an (an)aerobic respiration coupled to electron-transport phosphorylation in order to provide additional ATP (30). Modifications of the canonical ED and EM-pathways are mainly found in archaea (5) (4) (31).

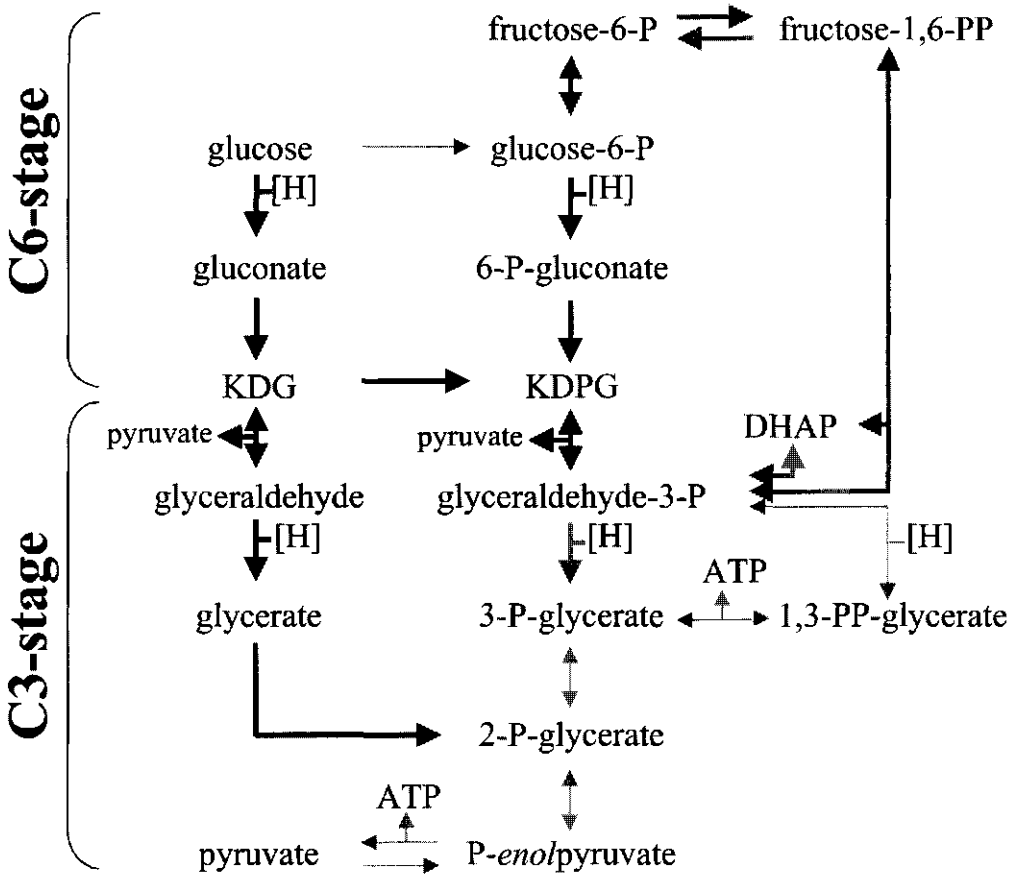

Figure 2. 1 Glucose metabolic pathways in archaea.

Reconstruction of archaeal sugar metabolism based on genes, enzyme activities and labeling studies. *Thick black arrows* indicated conversions specific for the (modified) ED-pathway. *Thick grey arrows* indicate conversions specific for the (modified) EM-pathway. *Thin grey arrows* indicate conversions present in both pathways. The conversions in which reducing equivalents (H) or ATP is formed are shown. It should be noted that the last step of the EM-pathway, *i.e.* the conversion of phospho*enol*pyruvate to pyruvate is still unclear in archaea (see text). KDG, 2-keto-3-deoxy-gluconate; KDPG, 2-keto-3-deoxy-phosphogluconate; DHAP, dihydroxy-acetone-phosphate; P, phosphate. Note that the phosphorylation-step of gluconate is missing in archaea.

EM-pathway in archaea and its modifications

The best-studied archaeal EM-pathway is the one of *P. furiosus*. Six of the ten glycolytic steps are chemically identical to the classical pathway. Novel enzymes and unique control points in the pyrococcal pathway have been elucidated and involve two phosphorylation and an oxidoreduction reaction (32) (33) (34) (35) (36) (37).

Instead of the classical ATP-dependent glucokinase and the ATP- (or PP_i)-dependent phosphofructokinase (PFKA), this archaeon contains novel ADP-dependent sugar kinases (32) (34). The genes that encode these enzymes from *P. furiosus* have been identified and found to be paralogs. After heterologous expression in *E. coli* the enzymes have been studied in detail (34) (C. Verhees, submitted). The ADP-dependent sugar kinases do not share overall sequence similarity with classical sugar kinase sequences. Interestingly, uncharacterized homologs were identified in several eucaryal, but not in bacterial genomes (38). The recently solved structure of the ADP-dependent glucokinase from the archaeon *Thermococcus litoralis*, closely related to *Pyrococcus*, shows a remarkable resemblance to adenosine kinase and ribokinase of the ribokinase family (Fig. 2.2). The minor phosphofructokinase (PFKB) from *E. coli* belongs to this family as well. Classical hexo-/glucokinases and phosphofructokinases belong to different monophyletic families. Hence, the primary sequence and the fold of the ADP-dependent kinases are not related to that of the ATP-dependent hexo-/glucokinases and ATP/PP_i-dependent phosphofructokinases (PFKA) (39).

Another major modification concerns the single-step conversion of glyceraldehyde-3-phosphate to 3-phospho-glycerate by the glyceraldehyde-3-phosphate ferredoxin oxidoreductase (GAPOR), instead of the two-step catalysis by the enzyme-couple glyceraldehyde-3-phosphate dehydrogenase and phosphoglycerate kinase (35). GAPOR is dependent on ferredoxin and appears to function solely in glycolytic direction. For its gluconeogenesis *P. furiosus* uses the conventional enzyme-couple phosphoglycerate kinase and glyceraldehyde-3-phosphate dehydrogenase (36).

An additional unique glycolytic enzyme has recently been studied from *P. furiosus*, *i.e.* the phosphoglucose isomerase. Based on its primary structure this enzyme is unrelated to the canonical phosphoglucose isomerases (37) (40). However, it contains a cupin domain, often involved in sugar binding, that is absent in the canonical phosphoglucose isomerases (37).

The existence of novel ADP-dependent sugar kinases, phosphoglucose isomerase and GAPOR are examples of non-homologous enzyme displacement in the pyrococcal glycolysis. This excessive replacement of enzymes in a metabolic pathway is a compelling example of functional convergent evolution. The non-homologous enzyme displacement of GAPOR is a special case, because the canonical enzyme-couple glyceraldehyde-3-phosphate dehydrogenase and phosphoglycerate kinase is still functionally present in *P. furiosus*. However, GAPOR has replaced the canonical enzyme-couple in glycolytic direction (36).

The modified EM-pathway as present in *P. furiosus* might also be operating in several *Thermococcus* species (4), and in the starch-degrading *Archaeoglobus fulgidus* strain 7324, in which ADP-dependent glucokinase, ADP-dependent phosphofructokinase and GAPOR activities have been demonstrated (41). Moreover, ADP-dependent phosphofructokinases appear to be present in thermophilic and mesophilic glycogen-degrading methanogenic species belonging to *Methanococcales* and *Methanosarcinales* (38). Interestingly, the crenarchaeon *Desulfurococcus amylolyticus* was found to contain a partially modified EM-pathway, including GAPOR activity, but with classical ATP-dependent phosphofructokinase activity (4). The latter was confirmed after purification and characterization of the ATP-dependent phosphofructokinase from *D. amylolyticus* (42). Another type of variation was observed in the EM-pathway of the crenarchaeon *Thermoproteus tenax*. Instead of GAPOR, a distinct NAD^+-dependent glyceraldehyde-3-phosphate dehydrogenase catalyzes the phosphate-independent, single-step oxidation of glyceradehyde-3-phosphate to 3-phospho-glycerate in glycolysis (43). Furthermore, the *T. tenax* EM-pathway includes an ATP-dependent glucokinase and a PP_i-dependent phosphofructokinase activity (4) (44).

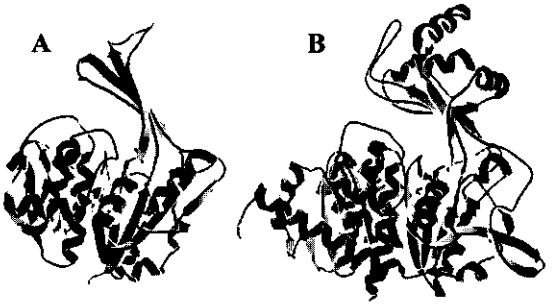

Figure 2.2 Structural similarity between ribokinase and ADP-dependent glucokinase.
Ribbon diagram of (*A*) *E. coli* ribokinase (1RKA; PDB) and (*B*) *Thermococcus litoralis* ADP-dependent glucokinase (1GC5; PDB) is shown. Both enzymes are (structural) members of the ATP-dependent ribokinase family (39).

ED-pathway in archaea and its modifications

Two main modifications in the archaeal ED-pathway have been described. Halophilic archaea (and some eubacteria) use a partially non-phosphorylated ED-pathway in which 2-keto-3-deoxy-gluconate (KDG) is phosphorylated to 2-keto-3-deoxy-6-phosphogluconate (KDPG) by KDG-kinase. Phosphorylation at a different level of the C6-stage in the pathway allows the gain of ATP by substrate-level phosphorylation during conversion of glyceraldehyde-3-phosphate via 1,3-diphosphoglycerate to 3-phosphoglycerate in the canonical EM-pathway (Fig. 2.1) (45). *Thermoproteus*, *Thermoplasma* and *Sulfolobus* use an ED-like pathway in which none of the hexose

intermediates are phosphorylated. However, at a late C3-stage phosphorylation of glycerate to 2-phospho-glycerate occurs, which is further metabolized to pyruvate via the EM-enzymes enolase and pyruvate kinase (46) (45) (47) (48) (4). Because most (if not all) archaea appear to lack a glyceraldehyde-3-phosphate oxidation system that allows substrate-level phosphorylation, it does not matter at what level phosphorylation occurs. The modified versions of the ED-pathway in archaea have often been referred to as "non-phosphorylating"-ED; however, phosphorylation occurs at another level in the pathway: not at the level of gluconate, but at the level of 2-keto-3-deoxy-gluconate or glycerate (Fig. 2.1).

The first enzyme of the ED-pathway, *i.e.* NADP-dependent glucose dehydrogenase activity was purified from *T. tenax* cell extract (49). Two unrelated types of glucose dehydrogenases have been described in literature: a pyrroloquinoline-quinone (PQQ)-dependent glucose dehydrogenase, which appear to be restricted to gram-negative bacteria, and a NAD(P)-dependent glucose dehydrogenase that has been isolated and characterized form all three domains of life (49). Non-homologous enzyme displacement of NADP-dependent glucose dehydrogenase by the PQQ-dependent glucose dehydrogenase might have occurred in some gram-negative bacteria. A novel non-phosphorylated KDG-aldolase has been purified and characterized from *S. solfataricus* (50). In the genome of *Halobacterium* a distantly related gene has been identified by similarity search and gene context and is predicted to encode the missing phosphorylated KDPG-aldolase (Table 2.2).

Pentose phosphate pathway in archaea

Two pathways have been proposed for the pentose biosynthesis in methanogens, *i.e.* a non-oxidative branch of the pentose phosphate pathway, or an oxidative decarboxylation of one of the hexoses (51) (52) (53). Isotope labeling studies have suggested that the oxidative branch of the pentose phosphate pathway is absent in *Methanococcus* (54). Genes encoding canonical enzymes of the oxidative branch of pentose phosphate pathway have not been found in archaea (55) (56) (57). Therefore, it would be unlikely that catabolism of glucose proceeds via the complete pentose phosphate pathway in archaea, but rather via an EM-like or ED-like pathway.

Novel pathways in archaea

A novel glycolytic pathway has recently been demonstrated in *Thermococcus zilligii* that makes use of a glucose-6-P dehydrogenase, a novel lyase and subsequent secretion of formate. Cells were grown on tryptone with or without glucose and after harvesting the cells the conversion of ^{13}C-glucose was recorded by NMR. A relative contribution of 2:1 (novel pathway versus EM-pathway) was calculated for cells grown on tryptone. The presence of glucose in the growth medium appears to repress the enzymes in this novel pathway, and results in inversion of the relative contributions of the two pathways (58). Alternatively, another route appears to be consistent with the labeling

pattern (H. Santos, pers. comm.) that would involve hexulose-6-P isomerase, hexulose-6-P synthase and formaldehyde ferredoxin oxidoreductase. The intermediate ribulose-5-P may be further degraded by the pentose phosphoketolase pathway, commonly found in lactic acid bacteria (59).

Genome based reconstruction of archaeal sugar metabolism

With the increasing number of completely sequenced archaeal genome sequences, a reconstruction can be made of glycolytic enzyme encoding genes present in archaea (Table 2.2). The identification of novel gene products involved in archaeal sugar catabolic and anabolic pathways allows for the compilation of a nearly complete set of enzymes involved in archaeal sugar metabolism. In the present paper the focus is on the main glycolytic pathways, *i.e.* EM-pathway and ED-pathway, and the non-oxidative branch of pentose phosphate pathway. However, genes that are yet to be identified in archaeal genomes concern the oxidative pentose phosphate pathway enzymes, and the (partially) non-phosphorylated ED-pathway enzyme gluconate dehydratase. The unsuccessful identification of the genes in genomic sequences suggests them to be either not present, highly diverged, or unique.

The identification of the novel paralogous ADP-dependent glucokinase and ADP-dependent phosphofructokinase, together with the GAPOR in *P. furiosus*, allowed us to genetically identify the major modifications in the pyrococcal EM-pathway (34) (36). Orthologs of the ADP-dependent phosphofructokinase were also identified in *M. jannaschii* (38). Interestingly, ADP-dependent kinase homologs were identified in several higher eukaryotes including man, suggesting these homologs to be distributed over at least two domains of life (38).

Genes encoding canonical phosphoglucose isomerases are present in *M. jannaschii* and *Halobacterium* NRC-1. However, a unique phosphoglucose isomerase, with a predicted cupin domain, was found in *P. furiosus*, *P. horikoshii* and *P. abyssi*. Remarkably, the distribution of this gene appears to be restricted to these Pyrococci (37). Phosphoglucose isomerase homologs have not been identified in the other available archaeal genomes. These organisms appear to contain a gluconeogenic pathway up to the level of fructose-6-phosphate, which probably acts as the intermediate to enter the non-oxidative pentose phosphate pathway.

A homolog of a canonical fructose-1,6-bisphosphatase (FBPase I) could be identified in the crenarchaeal genome sequence of *Halobacterium* NRC-1. No obvious orthologs of this gene are present in the other archaeal genomes. However, recent characterization of the bi-functional fructose-1,6-bisphosphatase/*myo*-inositol-1-phosphatase from *M. jannaschii* (MJ0109) (60) resulted in the identification of this gene in euryarchaeal genome sequences (FBPase IV) (C. Verhees, submitted). Putative homologs, but no orthologs of this fructose-1,6-bisphosphatase gene were identified in the crenarchaeal genomes (Table 2.2).

Table 2.1 Genome based reconstruction of archaeal and thermophilic sugar metabolism.

	Species code....										
	PF	PH	PAB	MJ	MT	AF	TA	SSO	APE	*VNG*	TM
EM-pathway/gluconeogenesis											
Hexokinase (ATP)							0825		2091		1469
Glucokinase (ADP)	0312	0589	0967								
Phosphoglucose isomerase (PGI/SIS)				1605						1992	1385
Phosphoglucose isomerase (CUPIN)	0196	1956	1199								
Phosphofructokinase (ATP)									0012		0209
Phosphofructokinase (PPi)											0289
Phosphofructokinase (ADP)	1784	1645	2013	1604							
Fructose-1,6-bisphosphatase (I)										0684	
Fructose-1,6-bisphosphatase (IV)	2014	1897	0189	0109	0871	2372					
Fructose-1,6-bisphosphatase (IV-related)								2418	1798	1379	1415
Fructose-1,6-bisphosphate aldolase (II)											0273
Fructose-1,6-bisphosphate aldolase (IA)	1956	0082	0049	0400 1585	0579	0108 0230		3226	0011	0683 0309	
Triose-phosphate isomerase	1920[1]	1884	1208	1528	1041	1304	0313	2592	1538	1027	0689
Glyceraldehyde-3-phosphate ferredoxin oxidoreductase	0464	0457	1315	1185							
Non-phosphorylating glyceraldehyde-3-phosphate dehydrogenase (NADH)	0755							3194[2]	1718		
Glyceraldehyde-3-phosphate dehydrogenase (NADH)	1874	1830	0257	1146	1009	1732	1103	0528	0171	0095	0688
Phosphoglycerate kinase	1057	1218	1679	0641	1042	1146	1075	0527	0173	1216	0689
Phosphoglycerate mutase (family A)							1347	2236			1374
Phosphoglycerate mutase (2,3-bisphosphoglycerate independent)										1887	
Phosphoglycerate mutase (archaeal)	1959	0037	2318	1612 0010	1591 0418	 1751 1425	0413	0417	1616		
Phosphopyruvate hydrolase (enolase)	0215	1942	1126	0232	0043	1132	0882	0913	2458	1142	0877
Pyruvate kinase	1188	0570	1441	0108			0896	0981[3]	0489	0324	0208
Phospho*enol*pyruvate synthase	0043	0092	0057	0542	1118	0710	0886	0883	0650	0330	0272
ED-pathway											
Glucose dehydrogenase (NADP+)							0897	3204 3003 3042		0446	
Glucose-6-phosphate dehydrogenase											1155
Gluconate kinase											0443
Gluconate dehydratase Phosphogluconate dehydratase											
KDG-kinase										0158	
KDPG-aldolase (hypothetical)										0444	0066
KDG-aldolase							0619	3197			
Glyceraldehyde dehydrogenase (NADP+) (hypothetical)				1411	0978			1629 1842			
Glycerate kinase	0024	0495	1021				0453	0666	0996		1585
Non-oxidative pentose phosphate pathway											
Ribose-5-phosphate epimerase	1258	1375	0522	1603	0608	0943	0878	0978	0665	2272	
Ribulose-phosphate 3-epimerase				0680			1315				1718
Transketolase	1689 1688		0296 0295	0679 0681			0617 0618	0299 0297	0583 0586		0953 0954 1762
Transaldolase				0960			0616				0295

Numbering of the genes is according to http://www-archbac.u-psud.fr/projects/sulfolobus/. PF = *P. furiosus*; PH = *P. horikoshii*; PAB = *P. abyssi*; MJ = *Methanococcus jannaschii*; MT = *Methanobacterium thermoautotrophicum*; AF = *A. fulgidus*; TA = *T. acidophilum*; SSO = *S. solfataricus*; APE = *Aeropyrum pernix*; VNG = *Halobacterium NRC-1*; TM = *Thermotoga maritima*. Experimentally confirmed gene products are underlined. [1]Characterized from *P. woesei* (97). [2]Characterized from *Thermoproteus tenax* (43). [3]Characterized from *T. tenax* (68). KDPG-aldolase and glyceraldehyde dehydrogenase is highly speculative and need to be experimentally confirmed.

A distantly diverged archaeal type of fructose-1,6-bisphosphate aldolase was recently identified in T. tenax and P. furiosus (61), confirming an earlier function prediction (53). Orthologs are present in all sequenced archaeal genomes, except for Thermoplasma acidophilum. Paralogs of the aldolase are present in M. jannaschii (MJ1585), A. fulgidus (AF0230), Halobacterium NRC-1 (VNG0309), and the encoded enzymes were predicted to function as deoxyribose phosphate aldolase or transaldolase (53).

Archaeal phosphoglycerate mutase, distantly related (11% amino acid identity) to its *E. coli* counterpart, has been predicted by comparative analysis of metabolic pathways in different genomes (62). The prediction has been confirmed experimentally for *P. furiosus* and *M. jannaschii* (MJ1612) (C. Verhees, unpublished). Interestingly, a gene duplication event has led to a second copy of this gene in *M. jannaschii* (MJ0010), *M. thermoautotrophicum* (MT0418), and *A. fulgidus* (AF1425), the physiological role of which is unknown (Table 2.2). The same holds true for the three copies of the *S. solfataricus* glucose dehydrogenase, which contrasts with a single copy of this gene in *T. acidophilum* (Table 2.2). Experimental work will have to determine the physiological role of these three copies in the former.

Regulation of archaeal glycolysis

Regulation of glycolysis is a very complex process. Swift initiation of the glycolytic flux relies on the coordinated triggering of multiple events, including allosteric regulation of enzymatic activities, protein modification and modulation of gene expression (2). In bacteria and eucarya transcriptional control of glycolysis can be positively or negatively regulated. In gram-positive bacteria the catabolite control protein (CcpA) was found to be a transcriptional activator of the *las* operon, consisting of genes encoding phosphofructokinase, pyruvate kinase and lactate dehydrogenase (63) (64). In gram-negative bacteria the fructose repressor protein (FruR) negatively regulates transcription of genes encoding glycolytic enzymes, and positively regulates transcription of genes encoding gluconeogenic enzymes (65). In yeast, a DNA-binding protein (GRC1) was found to strongly reduce the transcription levels of most glycolytic enzyme encoding genes (66) (67).

Glycolytic control in archaea is still poorly understood. However, novel insights have recently been gained in the control of the modified EM-pathways from *P. furiosus* and *T. tenax* (34) (37) (61) (44) (68) (36). The activities of *P. furiosus* glycolytic enzymes appear often to be higher in cells grown on sugars compared to cells grown on peptides or pyruvate (69) (32) (37) (70). Transcript analysis of *P. furiosus* glycolytic enzymes encoding genes revealed more abundant signals on sugar-grown cells then on peptide- or pyruvate-grown cells (36) (37) (61) (71). The co-

transcription of the genes coding for the *T. tenax* reversible PP_i-dependent phosphofructokinase and fructose-1,6-bisphosphate aldolase was 6-fold higher in heterotrophically then in autotrophically grown cells (61). In bacteria fructose-1,6-bisphosphate aldolase genes are sometimes co-transcribed with genes coding for other reversible enzymes of glycolysis, *e.g.* glyceraldehyde-3-phosphate dehydrogenase or phosphoglycerate kinase (72) (73). In the gram-positive bacterium *Lactococcus lactis* genes encoding irreversible phosphofructokinase and pyruvate kinase are organized as an operon and co-transcribed (74). Higher transcript levels under catabolic conditions might reflect the necessity of higher carbon flux rates through the glycolytic pathway.

Nothing is known about potential regulators of the transcription of glycolytic enzyme encoding genes in archaea. However, an inverted repeat has recently been identified in promoter sequences of the genes encoding glycolytic enzymes in *P. furiosus* (not shown) (C. Verhees, unpublished). This repeat was not present in promoter sequences of genes encoding fructose-1,6-bisphosphatase, glyceraldehyde-3-phosphate and phosphoglycerate kinase, enzymes that solely act in gluconeogenesis. Remarkably, it was apparent in the promoter structure of phosphoenolpyruvate synthase as well, but not in that of pyruvate kinase. Although it has been suggested before that phosphoenolpyruvate synthase rather than pyruvate kinase might be operating in glycolytic direction (75), this is still a matter of debate (76) (J. Tuininga, pers. comm.). Since the motif is present in promoter sequences of genes encoding glycolytic enzymes, it might represent a specific site for regulation the *P. furiosus* glycolytic pathway by a yet unidentified transcriptional regulator.

In classical glycolysis, the reactions catalyzed by hexokinase, phosphofructokinase and pyruvate kinase are virtually irreversible. Hence, they would be expected to have regulatory as well as catalytic roles. In fact, all three enzymes are allosterically regulated control sites. The ADP-dependent glucokinase from *P. furiosus*, the ADP-dependent phosphofructokinase and PP_i-dependent phosphofructokinase from *P. furiosus* and *T. tenax*, respectively, and the pyruvate kinase from *T. tenax* have been investigated on their regulatory roles (C. Verhees, unpublished) (34) (44) (68). Interestingly, none of these enzymes was allosterically regulated by any of the known allosteric effectors. Therefore, they presumably do not act as the major allosteric control point of the glycolytic pathway. Alternatively, GAPOR could be an important enzyme in control of the *Pyrococcus* glycolysis. GAPOR acts solely in glycolysis and the expression of its gene is induced by growth on sugars. In contrast, the expression of the glyceraldehyde-3-phosphate dehydrogenase gene is constitutively expressed. This confirms the involvement of GAPOR in the pyrococcal glycolysis, and has been proposed to be a novel site for glycolytic control (36).

It is concluded that regulation of the glycolytic flux in *P. furiosus* might involve modulation of gene expression rather than allosteric regulation of enzyme activities. Complete genome micro-arrays of *P. furiosus* are underway and will certainly provide more insight in the actual significance of regulation of gene expression in archaeal central metabolism (71) (M. Adams, pers. comm.).

Evolutionary aspects of archaeal glycolytic pathways

In most organisms glucose catabolism is accomplished by an EM-like, an ED-like or sometimes a pentose phosphate pathway, that converge at the level of glyceraldehyde-3-phosphate, which is subsequently converted by a common core pathway of enzymes to pyruvate (77). The non-phosphorylated ED-pathways in *Sulfolobus*, *Thermoproteus* and *Thermoplasma* form an exception since they converge with the EM-pathway at the level of 2-phospho-glycerate (Fig. 2.1). The common reversible core pathway that consist of the enzymes, glyceraldehyde-3-phosphate dehydrogenase, phosphoglycerate kinase, phosphoglycerate mutase, enolase, pyruvate kinase, and/or phospho*enol*pyruvate synthase, appears to be present in all organisms. The complete conservation of the reversible core pathway, or C3-stage of glycolysis might suggest it to represent an ancient pathway, that might have been present in the common ancestor.

The question remains which catabolic pathway, *i.e.* ED-pathway or EM-pathway represents the most ancient complete glycolytic pathway. It has been suggested that the ED-pathway predates the EM-pathway because the latter is more efficient from an energetic point of view, and thus less primitive (30) (78). However, the presence of an EM-pathway in anaerobic archaea and in deeply rooted bacteria would suggest the EM-pathway to represent a more ancient pathway (5). ED-pathways are commonly found in organisms capable of respiration. It has been proposed that the ED-pathway in aerobic organisms co-evolved in conjunction with the complete citric acid cycle and aerobic respiration (5). However, the complete citric acid cycle is proposed to have evolved first as partial cycle, with reductive biosynthetic capacity in anaerobic organisms (78) (79) and presumably predate complete cycles present in aerobic deeply rooted archaea like *Sulfolobus* (57). The presence of an ED-pathway (similar to halophiles) in strictly fermentative organisms such as *Zymomonas mobiles* and in the strictly anaerobic *Clostridium aceticum* raises questions about the implied requirement for ED-metabolism coupled to (an)aerobic respiration (30). Thus, the historical question which pathway was first remains to be answered, although it seems likely that both pathways have partly (from glucose to glyceraldehyde-3-phosphate) evolved independently, and that the energy-poor ED-pathway can be used efficiently in combination with energy-rich (an)aerobic respiration (5).

Modifications in the ED-pathway and EM-pathway appear to be mainly restricted to the C6-stage of the pathways, *i.e.* above the level glyceraldehyde-3-phosphate. Modifications in the EM-pathway include non-homologous enzyme displacements, natural inheritance and lateral gene transfer (37) (61). The modified versions of the ED-pathway mainly correspond to phosphorylation of the intermediates at a different level in the pathway and non-homologous enzyme displacement of at least the glucose dehydrogenase (49). The variations that occur above the level of

38. Verhees, C. H., Tuininga, J. E., Kengen, S. W., Stams, A. J., van der Oost, J., and de Vos, W. M. (2001) *J. Bacteriol.* 183, 7145-7153.
39. Ito, S., Fushinobu, S., Yoshioka, I., Koga, S., Matsuzawa, H., and Wakagi, T. (2001) *Structure* (Camb) 9, 205-214.
40. Hansen, T., Oehlmann, M., and Schonheit, P. (2001) *J. Bacteriol.* 183, 3428-3435.
41. Labes, A., and Schonheit, P. (2001) *Arch. Microbiol.* 176, 329-338.
42. Hansen, T., and Schonheit, P. (2000) *Arch. Microbiol.* 173, 103-109.
43. Brunner, N. A., Brinkmann, H., Siebers, B., and Hensel, R. (1998) *J. Biol. Chem.* 273, 6149-6156.
44. Siebers, B., Klenk, H. P., and Hensel, R. (1998) *J. Bacteriol.* 180, 2137-2143.
45. Danson, M. J. (1993) Central metabolism of the archaea. The biochemistry of archaea (archaeabacteria) (Kates, M., Kushner, D. J., and Matheson, A. T., Eds.), Elsevier, Amsterdam
46. De Rosa, M., Gambacorta, A., Nicolaus, B., Giardina, P., Poerio, E., and Buonocore, V. (1984) *Biochem. J.* 224, 407-414
47. Hensel, R., Laumann, S., Lang, J., Heumann, H., and Lottspeich, F. (1987) *Eur. J. Biochem.* 170, 325-333.
48. Budgen, N., and Danson, M. J. (1986) *FEBS Lett.* 196, 207-210
49. Siebers, B., Wendisch, V. F., and Hensel, R. (1997) *Arch. Microbiol.* 168, 120-127.
50. Buchanan, C. L., Connaris, H., Danson, M. J., Reeve, C. D., and Hough, D. W. (1999) *Biochem. J.* 343 Pt 3, 563-570.
51. Yu, J. P., Ladapo, J., and Whitman, W. B. (1994) *J. Bacteriol.* 176, 325-332.
52. Choquet, C. G., Richards, J. C., Patel, G. B., and Sprott, G. D. (1994) *Arch. Microbiol.* 161, 481-488.
53. Galperin, M. Y., Aravind, L., and Koonin, E. V. (2000) *FEMS Microbiol. Lett.* 183, 259-264.
54. Sprott, G. D., Ekiel, I., and Patel, G. B. (1993) *Appl. Environ. Microbiol.* 59, 1092-1098.
55. Selkov, E., Maltsev, N., Olsen, G. J., Overbeek, R., and Whitman, W. B. (1997) *Gene* 197, 11-26.
56. Makarova, K. S., Aravind, L., Galperin, M. Y., Grishin, N. V., Tatusov, R. L., Wolf, Y. I., and Koonin, E. V. (1999) *Genome Res.* 9, 608-628.
57. She, Q., Singh, R. K., Confalonieri, F., Zivanovic, Y., Allard, G., Awayez, M. J., Chan-Weiher, C. C., Clausen, I. G., Curtis, B. A., De Moors, A., Erauso, G., Fletcher, C., Gordon, P. M., Heikamp-de Jong, I., Jeffries, A. C., Kozera, C. J., Medina, N., Peng, X., Thi-Ngoc, H. P., Redder, P., Schenk, M. E., Theriault, C., Tolstrup, N., Charlebois, R. L., Doolittle, W. F., Duguet, M., Gaasterland, T., Garrett, R. A., Ragan, M. A., Sensen, C. W., and Van der Oost, J. (2001) *Proc. Natl. Acad. Sc.i* U. S. A. 98, 7835-7840.
58. Xavier, K. B., da Costa, M. S., and Santos, H. (2000) *J. Bacteriol.* 182, 4632-4636.
59. Kandler, O. (1983) *Antonie van Leeuwenhoek* 49, 209-224.
60. Stec, B., Yang, H., Johnson, K. A., Chen, L., and Roberts, M. F. (2000) *Nat. Struct. Biol.* 7, 1046-1050.
61. Siebers, B., Brinkmann, H., Dorr, C., Tjaden, B., Lilie, H., van der Oost, J., and Verhees, C. H. (2001) *J. Biol. Chem.* 276, 28710-28718.
62. Dandekar, T., Schuster, S., Snel, B., Huynen, M., and Bork, P. (1999) *Biochem. J.* 343, 115-124.
63. Luesink, E. J., van Herpen, R. E., Grossiord, B. P., Kuipers, O. P., and de Vos, W. M. (1998) *Mol. Microbiol.* 30, 789-798.
64. van den Bogaard, P. T., Kleerebezem, M., Kuipers, O. P., and de Vos, W. M. (2000) *J. Bacteriol.* 182, 5982-5989.
65. Ramseier, T. M., Bledig, S., Michotey, V., Feghali, R., and Saier, M. H., Jr. (1995) *Mol. Microbiol.* 16, 1157-1169.
66. Baker, H. V. (1986) *Molecular and Cellular Biology* 6, 3774-3784.

67. Baker, H. V. (1991) *Proc. Natl. Acad. Sci.* U S A 88, 9443-9447.
68. Schramm, A., Siebers, B., Tjaden, B., Brinkmann, H., and Hensel, R. (2000) *J. Bacteriol.* 182, 2001-2009.
69. Schäfer, T., and Schönheit, P. (1993) *Arch. Microbiol.* 159, 359-363.
70. Adams, M. W., Holden, J. F., Menon, A. L., Schut, G. J., Grunden, A. M., Hou, C., Hutchins, A. M., Jenney, F. E., Jr., Kim, C., Ma, K., Pan, G., Roy, R., Sapra, R., Story, S. V., and Verhagen, M. F. (2001) *J. Bacteriol.* 183, 716-724.
71. Schut, G. J., Zhou, J., and Adams, M. W. (2001) *J. Bacteriol.* 183, 7027-7036.
72. Plaumann, M., Pelzer-Reith, B., Martin, W. F., and Schnarrenberger, C. (1997) *Curr. Genet.* 31, 430-438.
73. van den Bergh, E. R., Baker, S. C., Raggers, R. J., Terpstra, P., Woudstra, E. C., Dijkhuizen, L., and Meijer, W. G. (1996) *J. Bacteriol.* 178, 888-893.
74. Wouters, J. A., Kamphuis, H. H., Hugenholtz, J., Kuipers, O. P., de Vos, W. M., and Abee, T. (2000) *Appl. Environ. Microbiol.* 66, 3686-3691.
75. Sakuraba, H., Utsumi, E., Kujo, C., and Ohshima, T. (1999) *Arch. Biochem. Biophys.* 364, 125-128.
76. Hutchins, A. M., Holden, J. F., and Adams, M. W. (2001) *J. Bacteriol.* 183, 709-715.
77. Fothergill-gilmore, L. A., and Michels, P. A. M. (1993) *Prog. Biophys. Molec. Biol.* 59, 105-235
78. Romano, A. H., and Conway, T. (1996) *Res. Microbiol.* 147, 448-455.
79. Huynen, M. A., Dandekar, T., and Bork, P. (1999) *Trends Microbiol.* 7, 281-291.
80. Ettema, T., van der Oost, J., and Huynen, M. (2001) *Trends Genet.* 17, 485-487.
81. Gonzalez, J. M., Masuchi, Y., Robb, F. T., Ammerman, J. W., Maeder, D. L., Yanagibayashi, M., Tamaoka, J., and Kato, C. (1998) *Extremophiles* 2, 123-130.
82. Barbier, G., Godfroy, A., Meunier, J. R., Querellou, J., Cambon, M. A., Lesongeur, F., Grimont, P. A., and Raguenes, G. (1999) *Int. J. Syst. Bacteriol.* 49, 1829-1837.
83. Zillig, W., Holz, I., Janekovic, D., Schäfer, T., and Reiter, W. D. (1983) *System. Appl. Microbiol.* 4, 88-94.
84. Ronimus, R. S., Reysenbach, A., Musgrave, D. R., and Morgan, H. W. (1997) *Arch. Microbiol.* 168, 245-248.
85. Ronimus, R. S., Koning, J., and Morgan, H. W. (1999) *Extremophiles* 3, 121-129.
86. Xavier, K. B., Peist, R., Kossmann, M., Boos, W., and Santos, H. (1999) *J. Bacteriol.* 181, 3358-3367.
87. Godfroy, A., Lesongeur, F., Raguenes, G., Querellou, J., Antoine, E., Meunier, J. R., Guezennec, J., and Barbier, G. (1997) *Int. J. Syst. Bacteriol.* 47, 622-626.
88. Canganella, F., Jones, W. J., Gambacorta, A., and Antranikian, G. (1998) *Int. J. Syst. Bacteriol.* 48 , 1181-1185.
89. Miroshnichenko, M. L., Gongadze, G. M., Rainey, F. A., Kostyukova, A. S., Lysenko, A. M., Chernyh, N. A., and Bonch-Osmolovskaya, E. A. (1998) *Int. J. Syst. Bacteriol.* 48, 23-29.
90. Godfroy, A., Meunier, J. R., Guezennec, J., Lesongeur, F., Raguenes, G., Rimbault, A., and Barbier, G. (1996) *Int. J. Syst. Bacteriol.* 46, 1113-1119.
91. Kobayashi, T., Higuchi, S., Kimura, K., Kudo, T., and Horikoshi, K. (1995) *J. Biochem.* (Tokyo) 118, 587-592.
92. Montera, C. G., Ventosa, A., Rodriguez-Valera, F., Kates, M., Moldoveanu, N., and Ruiz-Berraquero, F. (1989) *System. Appl. Microbiol.* 12, 167-171.
93. Rodriguez-Valera, F., Juez, G., and D.J., K. (1983) *System. Appl. Microbiol.* 4, 369-381.
94. Danson, M. J. (1989) *Can. J. Microbiol.* 35, 58-63.
95. Altekar, W., and Rangaswamy, V. (1990) *FEBS Microbiol. Letters* 69.
96. Rawal, N., Kelkar, S. M., and Altekar, W. (1988) *Indian J. Biochem. Biophys.* 25, 674-686.
97. Kohlhoff, M., Dahm, A., and Hensel, R. (1996) *FEBS Lett.* 383, 245-250.

Chapter 3

Molecular and biochemical characterization of the ADP-dependent phosphofructokinase from the hyperthermophilic archaeon *Pyrococcus furiosus*

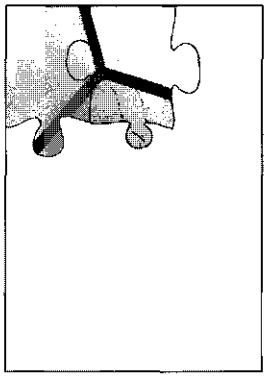

Judith E. Tuininga*, Corné H. Verhees*, John van der Oost, Servé W.M. Kengen, Alfons J.M. Stams and Willem M. de Vos

* both authors contributed equally

Journal of Biological Chemistry 274: 21023-21028 (1999)

Abstract

Pyrococcus furiosus uses a modified Embden-Meyerhof pathway involving two ADP-dependent kinases. Using the N-terminal amino acid sequence of the previously purified ADP-dependent glucokinase, the corresponding gene as well as a related open reading frame were detected in the genome of *P. furiosus*. Both genes were successfully cloned and expressed in *Escherichia coli*, yielding highly thermoactive ADP-dependent glucokinase and phosphofructokinase. The deduced amino acid sequences of both kinases were 21.1% identical but did not reveal significant homology with those of other known sugar kinases. The ADP-dependent phosphofructokinase was purified and characterized. The oxygen-stable protein had a native molecular mass of approximately 180 kDa and was composed of four identical 52-kDa subunits. It had a specific activity of 88 units/mg at 50 °C and a pH optimum of 6.5. As phosphoryl group donor, ADP could be replaced by GDP, ATP, and GTP to a limited extent. The K_m values for fructose 6-phosphate and ADP were 2.3 and 0.11 mM, respectively. The phosphofructokinase did not catalyze the reverse reaction, nor was it regulated by any of the known allosteric modulators of ATP-dependent phosphofructokinases. ATP and AMP were identified as competitive inhibitors of the phosphofructokinase, raising the K_m for ADP to 0.34 and 0.41 mM, respectively.

Introduction

During growth on poly- or disaccharides, the hyperthermophilic archaeon *Pyrococcus furiosus* uses a novel type of glycolytic pathway that is deviant from the classical Embden-Meyerhof pathway in several respects (1, 2). First, instead of the classical ATP-dependent hexokinase, the pathway involves a novel ADP-dependent glucokinase (3, 4). Second, a novel ADP-dependent phosphofructokinase replaces the more common ATP-dependent phosphofructokinase (3). Third, the pathway is modified in the degradation of glyceraldehyde 3-phosphate, which involves glyceraldehyde-3-phosphate ferredoxin oxidoreductase instead of the conventional couple glyceraldehyde-3-phosphate dehydrogenase and phosphoglycerate kinase (5, 6). Modifications of the classical Embden-Meyerhof pathway at one or more of these three steps have also been observed in members of the hyperthermophilic archaeal genera *Thermococcus*, *Desulfurococcus*, and *Thermoproteus* (2, 7). The presence of these modifications in *P. furiosus* and other hyperthermophilic microorganisms suggests that these are adaptations to elevated temperatures as a result of an altered biochemistry or a decreased stability of biomolecules.

Although ATP is regarded as the universal energy carrier and the most common phosphoryl group donor for kinases, several gluco- and phosphofructokinases with a different cosubstrate specificity have been described. Beside ADP-dependent gluco- and phosphofructokinases that have been demonstrated in *Pyrococcus* and *Thermococcus* spp. (3, 4, 7), polyphosphate-dependent

glucokinases have been found in several other microorganisms. In addition, the glucokinase of *Propionibacterium* can use both ATP and polyphosphate as phosphoryl group donor (8). Furthermore, PP_i-dependent phosphofructokinases have been described in several eukarya and bacteria and the hyperthermophilic archaeon *Thermoproteus tenax* (9).

Phylogenetic analyses of phosphofructokinases grouped these enzymes into three clusters. In a multiple alignment of representatives of each cluster, functionally important residues were identified that were highly conserved between all phosphofructokinases (9). ADP-dependent phosphofructokinases were not included in this study, because primary sequences of these enzymes were not yet available.

In this paper, we describe the cloning, expression, purification, and characterization of the ADP-dependent phosphofructokinase from *P. furiosus*. It is the first molecular and biochemical characterization of an ADP-dependent phosphofructokinase to date.

Experimental procedures

Materials

Acetyl phosphate (potassium-lithium salt, crystallized), ADP (disodium salt), AMP (disodium salt, crystallized), aldolase (D-fructose-1,6-bisphosphate D-glyceraldehyde-3-phosphate-lyase, EC 4.1.2.13; rabbit muscle), ATP (disodium salt), fructose 1,6-bisphosphate (trisodium salt, crystallized), GDP (dilithium salt), glucose 6-phosphate (disodium salt), glucose-6-phosphate dehydrogenase (D-glucose-6-phosphate:$NADP^+$ 1-oxidoreductase, EC 1.1.1.49; yeast), glycerol-3-phosphate dehydrogenase (*sn*-glycerol-3-phosphate:NAD^+ 2-oxidoreductase, EC 1.1.1.8; rabbit muscle), NADH (disodium salt), phosphoenolpyruvate (tricyclohexylammonium salt), phosphoglucose isomerase (D-glucose-6-phosphate ketol-isomerase, EC 5.3.1.9; yeast), and triosephosphate isomerase (D-glyceraldehyde-3-phosphate ketol-isomerase, EC 5.3.1.1; rabbit muscle) were obtained from Roche Molecular Biochemicals. D-Fructose-1-phosphate (barium salt), D-fructose 2,6-bisphosphate (sodium salt), D-fructose 6-phosphate (disodium salt), β-NADP (sodium salt), sea salts, sodium phosphate glass type 35, tetrapotassium pyrophosphate, tripolyphosphate pentasodium, and trisodium trimetaphosphate were from Sigma. All other chemicals were of analytical grade. *Pfu* DNA polymerase was obtained from Life Technologies Inc. Mono Q HR 5/5, Phenyl-Superose HR 5/5, Q-Sepharose fast flow, and Superdex 200 prep grade were obtained from Amersham Pharmacia Biotech, hydroxyapatite Biogel HT was from Bio-Rad. *P. furiosus* (DSM 3638) was obtained from the German Collection of Microorganisms (Braunschweig, Germany). *Escherichia coli* XL-1 Blue and *E. coli* BL21(DE3) were obtained from

Stratagene (La Jolla, CA). The expression vector pET9d was obtained from Novagen Inc. (Madison, WI).

Organisms and growth conditions

P. furiosus was mass-cultured (200 liters) in an artificial seawater medium supplemented with Na_2WO_4 (10 μM), yeast extract (1 g/liter), and vitamins, as described before (10) but with lower concentrations of Na_2S (0.25 g/liter) and NaCl (20 g/liter). The fermentor (Bioengineering AG, Wald, Switzerland) was sparged with N_2 , and potato starch was used as substrate (8 g/liter).

E. coli XL1 Blue was used as a host for the construction of pET9d derivatives. *E. coli* BL21(DE3) was used as an expression host. Both strains were grown in Luria Bertani medium with kanamycin (50 μg/ml) in a rotary shaker at 37 °C.

Preparation of cell-free extract from P. furiosus

P. furiosus cells from a 200-liter culture were harvested by continuous centrifugation (Sharples, Rueil, France) and stored at -20 °C until used. Cell-free extract was prepared by suspending cells in 2 volumes (w/v) of 50 mM Tris/HCl buffer, pH 7.8, and treatment in a French press at 100 megapascals. Cell debris was removed by centrifugation for 1 h at100,000 × *g* at 10 °C. The supernatant was used for purification of the phosphofructokinase.

Purification of the phosphofructokinase from P. furiosus cell-free extract

The phosphofructokinase was partially purified from cell-free extract of *P. furiosus*. All purification steps were done without protection against oxygen. To prevent microbial contamination, all buffers contained 0.02% sodium azide. Phosphofructokinase activity was recovered from cell-free extract following precipitation between 40 and 60% ammonium sulfate saturation. The subsequent purification included chromatography on phenyl-Superose HR 5/5, Q-Sepharose fast flow, hydroxyapatite Bio-Gel HT, mono Q HR 5/5, and Superdex 200 prep grade gel filtration. Alternatively, cell-free extract was applied to a dye affinity chromatography system as described before (11).

Cloning of the phosphofructokinase gene

The previously obtained N-terminal amino acid sequence of the ADP-dependent glucokinase from *P. furiosus*, partially published as MT*X*E*X*LYKN(I/A), where *X* = ambiguous residue (4), was used for BLAST search of the *P. furiosus* data base (http://www.genome.utah.edu). After exchanging the ambiguous residues with several possible amino acids, a putative glucokinase gene was identified. Using the sequence of this gene, another open reading frame was identified by nucleotide sequence similarity in the *P. furiosus* data base. The following primer set was designed

to amplify this open reading frame by polymerase chain reaction: BG447 (59-GCGCGTCATGATAGATGAAGTCAGAGAGCTCG, sense) and BG448 (59-GCGCGGGAT-CCTTACTGATGCCTTCTTAGGAGGGA, antisense), with *Bsp*HI and *Bam*HI restriction sites in bold.

The 100-μl polymerase chain reaction mixture contained 100 ng of *P. furiosus* DNA, isolated as described before (12), 100 ng each of primer BG447 and BG448, 0.2 mM dNTPs, *Pfu* polymerase buffer, and 5 units of *Pfu* DNA polymerase and was subjected to 35 cycles of amplification (1 min at 94 °C, 45 sec at 60 °C, and 3 min 30 sec at 72 °C) on a DNA Thermal Cycler (Perkin-Elmer Cetus). The polymerase chain reaction product was digested (*Bsp*HI/*Bam*HI) and cloned into an *Nco*I/*Bam*HI-digested pET9d vector, resulting in pLUW572, which was transformed into *E. coli* XL1 Blue and BL21(DE3). Sequence analysis on pLUW572 was done by the dideoxynucleotide chain termination method with a Li-Cor automatic sequencing system (model 4000L). Sequencing data were analyzed using the computer program DNASTAR.

Overexpression of the phosphofructokinase gene in E. coli

An overnight culture of *E. coli* BL21(DE3) containing pLUW572 was used as a 1% inoculum in 1 liter of Luria Bertani medium with 50 μg/ml kanamycin. After growth for 16 h at 37 °C, cells were harvested by centrifugation (2200 × *g* for 20 min) and resuspended in 10 ml of 20 mM Tris/HCl buffer, pH 8.5. The suspension was passed twice through a French press (100 megapascals), and cell debris was removed by centrifugation (10,000 × *g* for 20 min). The resulting supernatant was used for purification of the recombinant phosphofructokinase.

Purification of the recombinant phosphofructokinase

The *E. coli* cell-free extract was heated for 30 min at 80 °C, and precipitated proteins were removed by centrifugation. The supernatant was filtered through a 0.45-μm filter and loaded onto a Q-Sepharose column that was equilibrated with 20 mM Tris/HCl buffer, pH 8.5. Bound proteins were eluted by a linear gradient of NaCl (0 to 1 M in Tris/HCl buffer). Active fractions were pooled and desalted with 20 mM Tris/HCl buffer, pH 8.5, using a Centricon filter with a 30-kDa cutoff.

Protein concentration and purity

Protein concentrations were determined with Coomassie Brilliant Blue G250 as described before (13) using bovine serum albumin as a standard. The purity of the enzyme was checked by SDS-PAGE as described before (10). Protein samples for SDS-PAGE were heated for 5 min at 100 °C in an equal volume of sample buffer (0.1 M citrate-phosphate buffer, 5% SDS, 0.9% 2-mercaptoethanol, 20% glycerol, pH 6.8).

Determination of enzyme activity

ADP-dependent phosphofructokinase activity was measured aerobically in stoppered 1-ml quartz cuvettes at 50 °C as described before (3). The assay mixture contained 100 mM MES buffer, pH 6.5, 10 mM $MgCl_2$, 10 mM fructose 6-phosphate, 0.2 mM NADH, 2.5 mM ADP, 3.9 units of glycerol 3-phosphate dehydrogenase, 11 units of triosephosphate isomerase, 0.23 units of aldolase, and 5–25 µl of enzyme preparation. The absorbance of NADH was followed at 340 nm (ε = 6.18 $mM^{-1}cm^{-1}$). Care was taken that the auxiliary enzymes were never limiting. Specific enzyme activities were calculated from initial linear rates and expressed in units/mg of protein. 1 unit was defined as that amount of enzyme required to convert 1 µmol of fructose 6-phosphate/min. The activity of the enzyme in the reverse direction was measured in an assay containing 100 mM MES buffer, pH 6.5, 12.5 mM fructose 1,6-bisphosphate, 2.5 mM AMP, 0.5 mM NADP, 0.35 units of glucose-6-phosphate dehydrogenase, 1.4 units of phosphoglucose isomerase, and 5–25 µl of enzyme preparation. The absorbance of NADPH was followed at 340 nm (ε = 6.18 $mM^{-1}cm^{-1}$).

Molecular mass determination

The molecular mass of the partially purified phosphofructokinase from *P. furiosus* cell-free extract was determined on a Superdex 200 gel filtration column using 100 mM Tris/HCl buffer, pH 7.8, with 150 mM NaCl. The column was calibrated using the following standard proteins: ribonuclease A (13.7 kDa), chymotrypsinogen A (25 kDa), ovalbumin (43 kDa), bovine serum albumin (67 kDa), aldolase (158 kDa), and catalase (232 kDa).

Molecular mass determination of the purified recombinant phosphofructokinase was done by running PAGE gels at various acrylamide percentages (5, 6, 7, 8, 9, 10, 11, and 12%) as described before (14). The following molecular mass standards were used: lactalbumin (14.2 kDa), carbonic anhydrase (29 kDa), chicken egg albumin (45 kDa), bovine serum albumin monomer and dimer (66 and 132 kDa), and urease trimer and hexamer (272 and 545 kDa).

The subunit molecular mass of the purified recombinant protein was determined by SDS-PAGE, using a molecular mass standard mix of carbonic anhydrase (31.0 kDa), ovalbumin (45.0 kDa), serum albumin (66.2 kDa), and phosphorylase *b* (97.4 kDa).

pH optimum

The pH optimum of the phosphofructokinase was determined at 50 °C in 200 mM Tris/maleate buffer over the pH range 5.0 –8.0. Buffer pH values were adjusted at this temperature. Care was taken that the auxiliary enzymes were not limiting at the various pH values.

Substrate specificity

As possible phosphoryl group donors, ATP, GDP, GTP, pyrophosphate, phosphoenolpyruvate, acetylphosphate, tripolyphosphate, trimetaphosphate (each 2.5 mM), and polyphosphate (sodium phosphate glass type 35, 0.25 mg/ml) were used in the activity assay instead of ADP. The divalent cation requirement was tested by adding 10 mM $MnCl_2$, $CaCl_2$, $CoCl_2$ or $ZnCl_2$ instead of $MgCl_2$.

Kinetic parameters

Kinetic parameters were determined at 50 °C by varying the concentration of ADP (0.0125–5 mM) or fructose 6-phosphate (0.1–10 mM) in the assay mixture in the presence of 10 mM fructose 6-phosphate or 2.5 mM ADP, respectively. Data were analyzed by computer-aided direct fit to the Michaelis-Menten curve. Furthermore, the data were used to construct Hill plots (log $(V/V_{max} - V)$ *versus* log S).

Allosteric effectors

Regulation of phosphofructokinase activity by possible allosteric modulators was investigated by adding adenine nucleotides (ATP, ADP, or AMP; 2, 5, and 10 mM), metabolites (glucose, pyruvate, phosphoenolpyruvate, or citrate; 5 mM) or fructose 2,6-bisphosphate (0.1 and 1 mM) to the assay mixture. Furthermore, the effect of KCl and NaCl (30, 150 and 500 mM) on the enzyme activity was tested.

Results

Purification of the phosphofructokinase from P. furiosus cell-free extract

Cell-free extracts of *P. furiosus* showed a phosphofructokinase activity of 0.038 units/mg. However, despite the use of various chromatographic techniques, we were unable to obtain a highly purified enzyme, because it tended to stick to other proteins, resulting in similar band patterns upon PAGE after each purification step. When applied to a hydrophobic interaction column, phosphofructokinase activity was completely lost. Moreover, the use of dye affinity chromatography was not successful; although the phosphofructokinase did bind to a number of the tested dye ligands, it could not be eluted specifically with ADP. Aspecific elution with NaCl did not result in loss of contaminating proteins. Consequently, following chromatography on five different columns, the enzyme was purified 80-fold to a specific activity of 3 units/mg but still contained several contaminating proteins (Fig. 3.1).

Cloning of the phosphofructokinase gene

Using the previously obtained N-terminal amino acid sequence of the ADP-dependent glucokinase (4), a putative glucokinase gene was identified in the *P. furiosus* genome sequence. Expression of the gene in *E. coli* resulted in an ADP-dependent glucokinase activity of 20 units/mg in cell-free extracts at 50 °C, confirming that the gene indeed encoded the glucokinase (C. Verhees, in prep.). When the glucokinase gene, designated *glkA*, was used to search the *P. furiosus* genome, highest homology (25.7% nucleotide identity) was found with a 1365-base pair open reading frame predicted to encode a 455-amino acid protein. It was considered that this open reading frame might encode the ADP-dependent phosphofructokinase, and therefore the open reading frame was amplified by polymerase chain reaction and cloned into pET9d, resulting in plasmid pLUW572. DNA sequence analysis of pLUW572 confirmed the successful and faultless cloning of the open reading frame into pET9d (not shown).

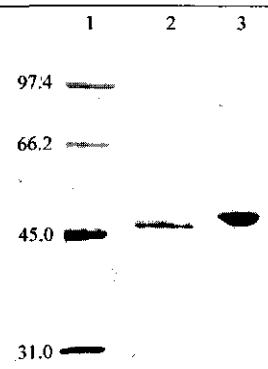

Figure 3.1 SDS-polyacrylamide gel electrophoresis of the phosphofructokinase from *P. furiosus*.
Lane 1 contained a set of marker proteins with their molecular mass indicated (kDa). *Lane 2* contained the partially purified phosphofructokinase from *P. furiosus* cell-free extract, and *lane 3* contained purified recombinant phosphofructokinase. Proteins were stained with Coomassie Brilliant Blue R250.

Overexpression of the phosphofructokinase gene in E. coli

SDS-PAGE analysis of a cell-free extract of *E. coli* BL21(DE3) harboring pLUW572 revealed an additional band of approximately 50 kDa, which corresponded with the calculated molecular mass (52.3 kDa) of the gene product. This band was absent in extracts of *E. coli* BL21(DE3) carrying the pET9d plasmid without insert. In a cell-free extract of *E. coli* BL21(DE3) harboring pLUW572, an ADP-dependent phosphofructokinase activity of 3.48 units/mg was measured at 50 °C, confirming that indeed the *P. furiosus* phosphofructokinase gene, designated *pfkA*, had been cloned and expressed. The enzyme could be produced for up to 5% of the total *E. coli* cell protein without inducing gene expression by adding isopropyl-1-thio-β-D-galactopyranoside. Therefore, no attempts were made to optimize the overexpression.

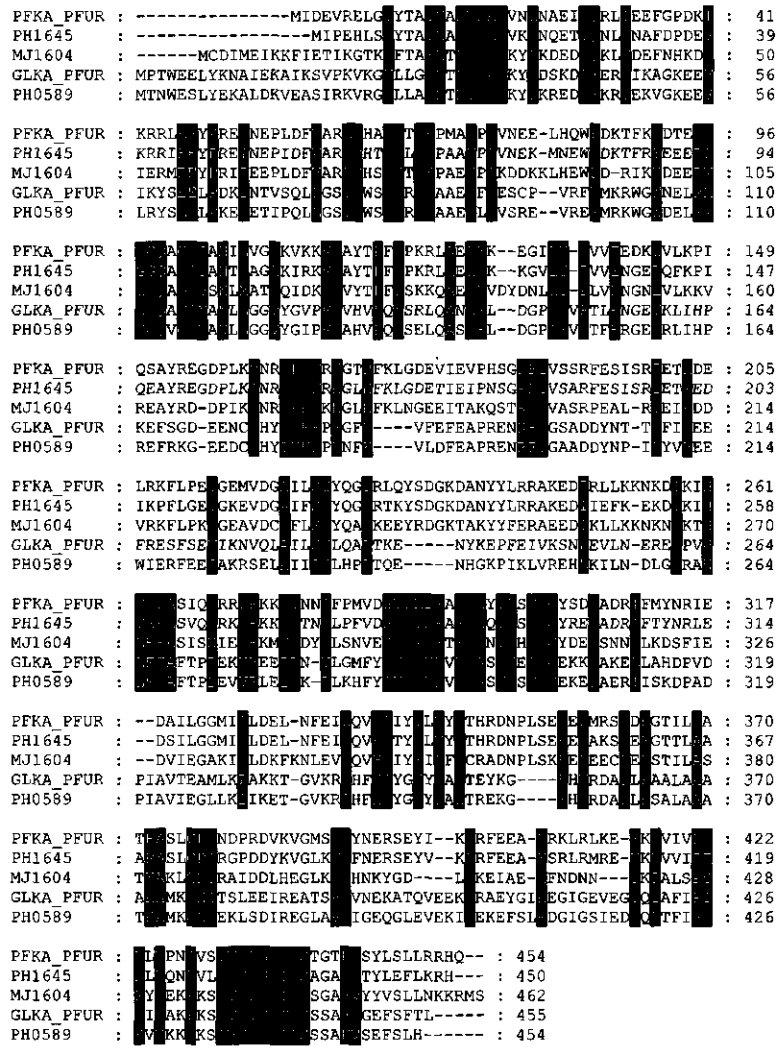

Figure 3.2 Multiple alignment of the deduced amino acid sequence of the *P. furiosus* ADP-dependent glucokinase and phosphofructokinase with the sequences of the hypothetical proteins from *P. horikoshii* and *M. jannaschii*, which were found to have high similarity with the phosphofructokinase. Gaps introduced for optimal alignment are marked by *hyphens*. Conserved regions are indicated as *black boxes*. *PFKA_PFUR*, ADP-dependent phosphofructokinase *P. furiosus* (accession number AF127909; Swiss-Prot); *PH1645*, putative ADP-dependent phosphofructokinase *P. horikoshii* (accession number 3258074; NCBI); *MJ1604*, putative ADP-dependent phosphofructokinase *M. jannaschii* (accession number 2128964; NCBI); *GLKA_PFUR*, ADP-dependent glucokinase *P. furiosus* (accession number AF127910; Swiss-Prot); *PH0589*, putative ADP-dependent glucokinase *P. horikoshii* (accession number 3256995; NCBI).

Primary sequence comparison

On an amino acid level, the identity between the glucokinase and phosphofructokinase from *P. furiosus* was 21.1%. Comparison of the deduced amino acid sequence of the phosphofructokinase with those of proteins present in the GenBank data base showed high similarity with two hypothetical proteins from *Pyrococcus horikoshii* (PH1645, 75.2% identity; PH0589, 23.1% identity). Cloning and expression of the corresponding genes demonstrated that the proteins are an ADP-dependent phosphofructokinase and an ADP-dependent glucokinase, respectively (data not shown). Furthermore, 48.6% identity was found with a hypothetical protein from *Methanococcus jannaschii* (MJ1604), which turned out to be an ADP-dependent phosphofructokinase (C. Verhees, in prep.). Multiple sequence alignment showed several conserved regions throughout the five proteins (Fig. 3.2). Comparison of the conserved regions with sequences present in the GenBank data base did not reveal additional similarities.

Purification and physical characterization of the recombinant phosphofructokinase

The recombinant phosphofructokinase was easily purified by a heat incubation and anion exchange chromatography to at least 95% homogeneity as judged by SDS-PAGE (Fig. 3.1). The specific activity of the purified protein was 88 units/mg at 50 °C. On SDS-PAGE, the purified recombinant protein did not appear at the same height as the most abundant band in the partially purified *P. furiosus* fraction.

However, because the phosphofructokinase activity of the partially purified *P. furiosus* cell-free extract is 3 units/mg, the enzyme represents only 3% of the total protein in the extract and can therefore not be most dominant band in *lane 2* of the SDS-PAGE gel.

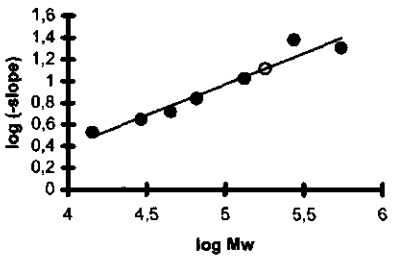

Figure 3.3 Calibration curve of molecular weight determination of the recombinant phosphofructokinase by native polyacrylamide gel electrophoresis. For each molecular weight marker protein, independent logarithmical plots were made of the relative mobility (R_f) against the acrylamide percentage of the gels. The slopes of these lines were plotted against the molecular weight of the marker proteins, depicted as *filled circles*. The slope of the phosphofructokinase was depicted as an *open circle*.

SDS-PAGE of the purified recombinant phosphofructokinase gave a single band at 52 kDa (Fig. 3.1). The native molecular mass of the partially purified phosphofructokinase from *P. furiosus* cell-free extract, as determined by gel filtration chromatography, was approximately 180 kDa. This is in good agreement with the molecular mass determination of the purified recombinant phosphofructokinase. A native molecular mass of the phosphofructokinase of 179 kDa was calculated from the calibration curve (Fig. 3.3), suggesting that the phosphofructokinase is a homotetramer. The phosphofructokinase showed activity between pH 5.5 and 7.0, with an optimum at pH 6.5 (data not shown).

Substrate specificity of the recombinant phosphofructokinase

The purified phosphofructokinase only showed activity in the forward direction. The enzyme showed highest activity with ADP as a phosphoryl group donor, which could be replaced by GDP, ATP, and GTP to a limited extent (Table 3.1). Divalent cations were required for activity of the enzyme, as shown by complete lack of activity in the presence of EDTA. Phosphofructokinase activity was highest in the presence of $MgCl_2$, followed by $CoCl_2$ (Table 3.1). The partially purified enzyme from *P. furiosus* cell-free extract showed the same substrate specificity pattern (data not shown).

Table 3.1 Substrate specificity and cation dependence of the ADP-dependent phosphofructokinase from *P. furiosus*.

Phosphoryl group donor	Relative activity	Divalent cation	Relative activity
	%		%
ADP	100	Mg^{2+}	100
GDP	28	Co^{2+}	81
ATP	<10	Mn^{2+}	43
GTP	<6	Ca^{2+}	8
Phosphoenolpyruvate	ND[a]	Zn^{2+}	ND
Pyrophosphate	ND		
Tripolyphosphate	ND		
Acetylphosphate	ND		
Trimetaphosphate	ND		
Polyphosphate	ND		

Enzyme assays were done at 50 °C as described under "Experimental Procedures." 100% activity corresponds to a specific activity of 88 units/mg.

[a]ND, not detectable.

Kinetic parameters of the recombinant phosphofructokinase

The purified phosphofructokinase showed Michaelis-Menten kinetics at 50 °C, with the following constants that were determined according to direct fit: K_m values of 2.3 ± 0.3 and 0.11 ± 0.01 mM for fructose 6-phosphate and ADP, respectively, and V_{max} values of 194 ± 13 and 150 ± 5 units/mg for fructose 6-phosphate and ADP, respectively. K_m values determined for the partially purified enzyme from *P. furiosus* cell-free extracts were in the same order of magnitude.

Furthermore, Hill coefficients of 1.1 (fructose 6-phosphate) and 0.95 (ADP) were determined, indicative of noncooperative binding of the substrates to each subunit of the tetrameric enzyme.

Allosteric effectors of the recombinant phosphofructokinase

The addition of glucose, pyruvate, phosphoenolpyruvate, citrate, or fructose 2,6-bisphosphate did not show any effect on the phosphofructokinase activity. Both NaCl and KCl had a negative effect on the phosphofructokinase activity (42 and 43% activity in 300 mM NaCl and KCl, respectively).

Furthermore, the phosphofructokinase activity was negatively affected by the addition of ATP or AMP to the assay mixture. Because subsequent addition of $MgCl_2$ did not restore activity, the negative effect was not because of binding of Mg^{2+} to the ATP or AMP, resulting in lower availability of the ions for the substrate ADP. The addition of 5 mM ATP or AMP resulted in an increase in K_m values for ADP from 0.11 to 0.34 ± 0.02 or 0.41 ± 0.03 mM, respectively, whereas the V_{max} did not change (Fig. 3.4). This indicates competitive inhibition of the phosphofructokinase by ATP and AMP. Apparently, the phosphofructokinase is not allosterically regulated by ATP, AMP, or any of the other tested compounds.

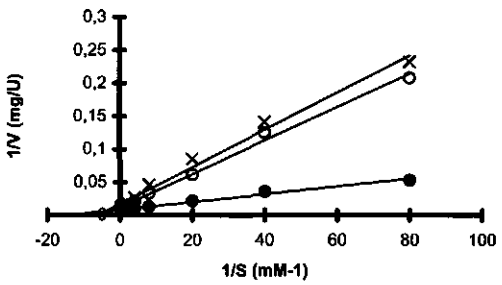

Figure 3.4 Lineweaver-Burk plot of recombinant *P. furiosus* phosphofructokinase with ADP as variable substrate, under normal assay conditions (•), in the presence of 5 mM ATP (o), or in the presence of 5 mM AMP (×).

Discussion

P. furiosus uses a modified Embden-Meyerhof pathway involving two novel-type kinases, *i.e.* an ADP-dependent glucokinase, which has previously been purified and characterized (4), and an ADP-dependent phosphofructokinase. In cell-free extracts of mass-cultured *P. furiosus* cells grown on starch, a phosphofructokinase activity of 0.038 units/mg was measured. Purification of the ADP-dependent phosphofructokinase from cell-free extracts of *P. furiosus* was hampered,

because the enzyme tended to stick to other proteins, and both dye affinity and hydrophobic interaction chromatography could not be used in the purification. However, an alternative approach became available following the identification of the *P. furiosus pfkA* gene encoding the phosphofructokinase, which was successfully overexpressed in *E. coli*.

The recombinant phosphofructokinase was purified from *E. coli* to 95% homogeneity in a two-step purification. The specific activity of the purified protein was 88 units/mg at 50 °C, which is approximately 2300-fold higher than the activity in crude cell-free extract of *P. furiosus* (0.038 units/mg). This suggests that the phosphofructokinase represents a very small fraction (0.043%) of the total *P. furiosus* cell protein, which is unexpected for a catalytic enzyme present in an important metabolic pathway. However, using the experimentally determined relationship between activity and temperature (Q_{10} = 2 (15)), it can be calculated that the specific activity at 100 °C would be 2816 units/mg. Furthermore, it has been calculated before that the specific activity of phosphofructokinase in cell-free extracts of *P. furiosus* is sufficiently high to sustain the glucose flux (3).

The ADP-dependent phosphofructokinase had a native molecular mass of 180 kDa and a subunit size of 52 kDa, in agreement with the deduced molecular mass of 52.3 kDa from the amino acid sequence. These data suggest that the phosphofructokinase has a tetrameric structure, which is most common for phosphofructokinases. ATP-dependent phosphofructokinases from bacteria and mammals are usually homotetramers with a subunit size of 33 and 85 kDa, respectively. Yeast phosphofructokinases show $\alpha_4\beta_4$ octameric structures with subunits of 112 and 118 kDa, whereas PP_i-dependent phospho-fructokinases have been described to be monomers (110 kDa), homodimers (subunits of 48–55 kDa), homotetramers (subunits of 45 kDa), or heterotetramers (subunits of 60 and 65 kDa) (16).

The reaction catalyzed by the phosphofructokinase was found to be irreversible. Therefore, *P. furiosus* needs a separate fructose-1,6-bisphosphate phosphatase to catalyze the conversion of fructose 1,6-bisphosphate to fructose 6-phosphate during gluconeogenesis. Indeed, this enzyme has been detected in cell-free extract with a specific activity of 0.026 units/mg at 75 °C (17). The irreversibility of the phosphofructokinase reaction has also been described for ATP-dependent phosphofructokinases, although PP_i-dependent phosphofructokinases catalyze reversible reactions (16).

Apparent K_m values of 2.3 and 0.11 mM were found for fructose 6-phosphate and ADP, respectively. These values were determined at 50 °C, which is much lower than the optimal growth temperature of *P. furiosus*. Because temperature can have a dramatic effect on K_m values (S. Kengen, unpublished), one has to realize that K_m values at the optimum growth temperature of 100 °C could differ considerably from the data obtained in this study. Apparent K_m values at 55 °C of the ADP-dependent phosphofructokinases from cell-free extracts of *Thermococcus celer* and *T.*

litoralis were 2.5 and 4 mM, respectively, for fructose 6-phosphate and 0.2 and 0.4 mM, respectively, for ADP (7). However, the possible temperature effect makes it difficult to compare kinetic values of microorganisms with different optimal growth temperatures (100 °C for *P. furiosus* and 85 °C for both *Thermococcus* strains). For the purified PP_i-dependent phosphofructokinase from *T. tenax* (optimal growth temperature 85 °C), much lower K_m values were found: 0.053 mM for fructose-6-phosphate and 0.023 mM for PP_i (9).

The ADP-dependent phosphofructokinase also showed activity with ATP, GTP, and GDP as phosphoryl group donors. In the case of ATP or GTP, however, the reaction product (ADP or GDP, respectively) is again an efficient phosphoryl group donor. Therefore, the relative activities with these compounds are probably overestimated. Furthermore, because of this fact, we were not able to determine kinetic values for ATP.

The phosphofructokinase was found to be inhibited by ATP and AMP through a competitive mechanism. In the case of ATP, this is not surprising, because ATP itself is a substrate and must therefore be able to bind to the catalytic site. In view of the role of phosphofructokinases in regulating the glycolytic pathway, it is surprising to see that ATP and AMP have the same (negative) effect on the activity of the phosphofructoki-nase. Allosterically regulated phosphofructokinases are usually inhibited by ATP but stimulated by AMP. ATP-dependent phosphofructokinases from *E. coli* and *Bacillus stearothermophilus* are allosterically activated by ADP and GDP and inhibited by phosphoenolpyruvate. Both yeast and mammalian phosphofructokinases are regulated by a large variety of effectors. Beside allosteric regulation by ATP and AMP, the enzymes are inhibited by citrate and activated by phosphate. Only mammalian enzymes are allosterically activated by fructose 1,6-bisphosphate. A very potent allosteric stimulator of eukaryotic phosphofructokinases is fructose 2,6-bisphosphate, which acts synergistically with AMP. This compound has been detected in most eukaryotes but never in prokaryotes (16). Apparently, the ADP-dependent phosphofructokinase from *P. furiosus* is not allosterically regulated at all, and therefore it can not act as the major control point of the glycolytic pathway. Alternatively, the glyceraldehyde-3-phosphate ferredoxin oxidoreductase could be an important enzyme in control of the glycolysis of *P. furiosus* (6). The PP_i-dependent phosphofructokinase from *T. tenax* is not allosterically controlled either, nor does it function as the major control point of the glycolytic pathway of this organism (9).

Hill plot analysis indicated that the phosphofructokinase did not cooperatively bind either of the substrates ADP and fructose 6-phosphate, in contrast to the ATP-dependent phospho-fructokinases from *E. coli* and *B. stearothermophilus*, which were found to show cooperative binding to fructose 6-phosphate but not to ATP (16).

The assumption that the open reading frame related to the *glkA*, found in the *P. furiosus* genome, might encode the ADP-dependent phosphofructokinase was based on the observation that

the N-terminal amino acid sequence of the glucokinase did not show any homology to known sugar kinases (4). Furthermore, in the *P. furiosus* genome data base, no sequence could be found that showed significant homology to either gluco-, hexo-, or phosphofructokinases. Because both enzymes are ADP-dependent kinases, they could have identical ADP and sugar binding sites and might therefore be homologous to each other.

This hypothesis was confirmed when the expressed open reading frame indeed turned out to encode the ADP-dependent phosphofructokinase. Primary sequence analysis of the deduced amino acid sequence of the glucokinase and the phosphofructokinase showed that the proteins are significantly homologous and share several conserved regions. The functionally important residues for substrate binding that have been described for ATP- and PP_i-dependent phosphofructokinases (9) did, however, not seem to be present in any of the sequences of the ADP-dependent kinases, suggesting they represent a novel group of kinases. Altogether, these findings suggest that the glucokinase and the phosphofructokinase from *P. furiosus* are phylogenetically related. Further research is focused on scientific evidence for this suggestion.

Acknowledgment

We thank George Ruijter (Wageningen Agricultural University, The Netherlands) for help with the dye affinity chromatography and Issei Yoshioka and Kiyofumi Fukufawa (Asahi-Kasei, Japan) for help in an early stage of the research project.

References

1. Kengen, S. W. M., Stams, A. J. M., and De Vos, W. M. (1996) *FEMS Microbiol. Rev.* 18, 119–137
2. De Vos, W. M., Kengen, S. W. M., Voorhorst, W. G. B., and Van der Oost, J. (1998) *Extremophiles* 2, 201–205
3. Kengen, S. W. M., De Bok, F. A. M., Van Loo, N.-D., Dijkema, C., Stams, A. J. M., and De Vos, W. M. (1994) *J. Biol. Chem.* 269, 17537–17541
4. Kengen, S. W. M., Tuininga, J. E., De Bok, F. A. M., Stams, A. J. M., and De Vos, W. M. (1995) *J. Biol. Chem.* 270, 30453–30457
5. Mukund, S., and Adams, M. W. W. (1995) *J. Biol. Chem.* 270, 8389–8392
6. Van der Oost, J., Schut, G., Kengen, S. W. M., Hagen, W. R., Thomm, M., and De Vos, W. M. (1998) *J. Biol. Chem.* 273, 28149–28154
7. Selig, M., Xavier, K. B., Santos, H., and Scho¨nheit, P. (1997) *Arch. Microbiol.* 167, 217–232
8. Phillips, N. F. B., Horn, P. J., and Wood, H. G. (1993) *Arch. Biochem. Biophys.* 300, 309–319
9. Siebers, B., Klenk, H.-P., and Hensel, R. (1998) *J. Bacteriol.* 180, 2137–2143
10. Kengen, S. W. M., Luesink, E. J., Stams, A. J. M., and Zehnder, A. J. B. (1993) *Eur. J. Biochem.* 213, 305–312
11. Hondmann, D. H. A., and Visser, J. (1990) *J. Chromatogr.* 510, 155–164
12. Sambrook, J., Fritsch, E. F., and Maniatis, T. (1989) *Molecular Cloning: A Laboratory Manual*, 2nd Ed., Cold Spring Harbor Laboratory, Cold Spring Harbor, NY

13. Bradford, M. M. (1976) *Anal. Biochem.* 72, 248–254

14. Hedrick, J. L., and Smith, A. J. (1968) *Arch. Biochem. Biophys.* 126, 155–164

15. Schäfer, T., and Schönheit, P. (1992) *Arch. Microbiol.* 158, 188–202

16. Fothergill-Gilmore, L. A., and Michels, P. A. M. (1993) *Prog. Biophys. Mol. Biol.* 59, 105–235

17. Schäfer, T., and Schönheit, P. (1993) *Arch. Microbiol.* 159, 354–363

Chapter 4

ADP-dependent phosphofructokinases in mesophilic and thermophilic methanogenic archaea

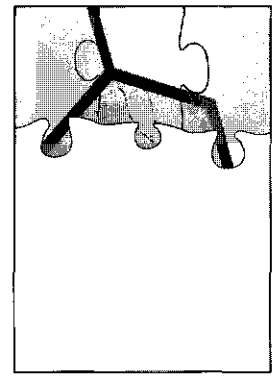

Corné H. Verhees*, Judith E. Tuininga*, Servé W.M. Kengen, Alfons J.M. Stams, John van der Oost and Willem M. de Vos

* both authors contributed equally

Journal of Bacteriology 183: 7145-7153 (2001)

Abstract

Phosphofructokinase (PFK) is a key enzyme of the glycolytic pathway in all domains of life. Two related PFKs, ATP- or PP_i-dependent, have been distinguished in bacteria, eucarya, as well as in some archaea. Hyperthermophilic archaea of the order *Thermococcales*, including *Pyrococcus* and *Thermococcus* spp., have recently been demonstrated to possess a unique ADP-dependent PFK (ADP-PFK) that appears to be phylogenetically distinct. Here, we report the presence of ADP-PFKs in glycogen-producing members of the orders *Methanococcales* and *Methanosarcinales*, including both mesophilic and thermophilic representatives. To verify the substrate specificities of the methanogenic kinases, the gene encoding the ADP-PFK from *Methanococcus jannaschii* was functionally expressed in *Escherichia coli*, and the produced enzyme was purified and characterized in detail. Compared to its counterparts from the two members of the order *Thermococcales*, the *M. jannaschii* ADP-PFK has an extremely low K_m for fructose 6-phosphate (9.6 μM), and it accepts both ADP and acetyl-phosphate as phosphoryl donor. Phylogenetic analysis of the ADP-PFK reveals it to be a key enzyme of the modified Embden-Meyerhof pathway of heterotrophic and chemolithoautotrophic archaea. Interestingly, uncharacterized homologs of this unusual kinase are present in several eucarya.

Introduction

The Embden-Meyerhof pathway is the most common route for the degradation of glucose. While several small variations in this glycolytic pathway are known, major modifications have been demonstrated in *Pyrococcus furiosus* and other hyperthermophilic archaea (4)(23). A combination of metabolic, biochemical and genetic approaches have established that the pyrococcal glycolysis differs from the Embden-Meyerhof pathway by incorporating new conversions, novel enzymes and unique control (9)(11)(27)(15)(28). First, the single-step conversion of glyceraldehyde-3-phosphate to 3-phospho-glycerate is catalyzed by a uniquely controlled glyceraldehyde-3-phosphate ferredoxin oxidoreductase (GAPOR) instead of the two-step reaction catalyzed by the conventional couple glyceraldehyde-3-phosphate dehydrogenase and phosphoglycerate kinase (28)(15). Second, instead of the classical ATP-dependent hexokinase, the pyrococcal pathway involves a novel ADP-dependent glucokinase (ADP-GLK) (11)(13). Third, a novel nonallosteric ADP-dependent phosphofructokinase (ADP-PFK) replaces the more common ATP-PFK (27).

The gene encoding an ADP-PFK was identified in the genome of *P. furiosus* and functionally expressed in *E. coli*, and the encoded protein was thoroughly characterized (27). Primary structure comparison revealed the ADP-PFK to be a member of a novel enzyme family that did not show homology to known PFKs, which are monophyletic and include both ATP- and pyrophosphate (PP_i)-dependent enzymes. However, the ADP-PFK appeared to have significant

similarity to the ADP-GLK from *P. furiosus*, suggesting that they belong to the same novel family of kinases. Recently, the crystal structure of the ADP-GLK from *Thermococcus litoralis* was solved. Unexpected structurally similarity was recognized with members of the ribokinase family (7).

Initial analysis of the first sequenced archaeal genome, that of the hyperthermophilic archaeon *Methanococcus (Methanocaldococcus) jannaschii* (29), suggested the presence of several glycolytic-enzyme-encoding genes, but indicated the absence of a gene encoding a classical PFK (2)(24). Hence, it was suggested that the PFK from *M. jannaschii* could be ADP-dependent and therefore undetectable in the sequence data (24). Indeed, an ortholog (MJ1604) with 48 % identity (on amino acid level) to the *P. furiosus* ADP-PFK was found to be encoded by the *M. jannaschii* genome (27). The presence of this hypothetical ADP-PFK in *M. jannaschii* suggests the presence of a modified Embden-Meyerhof pathway in methanogenic archaea as well. Previous studies on the genomic and enzyme levels indicated the presence of classical Embden-Meyerhof enzymes in bacteria, eucarya and archaea (3). However, no attention was given to enzymes involved in the modified Embden-Meyerhof pathway.

To obtain insight into the presence and function of ADP-PFKs in representatives from different phylogenetic lineages, we investigated their distribution on both the genomic and functional level. Moreover, the gene encoding the ADP-PFK from *M. jannaschii* was overexpressed in *E. coli* and the purified enzyme was thoroughly characterized. The results provided evidence for the presence of ADP-PFKs in both mesophilic and thermophilic archaea and led us to propose an evolutionary model.

Materials and methods

Organisms and growth conditions

All microorganisms were grown under H_2/CO_2 atmosphere in 50-ml and 250-ml medium, except that *Methanosaeta concilii* and *P. furiosus* were grown under N_2/CO_2 atmosphere. *P. furiosus* (100°C) (DSM 3638) *Methanococcus igneus* (80°C) (DSM 5666), *Methanococcus jannaschii* (80 °C) (DSM 2661), *Methanococcus maripaludis* (37°C) (DSM 2067), *Methanococcus thermolithotrophicus* (65°C) (DSM 2095), *Methanopyrus kandleri* (95°C) (DSM 6324), and *Methanobacterium thermoautotrophicum* Z-245 (65°C) (DSM 3720) were grown as described previously (10). *Methanosarcina mazei* (37°C) (DSM 2053) and *Methanosaeta concilii* (37°C) (DSM 3671) were grown as described previously (optimum temperatures given in parentheses) (26). *M. mazei* and *M. concilii* were supplemented with 50 mM methanol and 30 mM acetate, respectively. Nina Brunner (University of Essen, Germany) kindly provided cells of

Purification and characterization of the E. coli produced ADP-PFK from M. jannaschii

An overnight culture of *E. coli* BL21(DE3) harboring pLUW575 was inoculated (1%) into 1 liter of Luria-Bertani medium with 50 μg of kanamycin/ml. After growth for 16 h at 37°C, the cells were harvested by centrifugation (2,200 × *g* for 20 min) and resuspended in 10 ml of a 20 mM Tris/HCl buffer, pH 7.8. The suspension was passed twice through a French press (100 MPa), and cell debris was removed by centrifugation (10,000 × *g* for 20 min). The resulting supernatant was heat-treated for 30 min at 80°C, and precipitated proteins were removed by centrifugation.

The cell-free extract was filtered through a 0.45-μm-pore-size filter and applied to a Q-sepharose fast-flow column (Amersham Pharmacia Biotech) that was equilibrated with a 20 mM Tris/HCl buffer, pH 7.8 containing 1 mM CHAPS. ADP-PFK activity eluted at 0.3 M NaCl in a 125-ml gradient from 0 to 1 M NaCl. Active fractions were pooled and desalted by ultrafiltration using a 10 mM potassium phosphate buffer, pH 7.0. The desalted pool was applied to a hydroxyapatite CHT5-1 column (Bio-Rad) that was equilibrated with 10 mM potassium phosphate buffer. The enzyme eluted in a 75-ml linear gradient (10 to 500 mM potassium phosphate) at 250 mM potassium phosphate. Active fractions were pooled, the buffer was changed for a 25 mM Tris/HCl buffer, pH 7.8 containing 1 mM CHAPS by ultrafiltration and the pool was loaded onto a mono-Q HR 5/5 column (Amersham Pharmacia Biotech) that was equilibrated in the same buffer. The enzyme eluted from the column at 0.3 M NaCl in a 20-ml linear gradient from 0 to 1 M NaCl. Fractions showing ADP-PFK activity were pooled and concentrated 16-fold to a final volume of 460 μl. This concentrated pool was applied to a Superdex 200 HR 10/30 gelfiltration column (Amersham Pharmacia Biotech) that was equilibrated with a 100 mM Tris/HCl buffer, pH 7.8 containing 100 mM NaCl, from which the protein eluted after 15 ml. The purity of the ADP-PFK was confirmed by SDS-PAGE.

The purified enzyme was characterized by determining its specific activity, molecular mass, pH optimum, substrate specificity, kinetic parameters and allosteric effectors as described before (27).

Results

Genome analysis

To investigate the presence of genes that potentially encode enzymes involved in the modified Embden-Meyerhof pathway, we screened recent releases of complete and incomplete genome sequences of archaea and thermophilic bacteria (Table 4.1).

Orthologs of the novel GAPOR were identified in the genomes of all three *Pyrococcus* species (*P. furiosus*, *P. horikoshii* and *P. abyssi*) and in that of *M. jannaschii*. A classical NAD-dependent glyceraldehyde-3-phosphate dehydrogenase appeared to be present in all screened genomes. In *P. furiosus* this glyceraldehyde-3-phosphate dehydrogenase is involved in gluconeogenesis, whereas GAPOR functions in the glycolytic direction (28).

Orthologs of the ADP-GLK were identified only in the genomes of all three *Pyrococcus* species. Genes encoding classical ATP-dependent hexokinases were identified in *Halobacterium* sp. strain NRC-1, *Thermoplasma acidophilum*, *Aeropyrum pernix*, and the hyperthermophilic bacteria *Thermotoga maritima*, *Aquifex aeolicus*, and *Thermus thermophilus*.

Finally, ADP-PFK orthologs were identified in the three *Pyrococcus* genomes, the *M. jannaschii* genome, and the genome of *Methanosarcina mazei* Gö1. Remarkably, both an ATP-PFK and a PP_i-PFK ortholog were identified in the genome of *Thermotoga maritima*, whereas in the closely related *Aquifex aeolicus* only an ATP-PFK ortholog was identified.

Table 4.1 Enzymes of the classical and modified Embden-Meyerhof pathway encoded in the different genomes of archaea and (hyper)thermophilic bacteria.

GENOME	ATP-GLK	ADP-GLK	ATP-PFK	ADP-PFK	PP_i-PFK	GAPDH[b]	GAPOR
Pfu		AF127910		AF127909		PF1729232	AAC70892
Pho		PH0589		PH1645		PH1830	PH0457
Pab		PAB0967		PAB0213		PAB0257	PA1315
Mja				MJ1604		MJ1146	MJ1185
Mma				Present[c]		Present	
Afu						AF1732	
Mth						MT1009	
Hal	AAG20664					AAG18725	
Tac	TA0825					TA1103	
Sso						SSO0528	
Ape	APE2091		APE0012[d]			APE0171	
Tma	TM1469		TM0209		TM0289	TM0688	
Aae	AQ1496		AQ1708			AQ1065	
Tth	Present		Present			Present	

[a]Genome analyses were performed on the following organisms euryarchaea, Pfu, *Pyrococcus furiosus;* Pho, *Pyrococcus horikoshii*; Pab, *Pyrococcus abyssi*; Mja, *Methanococcus jannaschii*; Mma, *Methanosarcina mazei;* Afu, *Archaeoglobus fulgidus*; Mth, *Methanobacterium thermoautotrophicum*; Hal, *Halobacterium NRC-1;* Tac, *Thermoplasma acidophilum*. crenarchaea, Sso, *Sulfolobus solfataricus*; Ape, *Aeropyrum pernix*. bacteria, Tma, *Thermotoga maritima;* Aae, *Aquifex aeolicus*; Tth, *Thermus thermophilus*. [b]GAPDH, glyceraldehyde 3-phosphate dehydrogenase. [c]Present in the genome but not yet annotated. [d]APE0012 was detected using the N-terminal amino acid sequence of the ATP-PFK from *Desulfurococcus amylolyticus* (6) and was recently experimentally confirmed (21).

Interestingly, homologs of ADP-dependent sugar kinases (12 to 17% identity to the archaeal kinases) were identified in several eukaryotic genome sequences, *i.e.* those of *Drosophila melanogaster* (AAF49769), *Caenorhabditis elegans* (T32780), *Mus musculus* (BAB27619), and *Homo sapiens* (AAH06112) (query, ADP-GLK [AF127910]; blastP, E< 1e-07); no homologous

Overexpression of the M. jannaschii pfkC gene in E. coli

To gain insight into the substrate specificity of the methanogic ADP-PFK orthologs, we compared the properties of the enzyme of *M. jannaschii* to those of *P. furiosus* ADP-PFK. For this purpose, the *M. jannaschii pfkC* gene (MJ1604) was PCR-amplified and cloned into pET9d, resulting in plasmid pLUW575. DNA sequence analysis of pLUW575 confirmed that the cloned *pfkC* gene showed the expected sequence. SDS-PAGE analysis of a cell-free extract of *E.coli* BL21(DE3) harboring pLUW575 revealed an additional band of 51.5 kDa which corresponded to the calculated molecular mass (53.4 kDa) of the gene product (not shown). This band was absent in cell-free extracts of *E.coli* BL21(DE3) carrying the pET9d vector that also showed no ADP-PFK activity. In a cell-free extract of *E.coli* BL21(DE3) harboring pLUW575, an ADP-PFK activity of 0.8 U/mg was measured at 50°C, confirming that the cloned *M. jannaschii pfkC* gene indeed encoded an ADP-PFK. The enzyme could be produced up to 10% of total soluble cell protein after 16 h of cultivation at 37°C without inducing gene expression by adding isopropyl-1-thio-β-D-galactopyranoside.

Characteristics of the M. jannaschii ADP-PFK

The *E.coli*-produced *M. jannaschii* ADP-PFK was purified to homogeneity. The native molecular mass of the enzyme, as determined by native PAGE at various acrylamide percentages was approximately 50.1 kDa, indicating that the *M. jannaschii* ADP-PFK is a monomer (not shown).

Table 4.3 Phosphoryl group donor and cation dependence of the ADP-PFK from *M. jannaschii*[a].

phosphoryl group donor	divalent cation	specific activity (mU/mg)	relative activity (%)
ADP	Mg^{2+}	8200	100
GDP	Mg^{2+}	115	1.4
ATP	Mg^{2+}	24.6	0.3
GTP	Mg^{2+}	664	8.1
Acetyl-phosphate	Mg^{2+}	6806	83
Polyphosphate	Mg^{2+}	ND[b]	ND
Phosphoenolpyruvate	Mg^{2+}	ND	ND
Pyrophosphate	Mg^{2+}	ND	ND
ADP	Ca^{2+}	9840	120
ADP	Co^{2+}	6396	78
ADP	Mn^{2+}	4428	54
ADP	Zn^{2+}	ND	ND

[a]Standard enzyme assays were done at 50°C, except that phosphoryl group donors and cations were varied as described in the Materials and Methods.

[b]ND, not detectable, *i.e.* the activity was less than 0.3% of the activity under optimal conditions.

The purified enzyme had a specific activity of 8.2 U/mg at 50°C at the optimum pH of 6.5, only in the direction of phosphorylation. Apart from ADP, acetyl-phosphate could serve as an

efficient phosphoryl group donor to the enzyme (Table 4.3). Divalent cations were required for activity, as indicated by complete lack of activity in the presence of EDTA. ADP-PFK activity was highest in the presence of $CaCl_2$ followed by $MgCl_2$ (Table 4.3). Both KCl and NaCl had negative effects on the ADP-PFK activity (84 and 88 % activity in 500 mM KCl and NaCl, respectively). Furthermore, the enzyme activity was negatively affected by the addition of ATP or AMP to the assay mixture (53 and 24 % activity in 10 mM ATP and AMP, respectively). However, the addition of fructose 2,6-bisphosphate, pyruvate, glucose, phosphoenolpyruvate, or citrate to the assay mixture had no effect on the activity. The enzyme showed Michaelis-Menten kinetics at 50°C, with the following constants, which were determined according to a computer-aided direct fit using the Michaelis-Menten equation: apparent K_m values of 0.0096 ± 0.0007 mM and 0.49 ± 0.13 mM for fructose 6-phosphate and ADP, respectively, and apparent V_{max} values of 11.2 ± 0.3 and 9.59 ± 0.74 U/mg for fructose 6-phosphate and ADP, respectively. For acetyl-phosphate as phosphoryl group donor, an apparent K_m value of 11.9 ± 1.8 mM and an apparent V_{max} of 14.4 ± 1.0 U/mg at 50°C were determined. In a Hill plot, the kinetic data of fructose 6-phosphate, ADP and acetyl-phosphate showed noncooperative binding of the substrates (not shown).

Discussion

Following the discovery of ADP-PFK activity in *P. furiosus* (9) and characterization of this novel enzyme (27), ADP-PFK activity has been detected in various members of the order *Thermococcales* (18)(23). The presence of a glycolytic pathway in methanogens has recently been proposed based on (i) enzyme analyses of *M. maripaludis* (31), and (ii) analysis of the genome sequence of *M. jannaschii*, which revealed several glycolytic orthologs (2). However, no PFK gene was detected (24). Here, we demonstrate the functional presence of ADP-PFKs in methanogenic archaea, analyze their distribution and describe the unique catalytic properties of the purified enzyme from *M. jannaschii*.

The recent characterization of the amino acid sequence of the *P. furiosus* and *Thermococcus zilligii* ADP-PFK (27)(20), resulted in the identification of orthologs in the genomes of both chemolithoautotrophic (*M. jannaschii* and *M. mazei*) and heterotrophic (*P. abyssi, P. horikoshii*) Archaea (Table 4.1). These data already suggested that a modified Embden-Meyerhof pathway, as present in *P. furiosus*, might also be operational in methanogens. In addition, we determined PFK activity in all methanogens inverstigated, *i.e., M. jannaschii, M. thermolithotrophicus, M. igneus* and *M. maripaludis*, of the order *Methanococcales*, and *M. mazei* of the order *Methanosarcinales* (Table 4.2). Although ADP-PFK activity could de detected in *M. concilii* extracts, this activity was probably the result of the concerted action of ATP-PFK activity and high adenylate kinase activity (8). The high ADP-PFK activity (18 mU/mg) and relatively low ATP-PFK activity (3.8 mU/mg)

these kinases was lost in these organisms. Only the heterotrophic order *Thermococcales*, as well as the glycogen-degrading orders *Methanococcales* and *Methanosarcinales*, are found to contain a functional variant of the Embden-Meyerhof pathway, and, as such, benefit from harboring an ADP-PFK.

The observed presence of unique ADP-PFK activity and the corresponding genes in the phylogenetically closely related *Pyrococcus* spp. and *Methanococcus* spp., as well as the deeply branched *M. mazei*, suggests that the specific function of ADP-dependent sugar phosphorylation originated at least before the branching of *Thermococcales* and *Methanococcales* and that gene duplication in the order *Thermococcales* has led to two specific enzymes, *i.e,* ADP-PFK and ADP-GLK. The acquired sugar kinases and the gaining of specific glycosyl hydrolases and sugar transporters by *Pyrococcus* spp. (5) probably enabled these organisms to ferment sugars. The ADP-PFKs described here most likely function as a key step of a central metabolic pathway. Functional analysis of the eukaryal homologs will be the next step to gain more insight in the evolution of this enzyme family.

Addendum

While this manuscript was being evaluated, Labes *et al.* described an ADP-GLK and ADP-PFK activity in starch-degrading *Archaeoglobus fulgidus* strain 7324 (13). The corresponding genes have not yet been identified. In the genome sequence of type strain VC16 no genes encoding ADP-GLK or ADP-PFK could be identified (12).

Acknowledgments

This research was supported by the Earth and Life Sciences Foundation (ALW), which is subsidized by the Netherlands Organization for Scientific Research (NWO). The authors wish to thank Frank de Bok and Nina Brunner for providing cell-free extracts of methanogens. Erwin Zoetendal is gratefully acknowledged for constructing the phylogenetic tree. Finally, we wish to thank Andre Johann (Goettingen Genomics Laboratory) for providing the *M.mazei* PFK sequence.

References

1. **Bradford, M. M.** 1976. A rapid and sensitive method for the quantitation of microgram quantities of protein utilizing the principle of protein dye binding. Anal. Biochem. **72**:248-254.
2. **Bult, C. J., O. White, G. J. Olsen, L. Zhou, R. D. Fleischmann, G. G. Sutton, J. A. Blake, L. M. FitzGerald, R. A. Clayton, J. D. Gocayne, A. R. Kerlavage, B. A. Dougherty, J. F. Tomb, M. D. Adams, C. I. Reich, R. Overbeek, E. F. Kirkness, K. G. Weinstock, J. M. Merrick, A. Glodek, J. L. Scott, N. S.**

M. Geoghagen, and J. C. Venter. 1996. Complete genome sequence of the methanogenic archaeon, *Methanococcus jannaschii.* Science. **273:**1058-1073.

3. **Dandekar, T., S. Schuster, B. Snel, M. Huynen, and P. Bork.** 1999. Pathway alignment: application to the comparative analysis of glycolytic enzymes. Biochem. J. **343:**115-124.
4. **de Vos, W. M., S. W. M. Kengen, W. G. B. Voorhorst, and J. van der Oost.** 1998. Sugar utilization and its control in hyperthermophiles. Extremophiles. **2:**201-205.
5. **Ettema, T . J. G., J. van der Oost, and M. Huynen.** 2001. Modularity in the gain and loss of genes: applications for function prediction. TRENDS in Genetics. **17:** 485-487.
6. **Hansen, T., and P. Schönheit.** 2000. Purification and properties of the first-identified, archaeal, ATP-dependent 6-phosphofructokinase, an extremely thermophilic non-allosteric enzyme, from the hyperthermophile *Desulfurococcus amylolyticus*. Arch. Microbiol. **173:**103-109.
7. **Ito, S., S. Fushinobu, I. Yoshioka, S. Koga, H. Matsuzawa, and T. Wakagi.** 2001. Structural basis for the ADP-specificity of a novel glucokinase from a hyperthermophilic archaeon. Structure **9:** 205-214.
8. **Jetten, M. S. M., A. J. M. Stams, and A. J. B. Zehnder.** 1989. Isolation and characterization of acetyl-coenzyme A synthetase from *Methanothrix soehngenii.* J. Bacteriol. **171:**5430-5435.
9. **Kengen, S. W. M., F. A. M. de Bok, N-D. van Loo, C. Dijkema, A. J. M. Stams, and W. M. de Vos.** 1994. Evidence for the operation of a novel Embden-Meyerhof pathway that involves ADP-dependent kinases during sugar fermentation by *Pyrococcus furiosus.* J. Biol. Chem. **269:**17537-17541.
10. **Kengen, S. W. M., E. J. Luesink, A. J. M. Stams, and A. J. B. Zehnder.** 1993. Purification and characterization of an extremely thermostable beta-glucosidase from the hyperthermophilic archaeon *Pyrococcus furiosus*. Eur. J. Biochem. **213:**305-312.
11. **Kengen, S. W. M., J. E. Tuininga, F. A. M. de Bok, A. J. W. Stams, and W. M. de Vos.** 1995. Purification and characterization of a novel ADP-dependent glucokinase from the hyperthermophilic archaeon *Pyrococcus furiosus*. J. Biol. Chem. **270:**30453-30457.
12. **Klenk, H. P., R. A. Clayton, J. F. Tomb, O. White, K. E. Nelson, K. A. Ketchum, R. J. Dodson, M. Gwinn, E. K. Hickey, J. D. Peterson, D. L., Richardson, A. R. Kerlavage, D. E. Graham, N. C. Kyrpides, R. D. Fleischmann, J. Quackenbush, N. H. Lee, G. G. Sutton, S. Gill, E. F. Kirkness, B. A. Dougherty, K. McKenney, M. D. Adams, B. Loftus, J. C. Venter.** 1997. The complete genome of the hyperthermophilic, sulfate-reducing archaeon *Archaeoglobus fulgidus*. Nature. **390:** 364-370.
13. **Koga, S., I. Yoshioka, H. Sakuraba, M. Takahashi, S. Sakasegawa, S. Shimizu, and T. Ohshima.** 2000. Biochemical characterization, cloning, and sequencing of ADP-dependent (AMP-forming) glucokinase from two hyperthermophilic Archaea, *Pyrococcus furiosus* and *Thermococcus litoralis*. J. Biochem. **128:**1079-1085.
14. **Labes A., and P. Schönheit.** 2001. Sugar utilization in the hyperthermophilic, sulfate-reducing archaeon *Archaeoglobus fulgidus* strain 7324: starch degradation to acetate and CO2 via a modified Embden-Meyerhof pathway and acetyl-CoA synthetase (ADP-forming). Arch. Microbiol. DOI 10.1007/s002030100330
15. **Mukund, S., and M. W. W. Adams.** 1995. Glyceraldehyde-3-phosphate ferredoxin oxidoreductase, a novel tungsten-containing enzyme with a potential glycolytic role in the hyperthermophilic archaeon *Pyrococcus furiosus*. J. Biol. Chem. **270:**8389-8392.
16. **Murray, P. A., and S. H. Zinder.** 1984. Nitrogen fixation by a methanogenic bacterium. Nature. **312:**284-286.
17. **Pellerin, P., B. Gruson, G. Prensier, G. Albagnac, and P. Debiere.** 1987. Glycogen in *Methanotrix*. Arch. Microbiol.. **146:**377-381.

18. **Ronimus, R. S., J. Koning, and H. W. Morgan.** 1999. Purification and characterization of an ADP-dependent phosphofructokinase from *Thermococcus zilligii*. Extremophiles. **3:**121-129.

19. **Ronimus, R. S., H. W. Morgan, and Y. H. R. Ding.** 1999. Phosphofructokinase activities within the order *Spirochaetales* and the characterisation of the pyrophosphate-dependent phosphofructokinase from *Spirochaeta thermophila*. Arch. Microbiol. **172:**401-406.

20. **Ronimus, R. S., E. De Heus, and H. W. Morgan.** 2001. Sequencing, expression, characterisation and phylogeny of the ADP-dependent phosphofructokinase from the hyperthermophilic euryarchaeal *Thermococcus zilligii*. Biochim. Biophys. Acta. **1527:** 384-391.

21. **Ronimus, R. S., Y. Kawarabayasi, H. Kikuchi, and H. W. Morgan.** 2001. Cloning, expression and characterisation of a family B ATP-dependent phosphofructokinase activity from the hyperthermophilic crenarchaeon *Aeropyrum pernix*. FEMS Microbiol. Lett. **202:** 85-90.

22. **Sambrook, J., E. F. Fritsch, and T. Maniatis.** 1989. Molecular cloning: A laboratory Manual, 2nd ed. Cold Spring Harbor Laboratory, Cold Spring Harbor, NY.

23. **Selig, M., K. B. Xavier, H. Santos, and P. Schönheit.** 1997. Comparative analysis of Embden-Meyerhof and Entner-Doudoroff glycolytic pathways in hyperthermophilic archaea and the bacterium *Thermotoga*. Arch. Microbiol. **167:**217-232.

24. **Selkov, E., N. Maltsev, G. J. Olsen, R. Overbeek, and W. B. Whitman.** 1997. A reconstruction of the metabolism of *Methanococcus jannaschii* from sequence data. Gene. **197:**11-26.

25. **Siebers, B., H. P. Klenk, and R. Hensel.** 1998. PPi-dependent phosphofructokinase from *Thermoproteus tenax*, an archaeal descendant of an ancient line in phosphofructokinase evolution. J. Bacteriol. **180:**2137-2143.

26. **Stams, A. J. M., J. B. van Dijk, C. Dijkema, and C. M. Plugge.** 1993. Growth of syntrophic propionate-oxidizing bacteria with fumurate in the absence of methanogenic bacteria Appl. Environ. Microbiol. **59:**1114-1119.

27. **Tuininga, J. E., C. H. Verhees, J. van der Oost, S. W. M. Kengen, A. J. M. Stams, and W. M. de Vos.** 1999. Molecular and biochemical characterization of the ADP-dependent phosphofructokinase from the hyperthermophilic archaeon *Pyrococcus furiosus*. J. Biol. Chem. **274:**21023-21028.

28. **van der Oost, J., G. Schut, S. W. M. Kengen, W. R. Hagen, M. Thomm, and W. M. de Vos.** 1998. The ferredoxin-dependent conversion of glyceraldehyde-3-phosphate in the hyperthermophilic archaeon *Pyrococcus furiosus* represents a novel site of glycolytic regulation. J. Biol. Chem. **273:**28149-54.

29. **Whitman, W. B., D. R. Boone, and Y. Koga.** Bergey's Manual of Systematic Bacteriology, 2nd ed. Springer.

30. **Woese, C. R., O. Kandler, and M. L. Wheelis.** 1990. Towards a natural system for organisms. Proposal for the domains Archaea, Bacteria and Eucarya Proc. Natl. Acad. Sci. USA **87:**4576-4579.

31. **Yu, J. P., J. Ladapo, and W. B. Whitman.** 1994. Pathway of glycogen metabolism *in Methanococcus maripaludis*. J. Bacteriol. **176:**325-332.

Chapter 5

Biochemical adaptations of two sugar kinases from the hyperthermophilic archaeon *Pyrococcus furiosus*

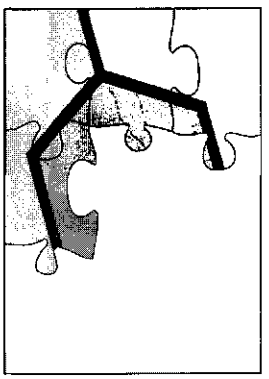

Corné H. Verhees, Denise G.M. Koot, Thijs J.G. Ettema, Cor Dijkema, Willem M. de Vos and John van der Oost

Biochemical Journal, in press (2002)

Abstract

The hyperthermophilic archaeon *Pyrococcus furiosus* possesses a modified Embden-Meyerhof pathway, including an unusual ADP-dependent glucokinase (ADP-GLK) and an ADP-dependent phosphofructokinase (ADP-PFK). We here report on the characterization of a *P. furiosus* galactokinase (GALK) and its comparison with the *P. furiosus* ADP-GLK. The pyrococcal genes encoding the ADP-GLK and the GALK were functionally expressed in *E. coli*, and the proteins were subsequently purified to homogeneity. Both enzymes are specific kinases with an optimal activity at approximately 90 °C. Biochemical characterization of these enzymes confirmed that the ADP-GLK is unable to use ATP as phosphoryl group donor but revealed that GALK is ATP-dependent and has an extremely high affinity for ATP. It is discussed that the unusual features of these two classes of kinases might reflect adaptations to a relatively low intracellular ATP concentration in the hyperthermophilic archaeon *P. furiosus*.

Introduction

During the catabolic conversion of carbohydrates sugar molecules are activated by specific kinases to a phosphorylated form (sugar + ATP → sugar-P + ADP). The universal energy carrier of biological systems and the preferred phosphoryl group donor in most kinase reactions is ATP. However, glucose can also be phosphorylated by polyphosphate or by phospho*enol*pyruvate as part of phosphotransferase systems (PTS), and fructose 6-phosphate by pyrophosphate (PP_i) instead of ATP (1,2,3). Sugar kinases of central catabolic pathways can be classified in at least four different monophyletic enzyme families (4) (http://www.scop.mrc-lmb.cam.ac.uk/scop/). Gluco/hexokinases generally belong to the hexokinase family. Phosphofructokinases belong to the phosphofructokinase (PFKA) family, or to the ribokinase (PFKB) family. Galactokinases are classified in the galactokinase family. Of the former three families crystal structures are available (5,6,7).

Two sugar kinases have recently been identified in the hyperthermophilic archaeon *Pyrococcus furiosus* that differ considerably from the canonical glycolytic kinases by being dependent on ADP rather than ATP (8). The ADP-dependent glucokinase (ADP-GLK) has been purified from *P. furiosus* cell extracts and the protein was biochemically characterized (9,10). The gene encoding the ADP-dependent phosphofructokinase (ADP-PFK) from *P. furiosus* was expressed in *E. coli* and the protein was studied in detail. Primary structure analyses revealed that the ADP-GLK and ADP-PFK belong to the same enzyme family (11). Recently, the crystal structure of the ADP-GLK from *Thermococcus litoralis* revealed a similar fold as the ATP-dependent ribokinase family (12).

An intriguing question is why *P. furiosus* contains ADP-dependent kinases (ADP-GLK, and ADP-PFK) in its central metabolic pathway. A plausible reason would be that the ADP-dependent

kinases would enable *P. furiosus* to recover more easily after periods of starvation. As soon as glucose becomes available, phosphorylation of glucose can proceed due to the high ADP level under these conditions. An alternative explanation would be the fact that ADP is more stable than ATP at elevated temperatures, with half-lifes at 90 °C of 750 and 115 min, respectively (13). However, several hyperthermophilic species with similar optimum growth temperatures (T-opt. ≥ 80 °C), such as *Thermotoga maritima* (T-opt. 80 °C) or *Desulfurococcus amylolyticus* (T-opt. 90 °C), are known to use ATP in the phosphorylation of sugars (14). Still, it can not be ruled out that the intracellular ATP concentration is relatively low in *P. furiosus*, either because of a distinct physiology, or because of the even more extreme optimum growth temperature (T-opt. 100 °C).

Recent genome analysis revealed that an ortholog of a galactokinase (GALK) gene is present in *P. furiosus* (http://www.utah.edu). The ATP-dependent GALK is a key enzyme in galactose metabolism in bacteria and eucarya (15), and has not been studied in archaea before. Here we describe that the *P. furiosus* GALK is ATP dependent, implying that ADP- and ATP-dependent sugar kinases co-exists in this hyperthermophilic archaeon. A comparison of the characteristics of the *E.coli*-produced kinases from *P. furiosus*, the ATP-dependent GALK and the ADP-GLK reveals distinct adaptations of sugar kinases to function optimally at extreme temperatures.

Experimental

Materials

ADP (monopotassium salt, less than 0.2% ATP), ATP (disodium salt), GDP (dilithium salt), glucose-6-phosphate dehydrogenase (D-glucose-6-phosphate: NADP oxidoreductase, EC 1.1.1.49; yeast), GTP (dilithium salt), phospho*enol*pyruvate (tricyclohexylammonium salt), lactate dehydrogenase (EC 1.1.1.27; pig heart), phosphoglucose isomerase (D-glucose-6-phosphate ketol-isomerase, EC 5.3.1.9; yeast), phosphomannose isomerase (D-mannose-6-phosphate ketol-isomerase, EC 5.3.1.8; yeast), and pyruvate kinase (EC 2.7.1.40; rabbit muscle), were obtained from Roche Molecular Biochemicals. CDP (sodium salt), D-galactose, 2-deoxy-D-glucose, kanamycin A (monosulfate, less than 5% kanamycin B), NADP (sodium salt), and NADH (disodium salt), were obtained from Sigma (Bornem, Belgium). D-glucose, D-fructose, D-glucosamine, and D-mannose were obtained from Merck (Darmstadt, Germany). These and all other chemicals were of analytical grade.

Organisms and growth conditions

P. furiosus (DSM 3638) was obtained from the German Collection of Microorganisms (DSM Braunschweig, Germany) and was routinely grown at 90 °C, as described before (16). *E.coli*

XL1 Blue (Stratagene) was used as a host for the construction of pET9d (Novagen) derivatives. *E.coli* BL21 (DE3) (Stratagene) was used as an expression host. Both strains were grown in Luria-Bertani medium with kanamycin (50 μg/ml) in a rotary shaker at 37 °C.

Cloning of the sugar kinase genes in E. coli

Based on the N-terminal sequence (9) the putative ADP-GLK gene was identified as described before (11). The following primer set was designed to amplify this open reading frame by polymerase chain reaction: BG451 (GCGCGCCATGGCACCCACTTGGGAGGAGCTTTA, sense) and BG452 (GCGCGGGATCCTTAGAGAGTGAATGAAAACTCACCAA, antisense), with *Nco*I and *Bam*HI restriction sites in bold.

An ortholog of a classical GALK was identified in the *P. furiosus* genome database (http://www.genome.utah.edu). The N-terminus was based on the presence and proper spacing of the ribosomal binding site and annotation from the genome sequence. The following primer set was designed to amplify this open reading frame by polymerase chain reaction: BG376 (5'-GCGCGCCATGGCAAGTAAAATCACTGTAAAATCT, sense) and BG377 (5'-GCGCGG-GATCCTCATACTCCCACACCATCGGAG, antisense), with *Nco*I and *Bam*HI restriction sites in bold.

The procedure for cloning of the GALK and ADP-GLK gene was essentially the same. Chromosomal DNA was isolated from *P. furiosus* as described by Sambrook *et al.* (17). The PCR mixture (100 μl) contained: 100 ng *P. furiosus* DNA, 100 ng of each primer, 0.2 mM dNTP's, *Pfu* polymerase buffer, 5 U *Pfu* DNA polymerase. The mixture was subjected to 35 cycles of amplification (1'at 94°C, 45"at 60°C and 3'30" at 72°C) on a DNA Thermal Cycler (PerkinElmer Life Sciences). The PCR products were digested with *Nco*I/*Bam*HI, and cloned into a *Nco*I/*Bam*HI-digested pET9d vector, resulting in pLUW570 and pLUW574, respectively. Sequence analyses on pLUW570 and pLUW574 was done by the dideoxynucleotide chain termination method with a Li-Cor automatic sequence system (model 4000L). Sequence data were analyzed using the computer program DNASTAR.

Overexpression of the sugar kinase genes in E.coli

An overnight culture of *E. coli* BL21(DE3) containing pLUW570 or pLUW574 was used as a 1% inoculum in 1 liter of Luria-Bertani medium with 50 μg/ml kanamycin. After growth for 16 h at 37 °C, cells were harvested by centrifugation (2200 × *g* for 20 min) and resuspended in 10 ml of 50 mM Tris/HCl buffer, pH 7.8. The suspension was passed twice through a French press (100 megapascals), and cell debris was removed by centrifugation (10,000 × *g* for 20 min). The resulting supernatant was used for purification of the *E.coli*-produced sugar kinases.

Purification of the sugar kinases

For the purification of the *E. coli*-produced GALK and ADP-GLK, the *E. coli* cell-free extracts were heated for 30 min at 70 °C, and precipitated proteins were removed by centrifugation. The supernatant containing GALK and ADP-GLK was filtered through a 0.45-µm filter and loaded onto a Q-Sepharose fast flow column (25 ml, Amersham Pharmacia Biotech) that was equilibrated with 50 mM Tris/HCl buffer, pH 8.5, and 50 mM Tris/HCl buffer, pH 7.8, respectively. Bound proteins were eluted by a linear gradient of NaCl (0 to 1 M in Tris/HCl buffer). The GALK and ADP-GLK eluted at 0.40 M NaCl and 0.27 M NaCl, respectively. Active fractions were pooled and desalted with 50 mM Tris/HCl buffer, pH 7.8, using a Centricon filter with a 10-kDa cutoff. The concentrated extracts were further purified on a Superdex 200 HR 10/30 gel filtration column (24 ml, Amersham Pharmacia Biotech), equilibrated with 50 mM Tris-HCl, pH 7.8, 100 mM NaCl. The *E. coli*-produced GALK and ADP-GLK eluted at 15.4 ml and 12.8 ml, respectively. The purified enzymes were desalted in 50 mM Tris/HCl, pH 7.8 as described above. To prevent microbial contamination, all the protein samples contained 0.02% sodium azide, and were stored at 4°C.

Determination of standard enzyme activity

GALK activity was determined by measuring the oxidation of NADH in a coupled assay with pyruvate kinase from rabbit muscle and lactate dehydrogenase from pig heart. One unit was defined as the amount of enzyme required to convert 1 µmol of galactose per min. The standard assay was performed at 50 °C. At this temperature the rabbit and pig enzymes remained active, and the *P. furiosus* enzyme was sufficiently active to measure its activity. The standard assay mixture contained 100 mM Tris/HCl, pH 7.8, 2 mM EDTA, 10 mM $MgCl_2$, 0.2 mM NADH, 15 mM D-galactose, 5 mM ATP, 2 mM phospho*enol*pyruvate, 2 U pyruvate kinase, 4 U lactate dehydrogenase, and 5-50 µl of enzyme preparation. The absorbance of NADH was followed at 340 nm (ε = 6.3 $mM^{-1}cm^{-1}$). The auxiliary enzymes were present in excess, to ensure that the detected NADH oxidation corresponded to the GALK activity.

ADP-GLK activity was determined by measuring the formation of NADPH in a coupled assay with yeast glucose-6-phosphate dehydrogenase. One unit was defined as the amount of enzyme required to convert 1 µmol of glucose per min. The assay was performed at 50 °C. At this temperature the yeast enzyme remained active, and the *P. furiosus* enzyme was sufficiently active to measure its activity. The standard assay mixture contained 100 mM Tris/HCl, pH 7.8, 2 mM EDTA, 10 mM $MgCl_2$, 0.5 mM NADP, 15 mM glucose, 2 mM ADP, 0.35 units of D-glucose-6-phosphate dehydrogenase, and 5-50 µl of enzyme preparation. The production of NADPH was measured at 340 nm (ε = 6.3 $mM^{-1}cm^{-1}$). The auxiliary enzyme was present in excess, to ensure that the detected NADPH formation corresponded to the ADP-GLK activity.

Protein concentrations were determined with Coomassie Brilliant Blue G-250 as previously described (18).

Substrate specificity

For the determination of the substrate specificity of GALK, the standard enzyme assay was used. Instead of D-galactose either D-glucose, D-fructose, D-mannose, 2-deoxy-D-glucose or D-glucosamine was added as substrate. The divalent cation requirement was tested by adding 10 mM of $MnCl_2$, $CaCl_2$, $ZnCl_2$, or $CoCl_2$ instead of $MgCl_2$ to the standard assay mixture. Phosphoryl group donor specificity of GALK was determined by high-performance liquid chromatography. The assay mixture contained 100 mM Tris/HCl buffer, pH 7.8, 2 mM EDTA, 10 mM $MgCl_2$, 10 mM galactose and 10 mM of phosphoryl group donor (either ATP, ADP, GTP, PEP, or PP_i). After incubation for an appropriate time at 50 °C, the reaction was stopped on ice and analyzed by high-performance liquid chromatography. To test whether GALK phosphorylates galactose into galactose-1-phosphate, ^{13}C-/^{31}P-NMR spectra of the conversion of [1-^{13}C]-galactose by the purified GALK were recorded at 76.47 MHz (^{13}C) and 125.5 MHz (^{31}P) on an AMX300 spectrometer (Bruker, Germany) using a 10 mm (outer diameter) probe. The incubation was continued for 12 min at 80 °C, whereas 1 min spectra were recorded. The presence of α-galactose-1-phosphate was confirmed by spiking with commercial α-galactose-1-phosphate (Sigma)

The use of 2-deoxy-D-glucose and D-galactose as possible substrates for the ADP-GLK was tested using the standard enzyme assay because the auxiliary enzyme from yeast is also able to use galactose-6-phosphate. For the determination of D-fructose as a possible substrate, phosphoglucose isomerase (1.4 units) was added to the standard assay mixture. D-mannose was tested by adding phosphomannose isomerase (0.6 units) and phosphoglucose isomerase (1.4 units) as auxiliary enzymes. All sugars were tested at a concentration of 15 mM. As possible phosphoryl group donor, ATP, GDP, CDP, PEP, or PP_i (each 2 mM) were used instead of ADP. The divalent cation requirement was tested by adding 10 mM of $MnCl_2$, $CaCl_2$, $ZnCl_2$, or $CoCl_2$ instead of $MgCl_2$ to the standard assay mixture.

Molecular mass determination

The molecular mass of GALK and ADP-GLK were determined on a Superdex 200 HR 10/30 gel filtration column (24 ml, Amersham Pharmacia Biotech) using 50 mM Tris/HCl buffer, pH 7.8, with 100 mM NaCl. The column was calibrated using the following standard proteins: ribonuclease A (13.7 kDa), chymotrypsinogen A (25 kDa), ovalbumin (43 kDa), bovine serum albumin (67 kDa), aldolase (158 kDa), and catalase (232 kDa).

pH optimum

The pH optimum of GALK and ADP-GLK were determined in the standard enzyme assay at 50 °C in 200 mM Tris/maleate buffer over the pH range 3.9-8.4. Buffer pH values were adjusted at the temperature of incubation.

Temperature optimum

The effect of temperature on the activity of the sugar kinases was determined by incubating an appropriate amount of purified enzyme in 1-ml crimp-sealed vials containing 200 mM Tris/maleate buffer, pH 8.5, 20 mM $MgCl_2$, and 20 mM galactose and glucose, respectively. The vials were submerged in an oil bath at temperatures from 30 to 110 °C, preheated for 5 min, and the enzyme reaction was started by injecting 10 µl of 100 mM ATP and ADP, respectively. After 1, 3, 5 min, the reaction was stopped by putting the vials on ice, and the amount of product formed was determined spectrophotometrically at room temperature, by measuring the oxidation of NADH and the reduction of NADP in the standard enzyme assays for GALK and ADP-GLK, respectively. Corrections were made for the chemical conversion of ATP in the absence of GALK.

Kinetic parameters

Kinetic parameters of GALK were determined at 50 and 90 °C, in 100 mM MOPS, pH 7.0 (50 °C and 90 °C) by varying the concentration of ATP (0.0005-5 mM) or galactose (0.05-10 mM), in the presence of 5 mM galactose or 2 mM ATP, respectively. Kinetic parameters of ADP-GLK were determined at 50 and 90 °C in 200 mM Tris/maleate, pH 7.0 (50 °C and 90 °C), by varying the concentration of ADP (0.02–2 mM) or glucose (0.1-10 mM) in the presence of 15 mM glucose or 2 mM ADP, respectively. At 50 °C a continuous assay was used, whereas at 90 °C a discontinuous assay was used, as described under "Temperature optimum". Data were analyzed by computer-aided direct fit to the Michaelis-Menten curve (program Tablecurve).

Results and discussion

Overexpression and purification of the GALK and ADP-GLK

The open reading frames predicted to encode the *P. furiosus* GALK (1062 bp) and ADP-GLK (1371 bp), were PCR-amplified and cloned into pET9d, resulting in plasmids pLUW570 and pLUW574, respectively. DNA sequence analysis of pLUW570 and pLUW574 confirmed the cloning of the correct open reading frames into pET9d. SDS-PAGE analysis (not shown) of a heat-treated cell-free extract of *E.coli* BL21(DE3) harboring either pLUW570 or pLUW574 revealed an additional band of approximately 38 kDa and 51 kDa, respectively, which was in good agreement

with the calculated molecular mass of the gene product (39.4 kDa and 51.3 kDa). A heat-treated cell-free extract of *E.coli* BL21(DE3) harboring pLUW570 was found to contain a thermoactive ATP-dependent GALK activity of 0.7 units/mg, confirming the identity of the gene. In a heat-treated cell-free extract of *E.coli* BL21(DE3) harboring pLUW574, an ADP-GLK activity of 17.5 units/mg was measured, confirming that the gene indeed encoded an ADP-GLK. In extracts of *E.coli* BL21(DE3) carrying the pET9d vector without insert, the additional protein bands in SDS-PAGE analyses were absent and neither GALK nor ADP-GLK activity was detected.

GALK and ADP-GLK could be produced up to 20% and 10% of total soluble cell protein, respectively, after growth for 16 h at 37 °C. Both enzymes were purified to apparent homogeneity (>95 %, not shown) by two successive chromatographic steps. The molecular mass of GALK and ADP-GLK was determined by gel filtration chromatography to be approximately 32 kDa and 89 kDa, respectively, suggesting GALK is a monomer and ADP-GLK is a dimer. The dimeric structure of the *E.coli*-produced ADP-GLK is in good agreement with that of the native ADP-GLK, which has a molecular mass of 93 kDa (9). Classical GALKs in general occur as monomers or dimers (19,20,21), which agrees well with the determined monomeric structure of the *P. furiosus* GALK.

Primary structure comparison and phylogeny

Orthologs of the *P. furiosus* GALK were identified in a wide range of bacteria and eucarya, with a high degree of identity (*E.coli*; 32% identity P06976 and Human; 31% identity NP_000145). No orthologs could be identified in any of the archaeal or hyperthermophilic bacterial genomes, except for *Pyrococcus horikoshii* (PH0369 putative GALK, 77% identity), *Thermotoga maritima* (TM1190 putative GALK, 41% identity), and *Thermotoga neapolitana* (putative GALK, 41% identity). Analysis of the primary structure of the *P. furiosus* GALK revealed the presence of all typical GALK motifs (Fig. 5.1). The presence of a GALK ortholog in both *P. furiosus* and *P. horikoshii*, and the absence of this gene in all other available archaeal genomes, including *Pyrococcus abyssi*, is an example of a gain of genetic information in these *Pyrococci*, probably the result of horizontal gene transfer (22).

The *P. furiosus* ADP-GLK is unrelated to classsical gluco/hexokinases and showed high similarity with ADP-GLKs and ADP-PFKs from several *Pyrococcus* species and from *Methanococcus jannaschii* (11). Recently, the functional presence of homologs has been identified in several methanogens, and homologs (with unidentified functions) have been identified in higher eukaryotes (23). In contrast to GALK, ADP-GLK is phylogenetically unrelated to its canonical counterparts, and presumably has evolved independently. The specific function of ADP-GLK (and ADP-PFK) might therefore have been invented in the archaea as an adaptation to function optimally under extreme conditions.

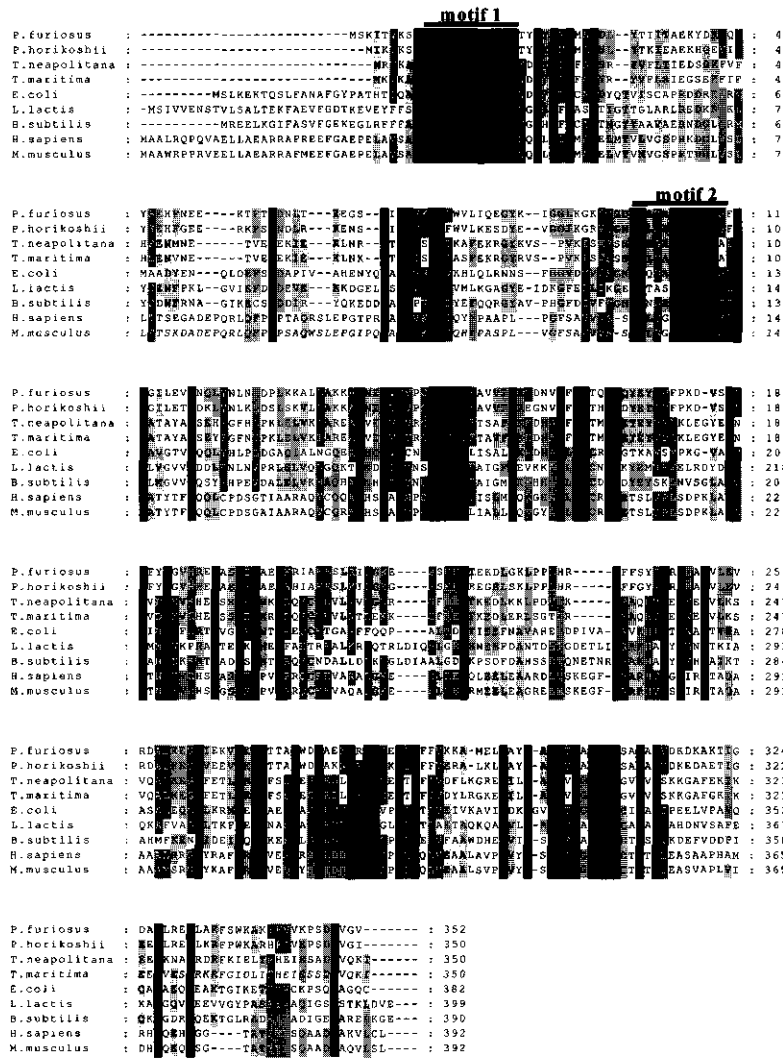

Figure 5.1 Multiple sequence alignment of the deduced amino acid sequence of the *P. furiosus* GALK with sequences of GALKs from bacteria and eucarya.

Sequences were deduced from the following accession numbers: *Pyrococcus furiosus* (AAG28454), *Pyrococcus horikoshii* PH0369 (NP_142343), *Thermotoga neapolitana* (O85253), *Thermotoga maritima* TM1190 (P56838), *Escherichia coli* (P06976), *Lactococcus lactis* (Q9R7D7), *Bacillus subtilis* (P39574), *Homo sapiens* (NP_000145), *Mus musculus* (AAF78226). Gaps introduced for optimal alignment are marked by *hyphens*. Completely conserved regions are indicated as *black boxes*. Highly conserved regions are *shaded grey*. Conserved motifs are indicated in *bars* above the alignment. Motif 1. G-R-x-N-[LIV]-I-G-[DE]-H-x-D-Y; GALK signature (PS00106). Motif 2. [LIVM]-[PK]-x-[GSTA]-x(0,1)-G-L-[GS]-S-S-[GSA]-[GSTAC]; GHMP kinases putative ATP-binding domain (PS00627).

Biochemical characteristics and physiology of GALK and ADP-GLK

Two distinct kinases, *i.e.* ATP-dependent and ADP-dependent, are potentially present in *P. furiosus* for galactose and glucose conversion, respectively. The presence of enzyme activities of GALK (0.001 units/mg)(C. Verhees, unpublished), ADP-GLK (0.4 units/mg) (9) and ADP-PFK (0.2 units/mg) (9) could be demonstrated in extracts of *P. furiosus* grown on starch. Moreover, the presence of both ADP-GLK and GALK transcripts has been established by RT-PCR and primer extension (C. Verhees, unpublished). As expected, ATP-dependent phosphorylation of glucose and ADP-dependent phosphorylation of galactose could not be detected in *P. furiosus* extracts.

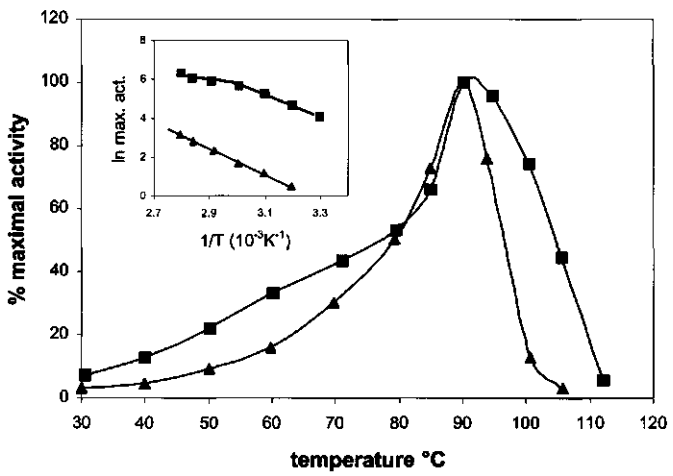

Figure 5.2 Dependence of GALK and ADP-GLK activity on temperature.

Activity was determined as described in Materials and Methods. 100% activity corresponds to 33.5 and 844 units/mg for GALK (▲) and ADP-GLK (■), respectively. *Inset,* Arrhenius plot indicating a break point at 60 °C for ADP-GLK.

The purified GALK was found to have a specific activity of 0.96 units/mg at 50 °C at its optimum pH of 5.0 in a Tris/maleate buffer, and retained >50% of its optimal activity between pH 4.5 and pH 8.5 (not shown). Classical GALKs from bacteria and eucarya generally have a more neutral or even alkalic optimum pH, *e.g. E. coli* pH 7.8 (24), *Saccharomyces cerevisiae* pH 8.3 (20), *Vicia faba* pH 7.3 (25). The *P. furiosus* GALK is the first archaeal and thermoactive GALK presently known, and showed maximal activity at approximately 90 °C (Fig. 5.2). The second most thermoactive GALK studied is the one from *Tetrahymena thermophila* with an optimum temperature of 41 °C (19). For its activity, the *P. furiosus* GALK required divalent cations, with highest activity in the presence of Mn^{2+} followed by Mg^{2+}. The enzyme was very specific for its substrate since the enzyme under the tested conditions could phosphorylate only galactose and ATP

was the only suitable phosphoryl group donor for the enzyme (Table 5.1). ^{13}C-NMR showed that GALK converted a mixture of α- and β-[1-^{13}C]-galactose (being in anomeric equilibrium) into only α-[1-^{13}C]-galactose 1-phosphate. This was confirmed by ^{31}P-NMR upon spiking with α-galactose 1-phosphate (not shown). It was thus determined that a single phosphate from ATP was transferred to the C_1 position of galactose producing α-galactose 1-phosphate and ADP. In contrast to the ADP-GLK, the *P. furiosus* GALK shows the same substrate preferences as its classical counterparts. GALK showed Michaelis-Menten kinetics at 50 °C, and apparent K_m values of 0.21 ± 0.02 and 0.006 ± 0.001 mM, and apparent V_{max} values of 3.66 ± 0.08 and 3.42 ± 0.006 units/mg for galactose and ATP, respectively, were determined. Apparent K_m values for GALK were not significantly different at 90 °C, 0.27 ± 0.03 and 0.008 ± 0.002 mM for galactose and ATP, respectively, and apparent V_{max} values of 43.2 ± 3.8 and 41.9 ± 3.2 units/mg for galactose and ATP, respectively, were determined at 90 °C.

Table 5.1 Substrate specificity and cation dependency of GALK and ADP-GLK from *P. furiosus*.

Sugar	Relative activity %		Divalent cation	Relative activity %		Phosphoryl group donor	Relative activity %	
	GALK	ADP-GLK		GALK	ADP-GLK		GALK	ADP-GLK
D-glucose	< 0.3	100	Mg^{2+}	100	88	ATP	100	< 0.3
D-galactose	100	< 0.3	Mn^{2+}	37	100	ADP	< 0.3	100
D-fructose	< 0.3	< 0.3	Co^{2+}	35	59	GTP	60	NM
D-mannose	< 0.3	2	Ca^{2+}	7	15	GDP	NM[a]	< 0.3
2-deoxy-D-glucose	< 0.3	8	Zn^{2+}	< 0.3	60	CDP	NM	66
D-glucosamine	< 0.3	< 0.3				PP_i	< 0.3	NM
						PEP	< 0.3	< 0.3

Standard enzyme assays were done, except that cations, carbon substrates, and phosphoryl group donors were varied, as described under "Experimental". 100% activity of GALK and ADP-GLK corresponds to a specific activity of 2.6 and 139 units/mg, respectively.

[a]NM : not measured

The successful heterologous production of the *P. furiosus* ADP-GLK in *E. coli*, allowed for comparing the properties of the *E. coli*-produced ADP-GLK with that of the native ADP-GLK at the optimum pH of 7.5. The purified *E.coli*-produced ADP-GLK was found to have a specific activity of 189 units/mg, similar to the native ADP-GLK (9). The ADP-GLK exhibited a similar optimum temperature as GALK of approximately 90 °C. (Fig. 5.2). Interestingly, the ADP-GLK was able to convert D-mannose to some extent, next to D-glucose and 2-deoxy-D-glucose (Table 5.1). ADP and CDP were potential phosphoryl group donors for ADP-GLK, while it could not use ATP. ADP-PFK from *P. furious*, on the other hand, was able to use ATP to some extent (11). Divalent cations were required for activity, with the highest activity in the presence of Mg^{2+}, similar to the native ADP-GLK (9). For the *E. coli*-produced ADP-GLK apparent K_m values of 1.12 ± 0.10

mM and 0.078 ± 0.007 mM, and apparent V_{max} values of 300 ± 8 and 213 ± 8 units/mg for glucose and ADP, respectively, were determined at 50 °C, similar to the kinetic parameters of the native enzyme. In general, the characteristics of the *E.coli*-produced ADP-GLK closely resemble those of the native ADP-GLK. The affinity of ADP-GLK for both glucose and ADP was lower at 90 °C, resulting in apparent K_m values of 2.61 ± 0.28 and 0.45 ± 0.09 mM, and apparent V_{max} values of 1740 ± 210 and 2260 ± 150 units/mg, respectively. Thus, the affinity of the ADP-GLK for glucose and ADP decreased 2- and 6-fold, respectively, between 50 °C and 90 °C. This might be explained by assuming that ADP-GLK encounters a conformational change upon raising the temperature, which affects the affinity for ADP. Indeed, a break was observed in the Arrhenius plot for the ADP-GLK at approximately 60 °C (Fig. 5.2), which can be interpreted as such a structural change.

Table 5.2 Comparison of GALK and ADP-GLK from *P. furiosus* with other GALKs and ATP-dependent hexo- (HK) and glucokinases (GLK).

			Sugar		Phosphoryl group donor		
Type	Species	Assay temp. °C	K_m mM	k_{cat}/K_m $mM^{-1}s^{-1}$	K_m mM	k_{cat}/K_m $mM^{-1}s^{-1}$	Ref.
GALK	*Pyrococcus furiosus*	90	0.27	105	0.008	3439	This study
GALK	*Escherichia coli*	37	0.70	13.8	0.10	96.7	24
GALK	*Saccharomyces cerevisiae*	30	0.60	89.9	0.15	360	20
GALK	*Homo sapiens*	37	0.12	568	0.35	195	21
GLK	*Pyrococcus furiosus*	90	2.61	570	0.45	4294	This study
GLK	*Escherichia coli*	37	0.78	117	3.76	24.3	26
GLK	*Saccharomyces cerevisiae*	25	0.03	631	0.05	378	27
HK	*Homo sapiens*	37	0.065	411	0.49	54.5	28

The catalytic efficiencies of both sugar kinases, determined at 90 °C, were compared to those from characterized galactokinases and hexo/glucokinases from mesophiles (Table 5.2). These data show that the catalytic efficiencies of the pyrococcal sugar kinases for galactose and glucose resemble that of respective sugar kinases from mesophilic bacteria and eukaryotes. On the contrary, the catalytic efficiency of the pyrococcal sugar kinases for the phosphoryl group donor is 10- to 150-fold higher compared to their mesophilic counterparts (Table 5.2). This difference is caused by the high V_{max} of ADP-GLK (2260 units/mg) and the extremely low K_m for GALK (0.008 mM) at 90 °C. The observation of a high catalytic efficiency for adenine nucleotides and a normal catalytic efficiency for carbohydrates might suggest that the availability of certain nucleotides in the hyperthermophilic *P. furiosus* cells is lower than in cells of mesophilic organisms. Interestingly, the ADP-GLK is strongly inhibited (competitively) by AMP (K_i ~0.06 mM) (C. Verhees, unpublished), and hence the AMP concentration should be kept low during sugar fermentation in *P. furiosus*. The concentration of both ATP and AMP can be kept low by their conversion into ADP by an adenylate kinase (0.045 units/mg) (29). The produced ADP can subsequently serve as energy carrier for glycolysis. In this scenario, the high affinity of GALK for ATP as well as the ADP-dependence of the glycolytic kinases (Table 5.2) could be interpreted as an adaptation to relatively low

concentrations of ATP, possibly as a result of thermal instability of ATP. Interestingly, the recent characterization of a glycerol kinase from the closely related *Pyrococcus (Thermococcus) kodakaraensis* KOD1 (T.-opt. 95 °C) revealed that this enzyme also has a relatively high affinity for ATP (K_m 15.4 μM) compared to a mesophilic counterpart (K_m 4 mM) (30). Studies are underway to determine the intracellular adenine nucleotide concentrations under different growth conditions in *P. furiosus*, to get more insight in the actually availability of energy carriers under extreme conditions.

Acknowledgements

This research was supported by the Earth and Life science Foundation (ALW), which is subsidized by the Netherlands Organization for Scientific Research (NWO).

References

1. Kulaev, I.S. and Vagabov, V.M. (1983) Polyphosphate metabolism in micro-organisms. Adv. Microbiol. Physiol. **24**, 83-171
2. Postma, P.W. and Lengeler, J.W. (1985) Phospho*enol*pyruvate:carbohydrate phosphotransferase system of bacteria. Microbiol. Rev. **49**, 232-269
3. Mertens, E. (1991) Pyrophosphate-dependent phosphofructokinase, an anaerobic glycolytic enzyme? FEBS Lett. **285**, 1-5
4. Bork, P., Sander. C. and Valencia, A. (1992) Convergent evolution of similar enzymatic function on different protein folds: the hexokinase, ribokinase, and galactokinase families of sugar kinases. Protein Science **2**, 31-40
5. Aleshin, A.E., Zeng, C., Bartunik, H.D., Fromm, H.J. and Honzatko, R.B. (1998) Regulation of hexokinase I: crystal structure of recombinant human brain hexokinase complexed with glucose and phosphate. J. Mol. Biol. **282**, 345-357
6. Rypniewski, W.R. and Evans, P.R. (1989) Crystal structure of unliganded phosphofructokinase from *Escherichia coli*. J. Mol. Biol. **207**, 805-821
7. Sigrell, J.A., Cameron, A.D., Jones, T.A. and Mowbray, S.L. (1998) Structure of *Escherichia coli* ribokinase in complex with ribose and dinucleotide determined to 1.8 Å resolution: insights into a new family of kinase structures. Structure **6**, 183-193
8. Kengen, S.W.M., de Bok, F.A.M., van Loo, N-D., Dijkema, C., Stams, A.J.M. and de Vos, W.M. (1994) Evidence for the operation of a novel Embden-Meyerhof pathway that involves ADP-dependent sugar kinases during sugar fermentation by *Pyrococcus furiosus*. J. Biol. Chem. **269**, 17537-17541
9. Kengen, S.W.M., Tuininga, J.E., de Bok, F.A.M., Stams, A.J.M. and de Vos, W.M. (1995) Purification and characterization of a novel ADP-dependent glucokinase from the hyperthermophilic archaeon *Pyrococcus furiosus*. *J. Biol. Chem.* **270**, 30453-30457
10. Koga, S., Yoshioka, I., Sakuraba, H., Takahashi, M., Sakasegawa, S., Shimizu, S and Ohshima, T. (2000) Biochemical characterization, cloning, and sequencing of ADP-dependent (AMP-forming) glucokinase from two hyperthermophilic archaea, *Pyrococcus furiosus* and *Thermococcus litoralis*. J. Biochem. **128**, 1079-1085

11. Tuininga, J.E., Verhees, C.H., van der Oost, J., Kengen, S.W.M., Stams, A.J.M. and de Vos, W.M. (1999) Molecular and biochemical characterization of the ADP-dependent phosphofructokinase from the hyperthermophilic archaeon *Pyrococcus furiosus*. J. Biol. Chem. **274**, 21023-21028
12. Ito, S., Fushinobu, S., Yoshioka, I., Koga, S., Matsuzawa, H. and Wakagi, T. (2001) Structural basis for the ADP-specificity of a novel glucokinase from a hyperthermophilic archaeon. Stucture **9**, 205-214
13. Kengen, S.W.M., Stams, A.J.M. and de Vos, W.M. (1996) Sugar metabolism of hyperthermophiles. FEMS Microbiol. Rev. **18**, 119-137
14. Selig, M., Xavier, K.B., Santos, H. Schönheit, P. (1997) Comparative analysis of Embden-Meyerhof and Entner-Doudoroff glycolytic pathways in hyperthermophilic archaea and the bacterium *Thermotoga*. Arch. Microbiol. **167**, 217-232
15. Frey, P.A. (1996) The leloir pathway: a mechanistic imperative for three enzymes to change the stereochemical configuration of a single carbon in galactose. FASEB J. **10**, 461-470
16. Kengen, S.W.M., Luesink, E.J., Stams, A.J.M. and Zehnder, A.J.B. (1993) Purification and characterization of an extremely thermostable β-glucosidase from the hyperthermophilic archaeon *Pyrococcus furiosus*. Eur. J. Biochem. **213**, 305-312
17. Sambrook, J., Fritsch, E.F. and Maniatis, T. (1989) Molecular cloning: a laboratory manual, 2nd ed. Cold Spring Harbor Laboratory, Cold Spring Harbor, New York
18. Braford, M.M. (1976) A rapid and sensitive method for the quantification of microgram quantities of protein utilizing the principle of protein dye binding. Anal. Biochem. **72**, 248-254
19. Lavine, J.E., Cantlay, E., Roberts Jr, C.T. and Morse, D.E. (1981) Purification and properties of galactokinase from *Tetrahymena thermophila*. Biochim. et. Biophys. Acta **717**, 76-85
20. Schell, M.A. and Wilson, D.B. (1977) Purification and properties of galactokinase from *Saccharomyces cerevisiae*. J. Biol. Chem. **252**, 1162-1166
21. Blume, K-G. and Beutler, E. (1971) Purification and properties of galactokinase from human red blood cells. J. Biol. Chem. **246**, 6507-6510
22. Ettema, T., van der Oost, J. and Huynen M. (2001) Modularity in the gain and loss of genes: applications for function prediction. Trends Genet. **17**, 485-487
23. Verhees, C.H., Tuininga, J.E., Kengen, S.W.M., Stams, A.J.M., van der Oost, J. and de Vos, W.M. (2001) ADP-dependent phosphofructokinases in mesophilic and thermophilic methanogenic archaea. J. Bacteriol. **183**, in the press
24. Sherman, J.R. and Adler, J. (1963) Galactokinase from *Escherichia coli*. J. Biol. Chem. **238**, 873-878.
25. Dey, P.M. (1983) Galactokinase of *Vicia faba* seeds. Eur. J. Biochem. **136**, 155-159
26. Meyer, D., Schneider-Fresenius, C., Horlacher, R., Peist, R. and Boos W. (1997) Molecular characterization of glucokinase from *Escherichia coli* K-12. J. Bacteriol. **179**, 1298-1306
27. Maitra, P.K. (1970) A glucokinase from *Saccharomyces cerevisiae*. J. Biol. Chem. **245**, 2423-2431
28. Zeng, C., Aleshin, A.E., Chen, G., Honzatko, R.B. and Fromm, H.J. (1998) The roles of glycine residues in the ATP binding site of human brain hexokinase. J. Biol. Chem. **273**, 700-704
29. Schäfer, T. and Schönheit, P. (1991) Pyruvate metabolism of the hyperthermophilic archaeon *Pyrococcus furiosus*. Arch. Microbiol. **155**, 366-377
30. Koga, Y., Morikawa, M., Haruki, M., Nakamura, H., Imanaka, T. and Kanaya, S. (1998). Thermostable glycerol kinase from a hyperthermophilic archaeon: gene cloning and characterization of the recombinant enzyme. Protein Engineering **11**, 1219-1227

Chapter 6

The phosphoglucose isomerase from the hyperthermophilic archaeon *Pyrococcus furiosus* is a unique glycolytic enzyme that belongs to the cupin superfamily

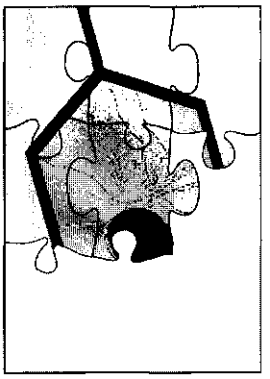

Corné H. Verhees, Martijn A. Huynen, Donald E. Ward, Emile Schiltz, Willem M. de Vos and John van der Oost

Journal of Biological Chemistry 276: 40926-40932 (2001)

Abstract

Pyrococcus furiosus uses a variant of the Embden-Meyerhof pathway during growth on sugars. All but one of the genes that encode the glycolytic enzymes of *P. furiosus* have previously been identified, either by homology searching of its genome or by reversed genetics. We here report the isolation of the missing link of the pyrococcal glycolysis, the phosphoglucose isomerase (PGI), which was purified to homogeneity from *P. furiosus* and biochemically characterized. The *P. furiosus* PGI, a dimer of identical 23.5-kDa subunits, catalyzes the reversible isomerization of glucose-6-phosphate to fructose-6-phosphate, with K_m values of 1.99 mM and 0.63 mM, respectively. An optimum pH of 7.0 has been determined in both directions, and at its optimum temperature of 90 °C the enzyme has a half-life of 2.4 h. The N-terminal sequence was used for the identification of the *pgiA* gene in the *P. furiosus* genome. The *pgiA* transcription start site has been determined, and a monocistronic messenger was detected in *P. furiosus* during growth on maltose and pyruvate. The *pgiA* gene was functionally expressed in *E. coli* BL21(DE3). The deduced amino acid sequence of this first archaeal PGI revealed that it is not related to its bacterial and eukaryal counterparts. In contrast, this archaeal PGI shares similarity with the cupin superfamily that consists of a variety of proteins that are generally involved in sugar metabolism in both prokaryotes and eukaryotes. As for the *P. furiosus* PGI, distinct phylogenetic origins have previously been reported for other enzymes from the pyrococcal glycolytic pathway. Apparently, convergent evolution by recruitment of several unique enzymes has resulted in the unique *Pyrococcus* glycolysis.

Introduction

The hyperthermophilic archaeon *Pyrococcus furiosus* is capable of metabolizing sugars via a modified Embden-Meyerhof pathway (1). Novel enzymes and unique control points in this pathway have been elucidated and involve two phosphorylation and an oxidoreduction reaction (2,3,4,5).

A first variation of the pyrococcal glycolysis concerns the unique ADP-dependent sugar kinases, *i.e.* ADP-dependent glucokinase (ADP-GLK) and ADP-dependent phosphofructokinase (ADP-PFK) have been characterized biochemically, and the paralogous genes were identified on the *P. furiosus* genome (2,3). The recently determined crystal structure of the ADP-GLK from the related archaeon *Thermococcus litoralis* revealed that the ADP-dependent sugar kinase family (ADP-GLK and most likely ADP-PFK) belong to the ribokinase family (6), whereas their bacterial and eukaryal counterparts belong to the hexokinase and PFK family, respectively (7,8).

A second variation concerns the glycolytic conversion of glyceraldehyde 3-phosphate to 3-phosphoglycerate in *P. furiosus* that was found to be catalyzed by the unique glyceraldehyde-3-phosphate ferredoxin oxidoreductase (GAPOR) enzyme (4,5). This ferredoxin-dependent, single-

step conversion of glyceraldehyde 3-phosphate was shown to represent a novel site of glycolytic regulation in *P. furiosus* (5).

With the increasing number of available sequence data from different species, including bacteria, eucarya and archaea, and functional characterization of the gene products, most of the genes encoding the other *P. furiosus* glycolytic enzymes (fructose-1,6-bisphosphate aldolase, triosephosphate isomerase, phosphoglycerate mutase, enolase, and pyruvate kinase) could readily be identified in its genome (9). Attempts to identify the gene encoding phosphoglucose isomerase (PGI) by a bioinformatics approach have hitherto been unsuccessful. Although significant PGI activity has previously been detected (0.2 units/mg) in a *P. furiosus* cell-free extract (1,2,10,11), no ortholog of a bacterial/eukaryal PGI could be identified in the *P. furiosus* genome. This suggested that *P. furiosus* might possess a distinct type of PGI. To complete the *P. furiosus* glycolytic pathway and to obtain insight in the anticipated novel type of PGI, we here report on the purification of the PGI enzyme from *P. furiosus*, its characterization, and the isolation of the corresponding *pgiA* gene. This is the first molecular and biochemical characterization of an archaeal PGI, that indeed represents a novel type of this enzyme.

Experimental procedures

Materials

All chemicals and enzymes were purchased from Sigma, Merck or Roche Molecular Diagnostic in analytical grade. *Aspergillus nidulans* mannitol-1-phosphate dehydrogenase was purified from an overproducing *A. nidulans* strain as described previously (12).

Organisms and growth conditions

P. furiosus was cultivated in artificial seawater medium as described before (3). *Escherichia coli* XL1 Blue was used as a host for the construction of pET24d derivatives. *E. coli* BL21 (DE3) was used as an expression host. Both strains were grown in Luria Bertani medium with kanamycin (50 μg/ml) in a rotary shaker at 37 °C.

Preparation of cell-free extract from P. furiosus

P. furiosus cells from a 200-liter culture were harvested by continuous centrifugation (Sharples, Rueil, France) and stored at –20 °C until use. Cell-free extract was prepared by suspending a cell paste in 2 volumes (w/v) of 50 mM Tris/HCl buffer, pH 7.5, and treatment in a French press at 100 megapascals. Cell debris was removed by centrifugation for 1h at 100,000 x *g* at 10 °C.

Purification of the PGI from P. furiosus cell-free extract

To prevent microbial contamination, all buffers contained 0.02% sodium azide. Cell-free extract (27 ml) was filtered (0.45 μm), brought to 1.7 M ammonium sulfate saturation and loaded onto a Phenyl-Sepharose fast flow column (69 ml, Amersham Pharmacia Biortech), equilibrated in 50 mM Tris/HCl buffer, pH 7.8, containing 1.7 M ammonium sulfate. During a 350-ml linear gradient (1.7-0.0 M ammonium sulfate) PGI activity eluted at 1.0 M ammonium sulfate. Active fractions were pooled and desalted by filtration (Macrosep, 10-kDa cutoff), using a 50 mM Tris/HCl buffer, pH 8.5. The desalted PGI pool was applied to a Q-Sepharose fast flow column (25 ml, Amersham Pharmacia Biotech) that was equilibrated in the same buffer. The PGI eluted in a 125-ml linear gradient (0.0-0.7 M NaCl) at 0.27 M NaCl. Active fractions were pooled and dialysed against 20 mM potassium phosphate buffer, pH 7.0. The desalted PGI pool was applied to a hydroxyapatite column (20 ml, Biorad) that was equilibrated in the same buffer. PGI activity eluted in a 200-ml linear gradient (20-500 mM potassium phosphate) at 140 mM potassium phosphate. Active fractions were pooled, the buffer was changed for a 50 mM Tris/HCl buffer, pH 7.6 by dialysis and the pool was loaded onto a mono-Q HR 5/5 column (1 ml, Amersham Pharmacia Biotech) that was equilibrated in the same buffer. PGI activity eluted in a 30-ml linear gradient (0.0-0.7 M NaCl) at 0.18 M NaCl. Fractions showing PGI activity were pooled and concentrated 10-fold to a final volume of 100 μl. This concentrated pool was applied to a Superdex 200 HR 10/30 gelfiltration column (24 ml, Amersham Pharmacia Biotech) that was equilibrated with a 50 mM Tris/HCl buffer, pH 7.8 containing 100 mM NaCl, from which the protein eluted after 14.5 ml. The purified PGI was desalted in 50 mM Tris/HCl, pH 7.8 using a Microsep filter with a 10-kDa cutoff.

Cloning of the PGI Gene

The N-terminal sequence of the purified PGI was determined by the Edman degradation method. The sample was subjected to SDS-PAGE and electroblotted on a polyvinylidene difluoride membrane prior to analysis. The N-terminal amino acid sequence was used for BLAST search of the *P. furiosus* database (http://www.genome.utah.edu), and identification of the PGI gene (*pgiA*, accession number AF381250, NCBI Genbank™). The following primer set was designed to amplify this open reading frame by PCR: BG902 (5'- GCGCGTCATGATGTATAAGGAACCT-TTTGGAGTG, sense) and BG903 (5'- GCGCGAAGCTTCTACTTTTTCCACCTGGGATTAT, antisense), with *Bsp*HI and *Hind*III restriction sites in bold.

The 100-μl PCR mixture contained 100 ng of *P. furiosus* DNA, isolated as described before (13), 100 ng each of primer BG902 and BG903, 0.2 mM dNTPs, *Pfu* polymerase buffer, and 5 units of *Pfu* DNA polymerase and was subjected to 35 cycles of amplification (1 min at 94 °C, 1 min at 56 °C, and 1 min at 72 °C) on a DNA Thermal Cycler (PerkinElmer Life Sciences). The PCR product was digested (*Bsp*HI/*Hind*III) and cloned into an *Nco*I/*Hind*III-digested pET24d vector,

resulting in pLUW557, which was transformed into *E. coli* XL1 Blue and BL21(DE3). Sequence analysis on pLUW557 was done by the dideoxynucleotide chain termination method with a Li-Cor automatic sequencing system (model 4000L). Sequencing data were analyzed using the computer program DNASTAR.

Overexpression of the PGI gene in E. coli

An overnight culture of *E. coli* BL21(DE3) containing pLUW557 was used as a 1% inoculum in 1 liter of Luria Bertani medium with 50 μg/ml kanamycin. Gene expression was induced by adding 0.1 mM isopropyl-1-thio-β-D-galactopyranoside at the A_{600} of 0.5. Growth was continued for 10 h at 37 °C, and cells were harvested by centrifugation (2,200 × *g* for 20 min) and resuspended in 10 ml of 50 mM Tris/HCl buffer, pH 7.6. The suspension was passed twice through a French press (100 megapascals), and cell debris was removed by centrifugation (10,000 × *g* for 20 min). The resulting supernatant was used for purification of the recombinant PGI.

Purification of recombinant PGI

The *E. coli* cell-free extract containing pLUW557 was heat-treated for 30 min at 80 °C, and precipitated proteins were removed by centrifugation. The heat-treated cell-free extract was filtered through a 0.45 μm filter and applied to a mono-Q HR 5/5 column (Amersham Pharmacia Biotech), equilibrated with 50 mM Tris/HCl pH 7.6. The PGI activity eluted at 0.18 M NaCl during a linear gradient of 0.0 – 1.0 M NaCl. Active fractions were pooled and concentrated 10-fold to a final volume of 100 μl using a Microsep filter with a 10-kDa cutoff. The concentrated pool was loaded onto a Superdex 200 HR 10/30 gelfiltration column (Amersham Pharmacia Biotech), equilibrated with 50 mM Tris/HCl, pH 7.8 containing 100 mM NaCl. The recombinant PGI eluted at 14.5 ml. The purified enzyme was desalted in 50 mM Tris/HCl, pH 7.8 using a Microsep filter with a 10-kDa cutoff.

Protein concentration and purity

Protein concentrations were determined with Coomassie Brilliant Blue G250 as described before (14) using bovine serum albumin as a standard. The purity of the enzyme was checked by SDS-PAGE as described before (15). Protein samples for SDS-PAGE were heated for 5 min at 100 °C in an equal volume of sample buffer (0.1 M citrate-phosphate buffer, 5% SDS, 0.9% 2-mercaptoethanol, 20% glycerol, pH 6.8).

Determination of enzyme activity

PGI activity was determined in 100 mM MOPS buffer, pH 7.0 (50 °C). Enzyme preparations were added in 5-50 µl. Enzyme activity on fructose-6-phosphate was determined by measuring the formation of NADPH in a coupled assay with yeast glucose-6-phosphate dehydrogenase. The assay mixture contained 0.5 mM NADP, 5 mM fructose 6-phosphate and 0.35 units of D-glucose-6-phosphate dehydrogenase. The activity of the PGI on glucose 6-phosphate was determined by measuring the decrease of NADH in a coupled assay with *Aspergillus nidulans* mannitol-1-phosphate dehydrogenase (12). The assay mixture contained 0.2 mM NADH, 5 mM glucose 6-phosphate and 1.4 units of mannitol-1-phosphate dehydrogenase. One unit was defined as the amount of enzyme required to convert 1 µmol of fructose-6-phosphate or glucose-6-phosphate per min. All enzyme assays were performed at 50 °C. At this temperature the yeast and *A. nidulans* enzyme remained active, and the *P. furiosus* enzyme was sufficiently active to measure its activity. The auxiliary enzymes were present in excess, to ensure that the detected NADPH and NADH absorbance at 340 nm ($\varepsilon = 6.3\ mM^{-1}cm^{-1}$) corresponded to the PGI activity.

Substrate specificity

Substrate specificity was investigated using purified PGI. The use of fructose 6-phosphate and glucose 6-phosphate as possible substrates for the PGI was tested using the standard enzyme assay. For the determination of mannose 6-phosphate as possible substrate the standard enzyme assay for glucose 6-phosphate was used. Glucose, fructose, galactose and mannose were tested as possible substrates by incubating an appropriate amount of PGI with 5 mM substrate for 30-60 min at 50 °C in 100 mM MOPS pH 7.0. The reactions were stopped on ice/ethanol and the products were analyzed by high performance liquid chromatography. The effect of cations ($MgCl_2$ and $MnCl_2$, 10 mM) and cofactors (ATP, NAD^+, arsenate and phosphate, 10 mM) on the isomerization of non-phosphorylated monosaccharides was investigated by the standard high performance liquid chromatography assay.

Inhibitors of PGI activity

Possible inhibitors (mannose 6-phosphate, fructose 1-phosphate, fructose 1,6-bisphosphate, fructose, glucose, mannose, galactose, pyruvate, phosphoenolpyruvate, AMP, ADP, or ATP) were tested on the activity of the *P. furiosus* PGI both in the direction of glucose-6-phosphate and fructose-6-phosphate formation by adding (1.25-10 mM) to the standard enzyme assays at 50 °C.

Kinetic analysis

Kinetic parameters were determined at 50 °C, in 100 mM MOPS buffer, pH 7.0, by varying the concentration of fructose 6-phosphate (0.05-3.50 mM) or glucose 6-phosphate (0.47-10.0 mM),

respectively. 2.0 μg of purified PGI was used for these determinations. Data were analyzed by computer-aided (Program Tablecurve) fit to the Michaelis-Menten curve.

Temperature optimum and thermal inactivation

The temperature optimum was determined in the direction of glucose 6-phosphate formation. Purified PGI (0.0064 mg/ml) was incubated in 1-ml crimp-sealed vials containing 100 mM sodium phosphate buffer, pH 7.0. The vials were submerged in an oil bath at temperatures varying from 30 to 120 °C, pre-heated for 2 min, and the enzyme reaction was started by injecting 20 mM fructose 6-phosphate. After 1, 2, and 3 min the reaction was stopped by transferring the vials on ice/ethanol, and the amount of glucose 6-phosphate formed was determined spectrophotometrically at room temperature by measuring the reduction of NADP (340 nm) in an assay with glucose-6-phosphate dehydrogenase. Corrections were made for the chemical isomerization of fructose 6-phosphate in the absence of PGI

Thermal inactivation of PGI was determined by incubating the enzyme (1.28 μg) in 200 μl of a pre-heated 100 mM sodium phosphate buffer, pH 7.0 at 60, 70, 80, and 90 °C in crimp-sealed vials, submerged in an oil bath. At certain time intervals, 200-μl aliquots were withdrawn and analyzed for activity in the standard assay. Studies were performed under V_{max} conditions, since substrate concentrations in the assays are approximately 30-fold higher than the K_m.

pH optimum

The pH optimum was determined at 50 °C in 200 mM Tris/maleate buffer over the pH range 6.0-9.5. Buffer pH values were adjusted at this temperature. Except for buffer and temperature, assay conditions were identical to analyze the enzyme's temperature optimum. In the case of fructose 6-phosphate conversion, glucose-6-phosphate dehydrogenase was used as following enzyme. When glucose 6-phosphate was used as substrate, mannitol-1-phosphate dehydrogenase was used as following enzyme.

Transcript analysis

RNA was isolated from maltose (10 mM) and pyruvate (40 mM) grown *P. furiosus* cells as described previously (16). For Northern blot analysis 15 μg of total RNA was separated on a 1.5% formaldehyde agarose gel and transferred to a Hybond N^+ membrane. Probes were generated by PCR with the primers BG902 and BG903. The PCR product was purified by Qiaquick (Qiagen) and labeled by nick translation with [α-^{32}P] dATP. The transcription start was determined with a fluorescence (IRD800)-labeled antisense oligonucleotide (5'- CTTTCCATGCCCTTTCATCAAC - 3', position 103-124 of the *pgiA* gene). Primer extension reactions were performed using the Reverse Transcription System (Promega) according to the instructions of the manufacturer with

following modifications. Hybridization of total RNA (15 µg) and oligonucleotide (5 pmol) was performed for 10 min at 68 °C before allowing to cool to room temperature. The reaction (20 µl final volume) was started by addition of dNTPs (1 mM), MgCl2 (5 mM), RNAsin (20 U), and avian myeloblastosis virus-reverse transcriptase (22.5 U). After incubation for 30 min at 45 °C the reaction volume was diluted to 50 µl with 10 mM Tris/HCl, pH 8.5, 1 µl of RNaseA (5 mg/ml) was added and the sample was incubated for 10 min at 37 °C. cDNA was precipitated with ethanol, dissolved in 3 µl loading buffer and 1 µl was applied to a sequencing gel in parallel with the sequencing reactions obtained with the same oligonucleotide.

Multiple sequence alignment and tree construction

The sequence alignment of homologs of the *P. furious* PGI was generated with T-coffee (17) followed by small, manual refinements. A neighbor joining (18) tree of the aligned sequences was generated with clustalX (19). Bootstrap values above 60 out of 100 are indicated. A secondary structure prediction was generated with Profile-based neural network system from HeiDelberg (20).

Results and discussion

Purification of the PGI from P. furiosus

Table 6.1. Purification of PGI from *P. furiosus*.

Purification step	Total activity	Protein	Specific activity[a]	Purification factor	Recovery
	units	*mg ml^{-1}*	*units mg^{-1}*	*-fold*	*%*
Cell-free extract	295.8	39.7	0.276	1.0	100
Phenyl-Sepharose	93.6	3.54	0.588	2.1	31.6
Q-Sepharose	90.2	0.670	2.99	10.8	30.5
Hydroxyapatite	38.1	0.426	3.58	13.0	12.9
Mono-Q	25.8	9.92	3.86	14.0	8.7
Superdex200	10.1	0.196	14.5	52.5	3.4

[a] Specific activities were determined at 50 °C, with fructose-6-phosphate as substrate.

Purification of the *P. furiosus* PGI was performed aerobically at ambient temperature. PGI was purified from a *P. furiosus* cell-free extract using a number of conventional chromatographic steps (Table 6.1). Anion exchange chromatography (Q-sepharose Fast Flow) and gelfiltration (Superdex 200 HR 10/30) resulted in PGI purification to apparent homogeneity as judged from SDS-PAGE analysis (Fig. 6.1). Additional native PAGE analysis resulted in a single protein band (not shown). The enzyme was purified 52.5-fold from the cell-free extract, suggesting that the PGI

accounts for approximately 2% of the soluble cellular protein in *P. furiosus*. The amino-terminal sequence has been identified by Edman degradation: MYKEPFGVKVNFETGIIEGA. This sequence had a perfect match with the N-terminal part of a 21 kDa hypothetical protein from *P. furiosus* as identified from the genome sequence (http://www.genome.utah.edu).

Heterologous production and purification of PGI

The putative 570-base pair PGI-encoding gene (*pgiA*) was PCR amplified and cloned into pET24d, resulting in plasmid pLUW557. DNA sequence analysis of pLUW557 confirmed that the cloned *pgiA* gene showed the expected sequence. SDS-PAGE analysis of a heat-treated cell-free extract of *E.coli* BL21(DE3) harboring pLUW557 revealed an additional band of 23 kDa which was in good agreement with the calculated molecular mass (21.6 kDa) of the gene product. This band was absent in a heat-treated cell-free extract of *E.coli* BL21(DE3) carrying the pET24d vector without insert, in which no PGI activity was detected (not shown). In a heat-treated cell-free extract of *E.coli* BL21(DE3) harboring pLUW557, a PGI activity of 8.3 units/mg was measured at 50 °C, confirming that the cloned *P. furiosus pgiA* gene indeed encoded a PGI. The recombinant PGI was easily purified by two successive chromatographic steps, *i.e.* anion exchange chromatography and gelfiltration. The recombinant enzyme eluted as the native enzyme, and was purified to apparent homogeneity as judged by SDS-PAGE analysis (Fig. 6.1).

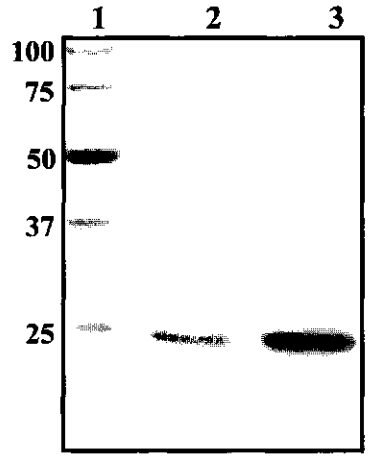

Figure 6. 1 SDS-polyacrylamide gel electrophoresis of the purified PGI from *P. furiosus*. *Lane 1* contained a set of marker proteins with their molecular mass indicated (kDa). *Lane 2* contained the purified PGI from *P. furiosus* cell-free extract. *Lane 3* contained purified recombinant PGI. Proteins were stained with Coomassie Brilliant Blue R250.

Physical and biochemical characterization of PGI

The molecular mass of both the native and recombinant PGI as determined by gelfiltration was 49.6 ± 0.3 kDa. SDS-PAGE analysis of the two enzymes resulted in identical bands of 23.5 ± 0.2 kDa, suggesting that the PGI is a homodimer. This homodimeric composition has been observed also for bacterial and eukaryal PGIs, although homotetrameric compositions occur as well. Furthermore, the *P. furiosus* PGI differs from all known PGIs by its subunit molecular mass, which is about half of its canonical counterparts (Table 6.2). Moreover, the *P. furiosus* PGI -the first archaeal PGI described to date- exhibits the lowest pH optimum and highest temperature optimum of all known PGIs (Table 6.2).

Table 6.2 Comparison of PGI from *P. furiosus* with other PGIs.

Domain	Species	T-opt.[a]	pH-opt.	Molecular mass		K_m		Reference(s)
				native	subunit	F6P	G6P	
		°C		kDa		mM		
Archaea								
	P. furiosus	90	7.0	49.3 (α_2)[c]	23.5	0.71	1.57	this work
Bacteria								
	B. caldotenax	77	8-9	202 (α_4)	50.6	ND	2.46	21
	E. coli (I)	ND[b]	8.0	125 (α_2)	59	0.2	ND	22
	E. coli (II)	ND	8.0	230 (α_4)	59	0.2	ND	22
Eucarya								
	A. niger	ND	7.5-10	118 (α_2)	60	0.32	0.48	12
	T. brucei	ND	7.5-9.5	ND	64	0.12	ND	23
	Yeast	ND	7.5-9.5	119 (α_2)	61	0.17	ND	23,24
	Rabbit	ND	7.5-9.5	125 (α_2)	64	0.12	ND	23,25

[a] T optimum determined for purified PGI.
[b] ND, not determined.
[c] The proposed subunit composition of the native enzyme is shown in parentheses.

The specific activities of the native and the recombinant PGI exhibited similar temperature or pH optima. The *P. furiosus* PGI showed reversible isomerization activity with fructose 6-phosphate and glucose 6-phosphate between pH 6.0 to 8.5, with an optimum at pH 7.0 (not shown). PGI showed maximal activity around 90 °C (Fig. 6.2). From the Arrhenius plot between 30 and 90 °C, an inactivation energy of 41 kJ/mol was calculated. Thermal inactivation was determined at 60, 70, 80, and 90 °C and followed first-order kinetics (Fig. 6.3). With a half-life of approximately 2.4 h at 90 °C it is the most thermostable PGI presently known. The second most thermostable PGI is the one from *B. caldotenax*, that exhibits a half-life of approximately 2 h at 65 °C (21).

The purified enzyme only showed activity in the isomerization of fructose 6-phosphate and glucose 6-phosphate (5mM), with specific activities at 50 °C of 14.5 and 29.1 units/mg, respectively (pH 7.0). The PGI activity was not affected by addition of cations (Mg^{2+} or Mn^{2+}), nor by addition of 10 mM EDTA to the assay mixture. Under the tested conditions the enzyme did not convert mannose 6-phosphate to fructose 6-phosphate. The PGI from *Escherichia intermedia* has been reported to catalyze the isomerization of non-phosphorylated sugars, like fructose and glucose,

but only in the presence of arsenate (26). The purified enzyme from *P. furiosus* was unable to isomerize non-phosphorylated sugars like glucose, fructose, mannose and galactose both in the absence or presence of cofactors like arsenate and phosphate. This suggests that the phosphoryl group at the C6 position of fructose 6-phosphate and glucose 6-phosphate plays an important role in substrate recognition of the *P. furiosus* PGI.

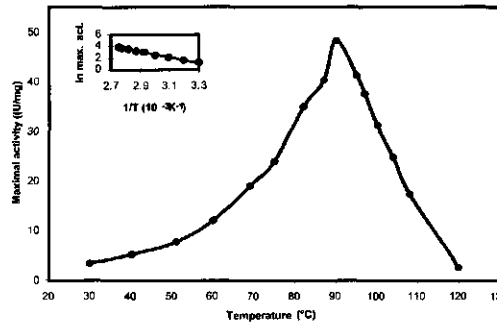

Figure 6.2 Dependence of PGI activity on temperature.

Activity of native PGI was determined by measuring the amount of glucose 6-phosphate formed after incubation for 1, 2, and 3 min at the desired temperature. *Inset*, Arrhenius plot of the data from 30 to 90 °C. Both native and recombinant PGI showed similar behaviors to temperatures (not shown).

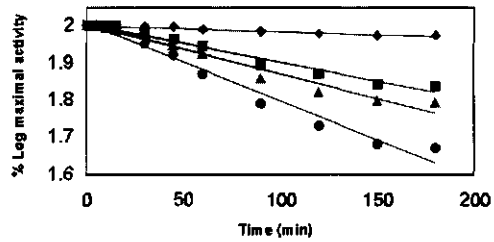

Figure 6. 3. Thermal stability of PGI.

The native enzyme (0.0064 mg/ml) was preincubated at 90 °C in 100 mM sodium phosphate buffer (pH 7.0) Residual activity was measured at 50 °C using fructose 6-phosphate as substrate. The 100% activity corresponds to 18.6 units/mg for the native PGI. Thermal inactivation is plotted on logarithmic scale to demonstrate first-order kinetics. The recombinant PGI showed similar inactivation profiles at the respective temperatures as the native PGI (not shown). Half-lifes of 1500, 300, 230, and 143 min were calculated at 60 (◆), 70 (■), 80 (▲), and 90 °C (●), respectively.

The native *P. furiosus* PGI showed Michaelis-Menten kinetics at 50 °C, K_m values of 0.63 ± 0.07 and 1.99 ± 0.11 mM for fructose 6-phosphate and glucose 6-phosphate, respectively, and V_{max} values of 20.1 ± 0.73 and 34.3 ± 0.71 units/mg for fructose 6-phosphate and glucose 6-phosphate, respectively. K_m values and V_{max} values determined for the recombinant PGI were in the same order of magnitude, with K_m values of 0.42 ± 0.03 and 2.00 ± 0.17 mM for fructose 6-phosphate and glucose 6-phosphate, respectively, and V_{max} values of 19.2 ± 0.37 and 47.7 ± 1.40 units/mg for fructose 6-phosphate and glucose 6-phosphate, respectively. The k_{cat}/K_m values for fructose 6-phosphate and glucose 6-phosphate conversion of the native PGI were 11.5 and 6.2 $sec^{-1}mM^{-1}$, and of the recombinant PGI 16.5 and 8.6 $sec^{-1}mM^{-1}$.

The effect of potential inhibitors was tested on the activity of the recombinant PGI (5 mM substrate). The addition of fructose, glucose, mannose, galactose (10 mM), pyruvate, phosphoenolpyruvate (10 mM), AMP, ADP or ATP (3.5 mM), did not show any effect on the PGI activity neither in the fructose 6-phosphate formation, nor in the glucose 6-phosphate formation. Typical PGI inhibitors like mannose 6-phosphate, fructose 1-phosphate, and fructose 1,6-bisphosphate negatively effected the PGI activity in both directions. Residual activities of 18 % and 38 % were monitored in the presence of 1.25 mM mannose 6-phosphate, in the direction of fructose 6-phosphate and glucose 6-phosphate formation, respectively. In the presence of 2 mM fructose 1-phosphate residual activities of 50 % and 69 % were measured, respectively. Finally, the addition of 10 mM fructose 1,6-bisphosphate to the assay mixture resulted in residual activities of 41 % and 53 %, respectively. Hence, the activity of the *P. furiosus* PGI is inhibited by classical PGI inhibitors (27), and the affinity of the *P. furiosus* enzyme for fructose 6-phosphate and glucose 6-phosphate (determined at 50 °C) was in the same order of magnitude as that of the classical PGIs (Table 6.2). Hence, catalytic properties of the *P. furiosus* PGI resemble that of the classical PGIs in most respects. When this paper was being evaluated, Hansen *et al.* (28) independently described a biochemical characterization of the phosphoglucose isomerase from *P. furiosus*, in general revealing features as reported in this study.

Transcript analysis

For an accurate assignment of the promoter region in *P.furiosus* the transcription start of the *pgiA* mRNA was determined by primer extension. The transcription is initiated at the thymine (T) 11 bp upstream of the ATG start codon (Fig. 6.4A). A putative ribosomal binding site (RBS) was identified at position +2 - +6. A putative TATA box is positioned around –24/-25 of the transcription start, and a clear transcription factor B Recognition Element (BRE site, consensus sequence A/GNA/TAAA/T) (29) is positioned around –33/-34 (Fig. 6.4B).

Northern blot analysis revealed a strong hybridization signal at 0.7 kilobase pairs with the *pgiA* probe, indicating the presence of a monocystronic transcript (Fig. 6.4C). As shown by primer

extension (4-fold) and Northern blot analysis (1.5-fold), *pgiA* transcription is slightly higher under catabolic (maltose) than under anabolic (pyruvate) conditions. Moreover, a 1.7-fold increase of PGI activity was detected when grown on maltose (0.32 units/mg) compared to pyruvate (0.19 units/mg). Similar observations were made for the reversible fructose-1,6-bisphosphate aldolase and phosphoenolpyruvate synthetase from *P. furiosus* (30,31). This might suggest a different flux through the pathway when used in the anabolic or in the catabolic direction.

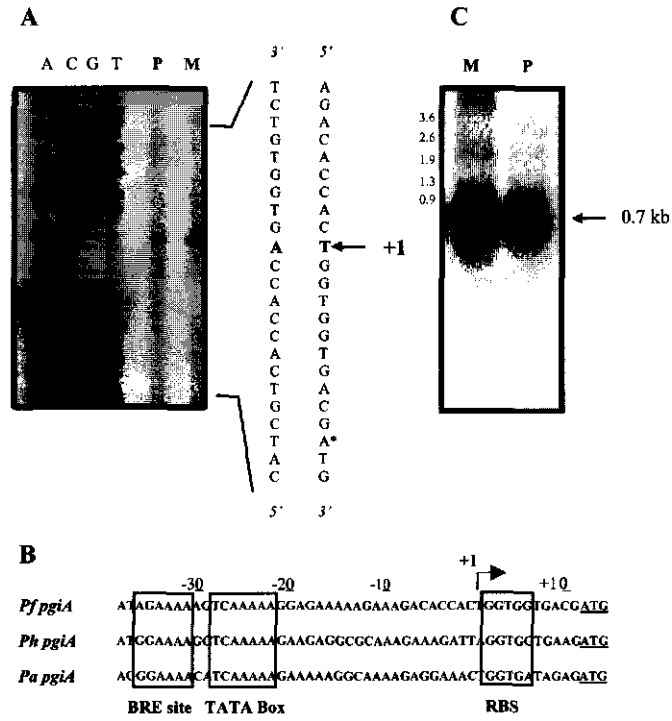

Figure 6.4 Transcript analyses of the *P. furiosus pgiA*.

(A) Mapping of the transcription start. The transcript begins at position +1 (*arrow*), an *asterisk* marks the start codon (ATG) and the sequence ladder (*lanes A, C, G* and *T*) is shown. **(B)** Upstream nucleotide sequence of the *P. furiosus pgiA* gene. The transcription factor B recognition element (*BRE site*), putative TATA box element and the ribosome-binding site (*RBS*) is marked. The mapped start site of transcription is marked by an *arrow* and the ATG start codon is *underlined*. Promoter regions of *Ph pgiA* (PH1956) and *Pa pgiA* (PAB1199) are included. **(C)** Northern blot analysis. For both primer extension and northern blot analysis 15 µg of total RNA was used from maltose (*M*) and pyruvate (*P*) grown cells.

Structural analysis

The amino acid sequence of PGI has full-length homologs with high levels of sequence identity (90% and 91% for *P.abyssi* and *P.horikoshii*, respectively) in the other two *Pyrococci*, suggesting that these genes most likely also function as PGIs. Homology with other sequences is limited to the positions 66 to 152 of the *P. furiosus* PGI (Fig. 6.5). Using profile based sequence comparisons (PSI-Blast, 9 iterations, E<0.002) this area can be shown to be homologous to a wide range of proteins belonging to the cupin superfamily, that consists of a variety of proteins that are generally involved in sugar metabolism in both prokaryotes and eukaryotes (33).

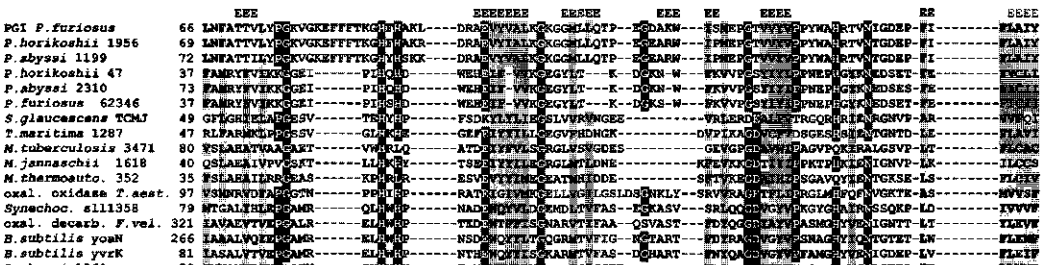

Figure 6.5 Alignment of the PGI of *P. furiosus* with 1) its most similar homologs (PSI-Blast 5 iterations E < 0.002) from completely sequenced genomes, 2) sequences with experimentally determined function, and 3) canavalin of which a three-dimensional structure is available (32). A secondary structure (above the alignment, *E* denotes beta-strand) is consistent with the secondary structure of canavalin (below the alignment). With each sequence is given the number of its gene in the genome. The species abbreviations with the genbank identifiers of the sequences: *P.furiosus* = *P. furiosus* (AF381250); *P.horikoshii* = *P. horikoshii* (g3258400 g3256432 g3256943); *P.abyssi* = *P. abyssi* (g5459164 g5457489 g5458926); *A.fulgidus* = *Archaeoglobus fulgidus* (g2649077 g2649495); *M.jannaschii* = *Methanococcus jannaschii* (g1499583 g1592216); *M. tuberculosis* = *Mycobacterium tuberculosis* (g2104394 g2113903), *T.aest.* = *Triticum aestivum* (g121129); *B.subtilis* = *Bacillus subtilis* (g2635821 g2634260); *Synechoc.* = *Synechocystis* (g1652630); *F.vel.* = *Flammulina velutipes* (g6468006); *S.typ.* = *Salmonella typhimurium* (g117277); *T.maritima* = *Thermotoga maritima* (g4981845); *S.glaucescens* = *Streptomyces glaucescens* (g153495); *M.thermo* = *Methanobacterium thermoautotrophicum* (g2621410); oxal. decarb. = oxalate decarboxylase; phos.man.isom. = phosphomannose isomerase; jack bean = *Canavalia ensimorfis*. The *P.furiosus* sequences are available from http://www.genome.utah.edu/sequence.html. Conserved amino acids are *shaded black*, conserved hydrophobic positions are *shaded grey*. The alignment was generated with T-Coffee (17) followed by small, manual refinements.

The molecular function of this cupin domain (consensus, $PG(X)_5HXH(X)_4E(X)_7G$ and $G(X)_5PXG(X)_2H(X)_3N$) is generally the binding of carbohydrates, and in some cases apparently to establish an interaction with other proteins (33,34). Among the homologs are two additional hypothetical proteins from *Pyrococcus* itself (PF_396648 and PF_62346), as well as several type-2 mannose-6-phosphate isomerases, oxalate decarboxylases, oxalate oxidases (germin), seed storage protein, canavalin (Fig. 5/6), as well as sugar-binding transcriptional regulators of the AraC family (33). No proteins with PGI activity have been reported to belong to this family before.

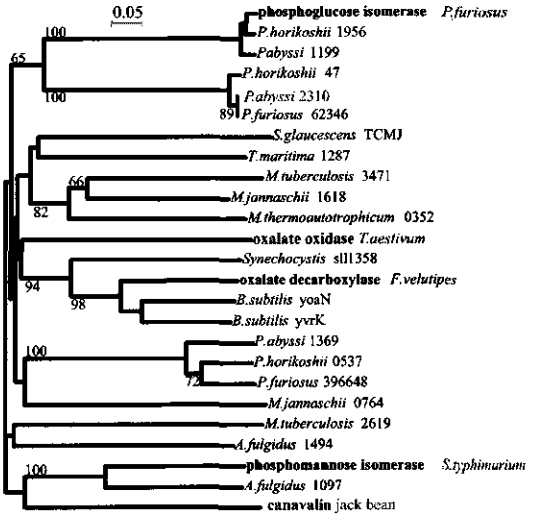

Figure 6.6 Neighbor joining tree of the aligned sequences.

The tree was generated with clustalX. Bootstrap values above 60 out of 100 are indicated. The genes PH1956 from *Pyrococcus horikoshii* and PAB1199 from *Pyrococcus abyssi* are clearly orthologous to the PGI from *P.furiosus*. No other orthologous are present in currently available genomes.

Recruitment of enzymes in unique "top" glycolysis

The identification of PGI allows a comparison of the nine-enzyme glycolysis in *Pyrococcus* with the classical ten-enzyme glycolysis in bacteria and eucarya. Notably four of the nine pyrococcal enzymes, that were identified experimentally, are non-homologous to their classical counterparts. Here we have shown, based on sequence comparison and on structural data, that the *P. furiosus* PGI (the second step in glycolysis) is not homologous to the bacterial and eukaryal PGI. The other five enzymes (fructose-1,6-bisphosphate aldolase, triosephosphate isomerase, phosphoglycerate mutase, enolase, and pyruvate kinase) have been predicted on the basis of

orthology with bacterial proteins (9). Four of these five are orthologous to their bacterial counterparts in the glycolysis. The fifth, fructose-1,6-bisphosphate aldolase, is not orthologous to the standard bacterial class II aldolase (35). This aldolase has recently been proposed to constitute a new family of aldolases, archaeal type ClassI aldolase (ClassIA), that is rare in bacteria and abundant in archaea, and only distantly related to ClassI fructose-1,6-bisphosphate aldolases (31).

The question remains whether or not a complete glycolytic pathway existed at the time that the non-homologous enzymes evolved in *Pyrococcus*; in other words, was (part of) the glycolytic pathway introduced by these newly evolving enzyme activities, or was it rather a substitution of their classical counterparts. Two patterns in these non-homologous replacements argue for an independent invention of the glycolysis that, made use of enzymes of an incomplete glyconeogenic pathway (from pyruvate to fructose-1,6-bisphosphate) that was already present: (i) three of the unique glycolytic steps in *Pyrococcus* are specifically catabolic (ADP-GLK, ADP-PFK and GAPOR); (ii) the first three unique steps (catalyzed by ADP-GLK, PGI, and ADP-PFK) form the part of the pathway that is rather *specific* for glucose degradation, whereas the more conserved part of the pathway (the interconversion of glyceraldehyde-3-phosphate and pyruvate) is made up by a more *general* set of enzymes that are potentially involved in numerous metabolic routes. This would argue for an independent invention of the glycolytic pathway in the lineage leading to *Pyrococcus*. Although non-homologous displacement of enzymes in *Pyrococcus* central carbohydrate metabolism has been observed before (36), this would be, to our knowledge, the first example of such excessive replacement of enzymes in a pathway, and is a compelling example of convergent evolution.

Acknowledgment

This research was supported by the Earth and Life Sciences Foundation (ALW), which is subsidized by the Netherlands Organization for Scientific Research (NWO).

References

1. Kengen, S.W.M., De Bok, F.A.M., Van Loo, N.D., Dijkema, C., Stams, A.J.M., and De Vos, W.M. (1994) *J. Biol.Chem.* **269**, 17537-17541
2. Kengen, S.W.M, Tuininga, J.E., De Bok, F.A.M., Stams, A.J.M., and De Vos, W.M. (1995) *J. Biol. Chem.* **270**, 30453-30457
3. Tuininga, J.E., Verhees, C.H., Van der Oost, J., Kengen, S.W.M., Stams, A.J.M, and De Vos, W.M (1999) *J. Biol. Chem.* **274**, 21023-21028
4. Mukund, S., and Adams, M.W.W. (1995) *J. Biol. Chem.* **273**, 28149-28154

5. Van der Oost, J., Schut, G., Kengen, S.W.M., Hagen, W.R., Thomm, M., and De Vos, W.M. (1998) *J.Biol. Chem.* **273**, 28149-28154
6. Ito, S., Fushinobu, S., Yoshioka, I., Koga, S., Matsuzawa, H., and Wakagi, T. (2001) *Structure* **9**, 205-214
7. Siebers, B., Klenk, H.-P., and Hensel, R. (1998) *J. Bacteriol.* **180**, 2137-2143
8. Bork, P., Sander, C., and Valencia, A. (1993) *Protein Science* **2**, 31-40
9. Dandekar, T., Schutser, S., Snel, B., Huynen, M., and Bork, P. (1999) *Biochem. J.* **343**, 115-124
10. Schäfer, T., and Schönheit, P. (1992) *Arch. Microbiol.* **158**, 188-202
11. Schäfer, T., and Schönheit, P. (1993) *Arch. Microbiol.* **159**, 354-363
12. Ruijter, G.J.G., and Visser, J. (1999) *Biochimie* **81**, 267-272
13. Sambrook, J., Fritsch, E.F., and Maniatis, T. (1989) *Molecular Cloning: A Laboratory Manual,* 2nd Ed., Cold Spring Harbor Laboratory, Cold Spring Harbor, NY
14. Bradford, M.M. (1976) *Anal. Biochem.* **72**, 248-254
15. Kengen, S.W.M., Luesink, E.J., Stams, A.J.M., and Zehnder, A.J.B. (1993) *Eur. J. Biochem.* **213**, 305-312
16. Ward, D.E., Kengen, S.W.M., Van der Oost, J., and De Vos, W.M. (2000) *J. Bacteriol.* **182**, 2559-2566
17. Notredame, C., Higgins, D.G., and Heringa, J. (2000) *J. Mol. Biol.* **8**, 205-217
18. Saitou, N., and Nei, M. (1987) *Mol. Biol. Evol.* **4**, 406-425
19. Jeanmougin, F., Thompson, J.D., Gouy, M., Higgins, D.G., and Gibson, T.J. (1998) *Trends Biochem. Sci.* **23**, 403-405
20. Rost, B. (1996) *Methods Enzymol.* **226**, 525-539
21. Takama, M., and Nosoh, Y. (1980) *J. Biochem.* **87**, 1821-1827
22. Schreyer, R., and Bock, A. (1980) *Arch. Microbiol.* **127**, 289-298
23. Marchand, M., Kooystra, U., Wierenga, R.K., Lambeir, A., Van Beeumen, J., Opperdoes, F.R., and Michels, P.A.M. (1989) *Eur. J. Biochem.* **184**, 455-464
24. Lowe, S.L., and Reithel, F.J. (1975) *J. Biol. Chem.* **250**, 94-99
25. Li, X., and Chirgwin, J.M. (2000) *Biochim. Biophys. Acta.* **1476**, 363-367
26. Nataka, M., Yoshimura, S. (1964) *Agric. Biol. Chem.* **28**, 510-516
27. Thomas, D.A. (1981) *J. Gen. Microbiol.* **124**, 403-407
28. Hansen, T., Oehlmann, M., and Schönheit, P. (2001) *J. Bacteriol.* **183**, 3428-3435
29. Bell, S.D, Kosa, P.L., Sigler, P.B., Jackson, S.P. (1999) *Proc. Natl. Acad. Sci. U.S.A.* **96**, 13662-13667
30. Robinson, K.A., and Schreier, H.J. (1994) *Gene* **151**, 173-176
31. Siebers, B., Brinkmann, H., Dörr, C., Tjaden, B., Lilie, H., Van der Oost, J, and Verhees, C.H. (2001) *J. Biol. Chem.* **276**, 28710-28718
32. Ko, T.P., Day, J., and McPherson, A. (2000) *Acta Crystallogr. D Biol. Crystallogr.* **56**, 411-420
33. Dunwell, J.M., Khuri, S., Gane, P.J. (2000) *Microbiol. Mol. Biol. Rev.* **64**, 153-179
34. Anantharaman, V., Koonin, E.V., and Aravind, L. (2001) *J. Mol. Biol.* **307**, 1271-1292
35. Galperin, M.Y., Aravind, L., and Koonin, E.V. (2000) *FEMS Microbiol. Lett.* **183**, 259-264
36. Huynen, M.A., Dandekar, T., and Bork, P. (1999) *Trends Microbiol.* 7, 281-291

Chapter 7

Archaeal fructose-1,6-bisphosphate aldolases constitute a new family of archaeal type class I aldolase

Bettina Siebers, Henner Brinkmann, Christine Dörr, Britta Tjaden, Hauke Lilie, John van der Oost and Corné H. Verhees

Journal of Biological Chemistry 276: 28710-28718 (2001)

Abstract

Fructose-1,6-bisphosphate (FBP) aldolase activity has previously been detected in several Archaea. However, no obvious orthologs of the bacterial and eucaryal Class I and II FBP aldolases have yet been identified in sequenced archaeal genomes. Based on a recently described novel type of bacterial aldolase, we report on the identification and molecular characterization of the first archaeal FBP aldolases. We have analyzed the FBP aldolases of two hyperthermophilic Archaea, the facultatively heterotrophic Crenarchaeon *Thermoproteus tenax* and the obligately heterotrophic Euryarchaeon *Pyrococcus furiosus*. For enzymatic studies the *fba* genes of *T. tenax* and *P. furiosus* were expressed in *E. coli*. The recombinant FBP aldolases show preferred substrate specificity for FBP in the catabolic direction and exhibit metal-independent Class I FBP aldolase activity, via a Schiff-base mechanism. Transcript analyses reveal that the expression of both archaeal genes is induced during sugar fermentation. Remarkably, the *fbp* gene of *T. tenax* is co-transcribed with the *pfp* gene which codes for the reversible PP_i-dependent phosphofructokinase. As revealed by phylogenetic analyses, orthologs of the *T. tenax* and *P. furiosus* enzyme appear to be present in almost all sequenced archaeal genomes, as well as in some bacterial genomes, strongly suggesting that this new enzyme family represents the typical archaeal FBP aldolase. Because this new family shows no significant sequence similarity to classical Class I and II enzymes, a new name is proposed, archaeal type Class I FBP aldolases (FBP aldolase Class IA).

Introduction

Fructose-1,6-bisphosphate (FBP) aldolase (EC 4.1.2.13) catalyzes the reversible aldol condensation of glyceraldehyde 3-phosphate (GAP) and dihydroxyacetone phosphate (DHAP) yielding FBP. The enzyme fulfills an amphibolic function being involved in catabolic (glycolysis) as well as anabolic pathways (gluconeogenesis, Calvin cycle). In spite of this central function in carbohydrate metabolism, up to now no archaeal genes coding for the respective enzyme activities have been analyzed.

Two distinct classes of FBP aldolases occur in nature, which differ in their enzymatic mechanisms (1, 2, 3, 4). Class I FBP aldolases form a Schiff-base intermediate between the carbonyl substrate (FBP, DHAP) and the ε-amino group of the active-site lysine residue, and are inactivated by borohydride ($NaBH_4$), whereas Class II FBP aldolases depend on divalent metal ions to stabilize the carbanion intermediate and are, therefore, inhibited by EDTA. Class II enzymes of bacterial and eucaryal origin generally form dimers with a subunit molecular mass of approx. 40 kDa, whereas the Class I pendants are heterogeneous: Eucaryal aldolases are homomeric tetramers with a subunit molecular mass of approx. 40 kDa and for bacterial enzymes oligomeric

arrangements from monomer to decamer and subunit molecular masses of 27 – 40 kDa have been described (5, 6).

Sequence comparisons of Class I and II FBP aldolases revealed no detectable sequence homology, suggesting convergent evolution (4, 5, 7, 8, 9, 10, 11). The latter is supported by comparisons of available crystal structures of rabbit muscle Class I and *E. coli* Class II FBP aldolases indicating that even though both classes adopt a common folding topology ($(\beta\alpha)_8$ triose-phosphate isomerase (TIM)-barrel fold) and catalyze identical reactions, they share no conserved catalytic residues and the location of their active sites is distinct (12). However, more recent analysis combining sequence, structure and functional information indicate that many of the $(\beta\alpha)_8$ (TIM) barrel superfamilies, such as aldolases, TIMs, enolases, share a common evolutionary origin (ancestral β/α barrel), although they adopt a wide range of enzymatic functions (13, 14).

The distribution of FBP aldolases during evolution is complex and still puzzling. Class II aldolases seem to be confined to more simple organisms such as bacteria and a few unicellular eukaryotes (fungi, including yeast), whereas Class I FBP aldolases are present in higher forms of life (animals, higher plants, ferns, mosses), and only a few bacteria possess a Class I enzyme, sometimes in addition to a Class II enzyme. Earlier-branching protists studied so far show a marked diversity of harboring Class I and/or Class II enzymes (for review see 5, 10).

Recently, Thomson *et al.* (6) described a new type of FBP aldolase in *E. coli*, which belongs to Class I aldolases according to its Schiff-base mechanism, but differs significantly from the other members of this class by its low sequence similarity. The *E. coli* Class I FBP aldolase was originally mis-annotated in the *E. coli* genome as dehydrin (DhnA, *dhnA* gene) due to its overall identity (13-20 %) to dehydrins in plants, which are stress proteins that are induced in response to dehydration (6).

Although Class I and Class II FBP aldolase activities have been demonstrated in Archaea (15, 16, 17, 18, 19, 20, 21), no genes encoding classical Class I or II enzymes have been identified in any of the sequenced archaeal genomes suggesting that Archaea possess novel types of aldolases that are either absent or not yet recognized as such in Bacteria and Eucarya. The latter is supported by initial database searches of Galperin *et al.* (22) who identified gene homologs of the unusual Class I FBP aldolase gene (*dhn*A) of *E. coli* in the sequenced archaeal genomes. However, none of this archaeal gene products was examined with respect to its enzymatic function. In order to prove that DhnA homologs in the two major archaeal kingdoms code for FBP aldolases, we expressed the *dhnA* gene homologs of the crenarchaeote *Thermoproteus tenax* and the euryarchaeote *Pyrococcus furiosus* in *E. coli* and we analyzed the function of their gene products. The two hyperthermophiles differ from each other not only with respect to phylogeny but also with respect to physiology: *T. tenax* is a facultative chemoorganotroph (23, 24) and *P. furiosus* is an obligate chemoorganotroph (25). *T. tenax* uses two different pathways for carbohydrate catabolism, *i.e.* a modified, non-

phosphorylative Entner-Doudoroff pathway and a variant of the reversible Embden-Meyerhof-Parnas pathway (19, 26). The latter is characterized by a PP_i-dependent phosphofructokinase (PP_i-PFK) (27), two different glyceraldehyde-3-phosphate dehydrogenase (28, 29) and a pyruvate kinase with reduced allosteric potential (30). *P. furiosus* possesses one catabolic pathway, a variant of the Embden-Meyerhof-Parnas pathway which differs significantly from the *T. tenax* variant (21) and involves an ADP-dependent glucokinase (31), an ADP-dependent PFK (32), a canonical glyceraldehyde-3-phosphate dehydrogenase and a ferredoxin-dependent glyceraldehyde-3-phosphate oxidoreductase (33, 34).

Experimental procedures

Chemicals and plasmids

DL-GAP was prepared from monobarium salts of the diethyl acetal, according to the manufacturer's instructions (Sigma). All other chemicals and enzymes were purchased from Sigma, Merck or Roche Diagnostic GmbH in analytical grade. For heterologuous expression the vector pET-15b and pET-24d (Novagen) and for generating antisense mRNA the vector pSPT 19 (Roche Diagnostics GmbH) were used.

Strains and Growth Conditions

Mass cultures of *T. tenax* Kra1 (DSM 2078) were grown as described previously (19). *P. furiosus* (DSM 3638) was grown in CDM medium as described previously (35) with the only exception that yeast extract was omitted and substituted by the individual amino acids (0.25 mM final concentration). Maltose (10 mM) or pyruvate (40 mM) was added as primary carbon source. *Escherichia coli* strains DH5α (Life Technologies, Inc.), XL1Blue (Stratagene), BL21(DE3) and BL21(DE3)pLysS (Novagen) for cloning and expression studies were grown under standard conditions (36) following the instructions of the manufacturer.

Enzyme Assay

The FBP aldolase activity was determined in catabolic direction (FBP cleavage) at 50 °C in a coupled assay with glycerol-3-phosphate dehydrogenase (EC 1.1.1.8) and (EC 5.3.1.1) of rabbit muscle as auxiliary enzymes. For the *T. tenax* enzyme the assay (total volume 1 ml) was performed in 100 mM Tris/HCl (pH 7.0, 50 °C) in the presence of 0.4 mM NADH, 5 mM FBP and 4 units of glycerol-3-phosphate dehydrogenase and 20 units of triose-phosphate isomerase. Enzymatic activities were measured by monitoring the increase in absorption at 366 nm ($\varepsilon_{50\,°C} = 3.36\ mM^{-1}cm^{-1}$). The assay mixture (1-ml volume) for the *P. furiosus* FBP aldolase contained 50 mM Tris/HCl

(pH 7.0, 50 °C), 0.2 mM NADH, 2.5 mM FBP, 4 units of glycerol-3-phosphate dehydrogenase and 11 units of triose-phosphate isomerase. The absorbance was followed at 340 nm (ε = 6.3 $mM^{-1}cm^{-1}$).

Reactions were started by addition of the substrate FBP and the enzyme concentrations ranged from 2 - 40 µg of protein/ml test volume. To determine the substrate specificity of the FBP aldolases, the standard enzyme assay was used substituting FBP by other substrates, such as fructose 1-phosphate (Fru-1-P). For effector studies citrate was added to an end concentration of 10 mM in the presence of half-saturating concentrations of FBP. To test the metal ion requirement up to 10 mM EDTA or different metal ions (0.1 and 1 mM) were added to the mixture. Protein concentration was measured according to the method of Bradford (37) using the Bio Rad Protein-Assay (Bio-Rad) with BSA as standard.

Active Site Labeling

To investigate the involvement of a Schiff-base mechanism the FBP aldolase of *T. tenax* (0.09 mg protein) was incubated at room temperature in 50 mM HEPES/KOH (pH 7.5), 100 mM $NaBH_4$ (1 M stock solution in 10 mM NaOH) in the presence or absence of saturating concentrations (10 mM) of D,L-GAP, DHAP or FBP (total volume: 250 µl). After 10 min the samples were dialyzed twice against 2 liters of 20 mM Tris/HCl (pH 8.5, 4 °C; overnight) and assayed for FBP aldolase activity. The assay was perfomed at 70 °C using the non-phosphorylating NAD^+-dependent glyceraldehyde-3-phosphate dehydrogenase (EC 1.2.1.9) (28) of *T. tenax* as auxiliary enzyme. The assay (total volume 1 ml) was performed in 100 mM Tris/HCl (pH 7.0, 70 °C) in the presence of 5 mM NAD^+, 5 mM FBP and 5 units of NAD^+-dependent glyceraldehyde-3-phosphate dehydrogenase. The increase in absorption was measured at 366 nm. ($\varepsilon_{70\,°C}$ = 3.15 $mM^{-1}cm^{-1}$).

Cloning and Sequencing of the Coding Genes

The identification of both genes encoding FBP aldolase (*fba*) was based on significant sequence similarity to the recently described *E. coli* Class I FBP aldolase (DhnA, GenBank™ accession number P71295). The *fba* gene of *T. tenax* (EMBL accession number AJ310483) was identified by sequencing the genomic clone (5.2 kb *Hin*dIII fragment) harboring the *pfp* gene (27). The *P. furiosus* gene (GenBank™ accession number AF368256, NCBI) was identified in the *P. furiosus* database (http://www.genome.utah.edu).

Expression of the FBP aldolases in E. coli

For expression of the *T. tenax* FBP aldolase the coding region was cloned into pET-15b via two new restriction sites (*Nco*I, *Bam*HI) introduced by PCR mutagenesis with the primers FBPA-f

(GCTCAAGCATCCATGGCAAA, sense) and FBPA-rev (CCCCCGTCAGGGATCCTATC, antisense). The following primer set was designed to amplify the *P. furiosus* open reading frame in pET-24d (*Nco*I, *Bam*HI) and to delete an internal *Nco*I restriction site using the PCR-based overlap extension method (38): BG749 (CGCGCGCGCCATGGAGGCCCCTCAAAATGTTGG, sense), BG750 (CCGTGGTCCATCGCGAAGATTAA, antisense), BG751 (TTAATCTTCGCGATGG-ACCACGG, sense) and BG688 (GCGCGGATCCTCAAATGAGACCTTCTGCCTTAGC, antisense). The introduced mutations are shown in boldface and introduced *Nco*I and *Bam*HI restriction sites are underlined. The sequence of both expression clones was confirmed by sequencing both strands. Expression of the *T. tenax* enzyme in *E. coli* BL21(DE3)pLysS and of the *P. furiosus* enzyme in BL21(DE3) was performed following the instructions of the manufacturer (Novagen).

Site-directed mutagenesis of the P. furiosus FBP aldolase

The active site mutation was introduced in the *P. furiosus fba* gene using *Pfu* polymerase in the PCR-based overlap extension method (38). The following primer set was designed to introduce mutation K191A: BG827 (AGCAGATATGATAGCGACCTATTGGAC, sense) and BG828 (GTCCAATAGGTCGCTATCATATCTGCT, antisense), the introduced mutations are shown in boldface.

Purification of recombinant FBP aldolases of T. tenax and P. furiosus

For purification of the recombinant *T. tenax* enzyme 10 g of *E. coli* cells were resuspended in 20 ml of 100 mM HEPES/KOH (pH 7.5) containing 300 mM 2-mercaptoethanol and passed three times through a French press cell at 150 megapascals. After centrifugation (20,000 x g, 45 min, 4 °C) the crude extract was heat-precipitated (90 °C, 30 min), centrifuged again and dialyzed over night against 50 mM HEPES/KOH (pH 7.5) containing 5 mM dithiothreitol (2-liters volume, 4 °C). The dialyzed fraction was applied to Q-Sepharose fast-flow (Amersham Pharmacia Biotech) equilibrated in the same buffer and eluted with a linear salt gradient of 0 - 500 mM KCl. Fractions containing the homogeneous enzyme solution were pooled.

For the purification of the recombinant FBP aldolase from *P. furiosus*, 3 g of *E. coli* cells were resuspended in 10 ml of 50 mM Tris/HCl (pH 7.8). The suspension was passed twice through a French press cell (100 megapascals), and cell debris was removed by centrifugation (10,000 x g, 20 min, 4 °C). After heat precipitation (70 °C, 30 min) and centrifugation the supernatant was filtered through a 0.45-µm filter and loaded onto a mono Q HR 5/5 column (Amersham Pharmacia Biotech) equilibrated in 50 mM Tris/HCl (pH 7.8). Proteins were eluted by a linear salt gradient of 0 - 1000 mM NaCl. Active fractions were pooled, concentrated by microfiltration (Centricon 30, Amicon) and applied to a Superdex 200 prep grade column (Amersham Pharmacia Biotech),

equilibrated in 50 mM Tris/HCl (pH 7.8), 100 mM NaCl. Fractions containing the homogeneous enzyme were pooled.

Analytical ultracentrifugation of the T. tenax FBP aldolase

Sedimentation velocity and equilibrium analyses were conducted using an analytical ultracentrifuge Optima X-LA (Beckman Instruments, Palo Alto, CA) equipped with double sector cells and an AnTi 50 rotor. The protein was dissolved in 50 mM HEPES/KOH (pH 7.5) containing 100 mM KCl and 2 mM dithiothreitol at a concentration of 0.48 mg protein/ml. Sedimentation velocity experiments were performed at 30,000 rpm (20 °C) and the data were analyzed according to the sedimentation time derivative method (39). Sedimentation equilibrium was analyzed at 6,000 rpm (20 °C) using the software provided by Beckman Instruments. Gel filtration experiments were performed as described previous (27).

Northern blot analyses of the T. tenax fba transcript

Preparation of total RNA from auto- and heterotrophically grown *T. tenax* cells and Northern blot analyses were performed as described before (30). Digoxigenin-labeled antisense mRNA of FBP aldolase and PP_i-PFK were obtained by *in vitro* transcription from the T7 promoter of vector pSPT 19 (Roche Diagnostics GmbH). A part of the coding region of FBP aldolase (502 bp) and the coding region of PP_i-PFK (1011 bp) was cloned into the *Eco*RI and *Bam*HI restriction sites of the vector by PCR mutagenesis using the primer sets CGAGGAGGGGGAATTCCATA (sense) and GAAGGTCTTGGGATCCCCCG (antisense) for FBP aldolase and GCTGGCCG-AGCCTCTGAATTCATGAAGATAG (sense) and CTAGGCAAAGAGGGATCCGGGGCCT-AGC (antisense) for PP_i-PFK. The introduced mutations are shown in boldface and the *Eco*R1 and *Bam*H1 restriction sites are underlined.

Primer extension analyses

Primer extension analyses for *T. tenax* were performed as described previously (30). To map the transcription start site of the *fba–pfp* transcript the 5'-^{32}P-labeled antisense oligonucleotide (5'-CCGTGCTCAATGCCGTGG-3', position 72 – 89 of the *fba* gene) was used as primer for cDNA synthesis. For *P. furiosus* total RNA was isolated from maltose and pyruvate grown cells as described previously (40), and the transcription start was determined with a fluorescence (IRD800)-labeled antisense oligonucleotide (5'-CAAAGTCCGTAGGGCCGTGC-3' (MWG), position 99 - 118 of the *fba* gene). The primer extension reaction was performed using the Reverse transcription System (Promega) according to the instructions of the manufacturer with following modifications. Hybridization of total RNA (15 µg) and oligonucleotide (5 pmol) was performed for 10 min at 68 °C before allowing to cool to room temperature. The reaction (20-µl final volume) was started by

addition of dNTPs (1 mM), $MgCl_2$ (5 mM), RNAsin (20 units) and Avian Myeloblastosis Virus reverse transcriptase (22.5 units). After incubation for 30 min at 45 °C, the reaction volume was diluted to 50 µl with 10 mM Tris/HCl (pH 8.5), 1 µl of RNaseA (5 mg/ml) was added and the sample was incubated for 10 min at 37 °C. cDNA was precipitated with ethanol, dissolved in 3 µl loading buffer and 1 µl was applied to a sequencing gel in parallel with the sequencing reactions obtained with the same oligonucleotide.

Sequence retrieval and phylogenetic analyses

Protein sequences were extracted from GenBank™ and the TIGR microbial data base using BLAST and first aligned with CLUSTALW (41), this alignment was manually refined using the MUST program package (42). Regions of uncertain alignment and partial sequences were omitted from the analyses leaving a total of 27 sequences and 172 amino acid positions. The topology of the phylogenetic tree was inferred using the PROTML program of the MOLPHY v. 2.3 package (43), starting with the NJDIST tree using the local rearrangement and the JTT-F options. A gamma parameter based maximum likelihood estimate of the branch length of the tree as well as of the statistical support for internal nodes (quartet puzzling support values) was performed using the program puzzle v.5 (44). Distance analyses including 1000 bootstrap replicates were performed with the MUST package using the Kimura correction and the neighbour joining method (45). Parsimony bootstrap analysis was performed using PAUP* with 2000 bootstrap replicates and 10 times random addition (46). Secondary structure prediction was performed using the predictprotein program (http://www.embl-heidelberg/predictprotein/) (47, 48).

Results

Nucleotide sequence of the fba genes of T. tenax and P. furiosus

Both *fba* genes were identified due to their sequence similarity with the recently characterized Class I FBP aldolase from *E. coli* (DhnA, *dhn*A gene) (6). The *T. tenax* enzyme was identified by sequence analysis of the genomic clone comprising the *pfp* gene (5.2 kb *Hin*dIII fragment), which revealed an additional open reading frame of 792 bp (Fig. 7.1) preceding the *pfp* gene (1014 bp) (27). This open reading frame codes for a polypeptide of 263 amino acid residues with a calculated molecular mass of 28.7 kDa and showed high overall similarity (26 % identity, blast database search) to the Class I FBP aldolase (DhnA) of *E. coli* (6). Strikingly, the coding regions of both *T. tenax* genes *fba* and *pfp* overlap by 1 bp with the A of the start codon (ATG) of the *pfp* gene being the last nucleotide of the triplet encoding the C-terminal valine (GTA) of the *fba* gene (Fig. 7.1). The *fba* gene of *P. furiosus* (846 bp) was identified in the *P. furiosus* database by

similarity of the translated 31.1 kDa polypeptide (282 amino acid residues) to *E. coli* DhnA (26 % identity, blast database search). Contrary to *T. tenax*, the *P. furiosus fba* gene is separated from the next neighbored downstream open reading frame with similarity to agmatinase (*speB* gene) by 61 nucleotides and therefore is presumably not organized in an operon structure (Fig. 7.1).

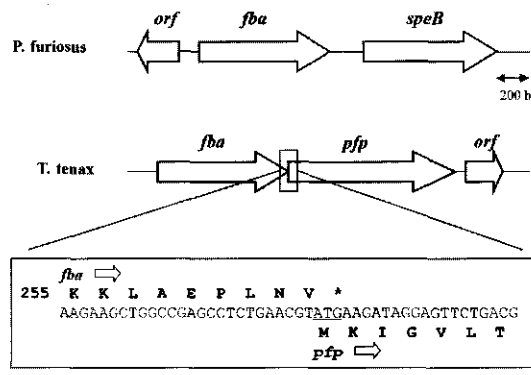

Figure 7.1 Genomic organization and flanking regions of the *P. furiosus fba* gene and the *T. tenax fba-pfp* operon. *Arrows* represent the open reading frames and their orientation. The enlargement shows the overlapping regions of the *fba* and *pfp* gene in *T. tenax*, the respective protein sequence is shown in *bold letters*. The *fba* stop codon is marked by asterisk and the ATG start codon of the *pfp* gene is *underlined*.

Expression of the fba genes from T. tenax and P. furiosus in E. coli and purification of recombinant FBP aldolases

The *fba* gene products of *T. tenax* and *P. furiosus* were expressed in *E. coli* and their FBP aldolase activity was confirmed for both enzymes using a coupled enzyme assay. For further biochemical studies both recombinant enzymes were purified. From 10 g wet cells of recombinant *E. coli*, 14 mg of homogeneous *T. tenax* FBP aldolase with a specific activity of 0.23 units/mg protein (50 °C) and from 3 g wet cells of recombinant *E. coli* 5 mg of homogeneous *P. furiosus* protein with a specific activity of 0.58 units/mg (50 °C) were recovered, respectively.

Enzymatic properties of the recombinant FBP aldolase of T. tenax and P. furiosus

The purified, recombinant FBP aldolases of *T. tenax* and *P. furiosus* exhibit Michaelis-Menten kinetics for FBP in the catabolic (aldol cleavage) direction. The K_m and V_{max} values for FBP were 9 µM and 0.23 units/mg for *T. tenax* and 3.6 µM and 0.61 units/mg for *P. furiosus* and as such comparable to the *E. coli* Class I FBP aldolase (DhnA) (Table 7.1) (6). Like the *E. coli* enzyme both archaeal FBP aldolases showed additional activity with Fru-1-P, although the much higher K_m for Fru-1-P (*T. tenax* 498-fold, *P. furiosus* 197-fold, *E. coli* 1650-fold) of all three enzymes strongly

suggests that FBP is the physiological substrate (Table 7.1). As shown for the FBP aldolase of *T. tenax* other sugar phosphates such as fructose 6-phosphate, glucose 6-phosphate, fructose 2,6-bisphosphate, and 6-phosphogluconate (concentration range of 5 - 10 mM) do not serve as substrates in the catabolic direction. Both archaeal FBP aldolases, however, like the *E. coli* enzyme, were activated in presence of saturating concentrations of citrate (10 mM) by factor 2.2 and 2.4, respectively (Table 7.1).

Table 7.1. Comparative analysis of archaeal type Class I FBP aldolases.

	Crenarchaea *T.tenax*	*Euryarchaea* *P. furiosus*	Bacteria *E. coli* (6)
Molecular mass of native enzyme (kDa)	241 (small form)	272	340
Molecular mass of subunit size (kDa)	28.7	31.1	38.0
Oligomeric structure	8 (small form)	8	8-10
Active site	Lys-177	Lys-191	Lys-237
Activation by citrate (10 mM)	2.2x	2.4x	14.6x
K_m FBP (mM)	0.009	0.0036	0.02
V_{max} FBP (units/mg)	0.23	0.61	0.34
k_{cat}/K_m ($mM^{-1}min^{-1}$)	734.4	5278	646
K_m Fru-1-P (mM)	4.48	0.71	33
V_{max} Fru-1-P (units/mg)	0.3	0.75	0.18
k_{cat}/K_m ($mM^{-1}min^{-1}$)	1.89	32.8	0.21

Enzyme assays for *T. tenax* and *P. furiosus* were performed at 50 °C.

The involvement of a Schiff-base mechanism in the FBP aldolase reaction was examined for the *T. tenax* enzyme by treating the enzyme with sodium borohydride in the presence and absence of the substrates GAP, DHAP and FBP. The significant reduction of the specific activity in the presence of the carbonyl substrates DHAP (38 % residual activity) and FBP (29 % residual activity) as compared to the presence of GAP (80 % residual activity) and the control, after $NaBH_4$ treatment (100 % activity, 0.8 U/mg protein, 70 °C), accounts for the formation of a Schiff-base in the enzyme reaction. In accordance with these results, a lysine residue is conserved at position 177 in the *T. tenax* sequence (Fig. 7.4) which corresponds to the active site Lys-237 (falsely marked as Lys-236) in the *E. coli* Class I FBP aldolase (DhnA) (6). Finally, the observation that neither metal ions such as Mn^{2+}, Mg^{2+}, Zn^{2+}, Ca^{2+} and Fe^{2+} (concentrations tested: 0.1 and 1 mM) nor EDTA (concentrations tested: 0.1 mM, 1 mM, 10 mM) affect the enzyme activity supports the biochemical classification of the *T. tenax* enzyme as Class I aldolase. As shown in Fig. 7.4 also the *P. furiosus* FBP aldolase exhibits the active site lysine residue (position 191) and the assumed involvement of a Schiff-base mechanism was supported by site-directed mutagenesis of the active site lysine to alanine (K191A) resulting in a virtually inactive mutant enzyme (not shown).

Molecular mass

The homogenous FBP aldolases from *T. tenax* and *P. furiosus* revealed similar subunit sizes in SDS-PAGE of approx. 30 kDa and 33 kDa, respectively, thus being in good agreement with the calculated molecular mass of 28.7 kDa and 31.1 kDa. However, differences between the two enzymes are obvious concerning their oligomeric state under native conditions (Table 7.1). Gel filtration experiments revealed for the recombinant *P. furiosus* enzyme an apparently uniform oligomer with a molecular mass of 272 kDa (representing presumably octamers), whereas for the *T. tenax* FBP aldolase two different oligomeric forms were identified. As shown by repeated chromatography of the separated oligomers, both forms are convertible to one another. Sedimentation velocity experiments revealed two distinct oligomers with apparent sedimentation coefficients of 9.34 S and 14.5 S indicating a slow equilibration reaction between the two forms of the *T. tenax* FBP aldolase. For the smaller association form an apparent molecular mass of 237-245 kDa was determined by sedimentation equilibrium centrifugation suggesting a stoichiometry of eight monomers per oligomer.

Transcript analyses

To determine if the expression of FBP aldolase of *T. tenax* and *P. furiosus* are controlled at transcriptional level, we examined the effect of the carbon source on *fbp* transcription. Since the juxtaposition of *fba* and *pfp* gene in *T. tenax* suggests an operon organization specific antisense mRNA probes for the *pfp* and *fba* gene were used to test for the formation of co-transcripts (Fig. .2).

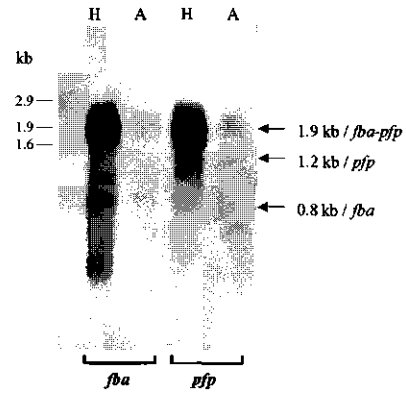

Figure 7.2 Transcript analysis of the *T. tenax fba-pfp* operon.

Northern blot analysis with digoxigenin-labeled, *fba*- and *pfp*-specific antisense mRNAs and total RNA (5 µg) from autotrophically (*A*) as well as heterotrophically (*H*) grown cells. The RNA molecular size standard (*left*) and the derived transcript size (*arrows, right*) are shown.

Northern blot experiments were performed with total RNA from autotrophically (in the presence of CO_2 and H_2) and heterotrophically (in the presence of glucose) grown *T. tenax* cells.They revealed a strong hybridization signal for both probes at 1.9 kb and two additional, weaker, probe-specific signals at 1.2 kb for the *pfp* probe and 0.8 kb for the *fba* probe, thus indicating the presence of bicistronic as well as monocistronic messages. The signals of both probes were much stronger with mRNA from heterotrophically compared to autotrophically grown cells (Fig. 7.2). Densitometric quantification of slot blot analysis using the *pfp* probe and different concentrations of total RNA (10 – 0.625 µg) from auto- or heterotrophically grown cells, revealed a six-fold higher transcript abundance in the latter (data not shown). Also in *P. furiosus* cells grown on maltose or pyruvate the transcript level of the *fba* gene varied similarly (dot blot analysis, data not shown). Like in *T. tenax* conditions favoring the catabolic direction (growth on maltose) induce a higher transcript amount (2-3 fold increase) as compared to anabolic conditions (growth on pyruvate).

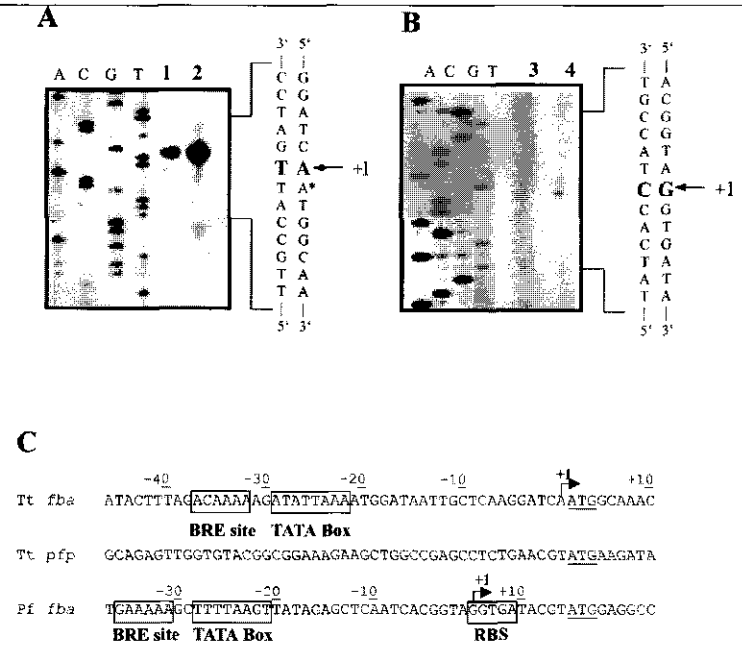

Figure 7. 3 Determination of transcript start sites and identification of putative promoter elements.

(**A**) Mapping of the transcription start of the *T. tenax fba-pfp* operon and (**B**) the *P. furiosus fba* gene by primer extension. The transcripts begin at position +1 (*arrow*), the start codon (ATG) is marked by an *asterisk*, and the sequence ladder (*lanes A, C, G* and *T*) is shown. cDNA synthesis for *T. tenax* was performed with total RNA from autotrophically (CO_2, *lane 1*) and heterotrophically (glucose, *lane 2*) grown cells and for *P. furiosus* with total RNA from pyruvate- (*lane 3*) and maltose (*lane 4*)-grown cells. (**C**) Upstream nucleotide sequences of the *T. tenax* (Tt) *fba* and *pfp* gene and the *P. furiosus* (Pf) *fba* gene. The putative transcription factor B recognition elements (*BRE site*), the TATA box promoter elements and the ribosome-binding sites (*RBS*) are marked. The mapped starting points of transcription are marked by an arrow and the ATG start codons are *underlined.*

For a more accurate assignment of the promoter region in *T. tenax* and *P. furiosus* the transcription starts of the *fba-pfp* mRNA and the *fba* mRNA, respectively, were determined by primer extension analyses. For the *T. tenax fbp-pfp* operon an antisense oligonucleotide binding at position 72 - 89 of the *fba* gene was used. As shown in Fig. 7.3A transcription is initiated at the adenosine (A) immediately in front of the start codon (ATG) of the *fba* gene (position +1). A similar proximity of transcription and translation start site was already observed for the *pyk* gene, coding for the pyruvate kinase of *T. tenax* (30) and corresponds with the observation that some Archaea contain a high portion of mRNAs lacking Shine-Dalgano sequences in front of their coding genes (49, 50). In accordance with the Northern analyses the amount of copy DNA in the primer extension studies was by factor 4.5 - 7.1 higher in hetero- than in autotrophically grown *T. tenax* cells. The transcription start of the *P. furiosus fba* mRNA (Fig. 7.3B) was initiated at the guanosine 10 bp upstream of the ATG start codon (position +1) and in contrast to *T. tenax* a putative RBS was identified.

Inspection of the 5' flanking regions (Fig. 7.3C) revealed for the *fba* genes of *T. tenax* and *P. furiosus* AT-rich regions 20-30 nucleotides upstream of their transcription start sites, which correspond well with the archaeal promoter consensus sequences (51, 52, 53). In *T. tenax* the TATA box (crenarchaeal consensus sequence C/TTTTTAAA) is centered around position -25/-26 and 2 bp (-30 GA -31) upstream of the TATA box is the putative transcription factor B (TFB) recognition element (BRE site, consensus sequence A/GNA/TAAA/T). A putative ribosome-binding site (RBS, GGAGG) seems to be absent. In *P. furiosus* a putative RBS (GGTGA) is identified at position +1 - +5, the TATA box is positioned around –24/-25 and 2 bp upstream is the putative purine-rich BRE site (54).

Phylogenetic analyses

Databank searches with the *fba* genes of *T. tenax* and *P. furiosus* revealed sequences with apparent similarity to the Class I FBP aldolases of *E. coli* (DhnA) in some bacterial and all archaeal genomes, with the only exception being *Thermoplasma acidophilum*. Whereas most of the genomes analyzed contain only a single *dhnA* like gene, *Archaeoglobus fulgidus*, *Methanococcus jannaschii*, *Halobacterium* sp. NRC-1, and *E. coli* possess two paralogous genes (22). This new FBP aldolase family represents a divergent group with sequence similarities as low as about 20 % identity (based on the 172-amino acid core region used for the phylogenetic analyses) between the different groups. Nevertheless, despite this substantial divergence, the universal conservation of the active site lysine (Lys-177, *T. tenax*; Lys-191, *P. furiosus*; and Lys-237, *E. coli* DhnA) and an additional conserved sequence motif preceding the active site lysine (position 171-176 *T. tenax*) as well as three further conserved regions ranging from position 20-27, 98-109, 199-204 (numbering of *T. tenax fba* gene), characterize them unequivocally as homologs of *E. coli* Class I FBP aldolase (DhnA) (Fig. 7.4).

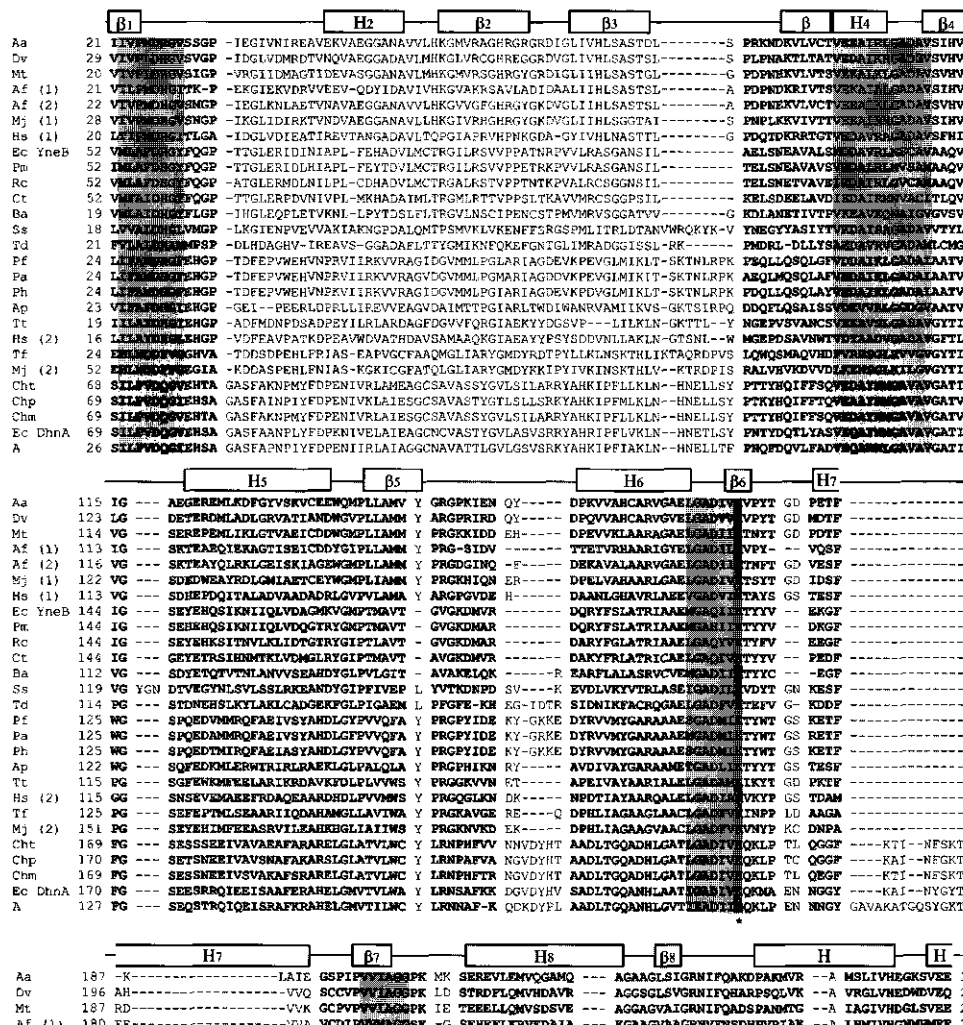

Figure 7.4 Multiple sequence alignment of archaeal type Class I FBP aldolases.

Boldface letters indicate amino acid residues used in the phylogenetic analyses. The predicted secondary structure of the *T. tenax* enzyme is shown *above* the sequences (47, 48). Conserved sequence motifs are *shaded*. The predicted phosphate-binding motif of many TIM barrel proteins is indicated by (P) and the catalytic lysine residue (Lys-237) determined for the *E. coli* Class I FBP aldolase (DhnA) (6) and the *P. furiosus* enzyme (this study) by an *asterisk*. The abbreviations used are as follows (accession numbers are in parentheses; for bigger nucleotide sequences with multiple open reading frames, first the protein and then the nucleotide accession numbers are given): Aa, *Aquifex aeolicus* (O67506, AE000745); Dv, *Desulfovibrio vulgaris* (TIGR); Mt, *Methanobacterium thermoautotrophicum* (O26679, AE000745); Af, *Archaeoglobus fulgidus* ((1) NP068949, AE001090, (2)NP069068, AE001099); Mj, *Methanococcus jannaschii* ((1) Q57843, U67492, (2) Q58980, U67598); Hs *Halobacterium* spec. NRC-1((1) AAG18889, AE004991, (2) AAG19176, AE005014); Ec, *E. coli* (DhnA P71295, U73760 and YneB AAC74590, AE000249); Pm, *Pasteurella multicoda* (AAK03362, AE006166); Rc, *Rhodobacter capsulatus* (U57682); Ct, *Chlorobium tepidum* (TIGR); Ba, *Bacillus anthracis* (TIGR); Ss, *Sulfolobus solfataricus* (AAK43321, Sso3326); Td *Treponema denticola* (TIGR); Pf, *Pyrococcus furiosus* (AF368256); Pa, *P. abyssi* (NP125781, AL096836); Ph, *P. horikoshii* (O57840, AP000001); Ap, *Aeropyrum pernix* (Q9YG90, AP000058); Tt, *T. tenax* (AJ310483); Tf, *Thiobacillus ferrooxidans* (TIGR); Cht, *Chlamydia trachomatis* (O84217, AE001273); Chm, *Ch. muridarum* (AAF39333, AE002317); Chp, *Ch. pneumoniae* (AAD18430, AE001613); A, *Anabaena* PCC7120 (AF047044).

Strikingly, DhnA homologs do not display significant overall similarity with the members of the classical Class I and Class II FBP aldolases as deduced from automated sequence comparison programs (*e.g.* Blast search). However, by closer inspection, sequence signatures could be identified resembling the active site region (position 177, *T. tenax*) and the phosphate binding motif (position 203 - 204, *T. tenax*) of some members of the $(\beta\alpha)_8$ TIM barrel superfamilies (13) strongly suggesting that this new family of Class I FBP aldolases is at least distantly related to classical Class I FBP aldolases. Moreover, secondary structure predictions (47, 48) performed with the aldolase sequences of *T. tenax*, *P. furiosus* and *Sulfolobus solfataricus* not only identified these enzymes as $(\beta\alpha)_8$ barrel proteins but also locate the functional important residues at equivalent positions to the ones found in classical Class I FBP aldolases as well as in other enzymes of the $(\beta\alpha)_8$ TIM barrel superfamilies (active site lysine in β6, phosphate binding region at the end of β7; Fig. 7.4) (13). From the high conservation of these key residues we further conclude that the new type of Class I FBP aldolase generally functions as a Schiff-base aldolase acting on phosphorylated substrates.

To analyze the phylogenetic relationships between the various DhnA homologs of Bacteria and Archaea we aligned 27 sequences of 23 different species and selected a sequence fragment of 172 amino acid residues (Fig. 7.4) for construction of phylogenetic trees (Fig. 7.5). The phylogenetic analyses include the three mostly used methods (maximum likelihood, maximum parsimony, and distance-based neighbor joining) and resulted in a complex tree topology with at least 7 deeply rooting branches. Two of them bear exclusively bacterial (branch 1B and 4B) or

archaeal sequences (branch 2 and 3) and three comprise both archaeal and bacterial sequences (branch 1A, 1C, and 4A).

Discussion

Aldolases of T. tenax and P. furiosus, members of a new type of class I FBP aldolase

The FBP aldolases of *T. tenax* and *P. furiosus* resemble specifically the Class I FBP aldolase of *E. coli* (DhnA) not only on sequence level but also in regard to biochemical properties. In common with *E. coli* Class I FBP aldolase (DhnA), catalysis of both archaeal enzymes proceeds via a Schiff-base mechanism. The archaeal enzymes, like the *E. coli* enzyme exhibit (i) additional enzyme activity with Fru-1-P, albeit at a much higher K_m than for FBP and (ii) maximal turnover rates that are stimulated by citrate (Table 7.1). Finally, also with respect to quarternary structure both archaeal aldolases show specific resemblance to the Class I enzyme of *E. coli* (DhnA). All three enzymes tend to form higher oligomerization states representing octa- / decamers or even higher oligomers, whereas the members of the classical Class I and II FBP aldolases form mostly tetramers or dimers, respectively. Thus, structural features and mode of enzyme mechanism classify the FBP aldolases of *T. tenax* and *P. furiosus* as members of a new type of Class I FBP aldolase, distinct from classical Class I enzymes, which consists of homologs in almost all Archaea and some Bacteria.

Transcription of the fba genes of T. tenax and P. furiosus, integration of the FBP aldolases in the physiological framework

The PP_i-PFK (27) and the FBP aldolase catalyze reversible reactions of successive steps in the variant of the Embden-Meyerhof-Parnas pathway of *T. tenax*, and as such both enzymes fulfill equivalent function in anabolic as well as catabolic direction of the pathway. Therefore the co-transcription of the *fba* and *pfp* gene gives rise to the coordinated expression of both enzymes in *T. tenax*. On the contrary, in most organisms using pathways characterized by an unidirectional working PFK, either dependent of ATP or like in *P. furiosus* of ADP (21, 32), a linkage of FBP aldolase and PFK coding genes does not seem to be meaningful. Sometimes FBP aldolase genes are co-transcribed with genes coding for other reversible enzymes of glycolysis (*e.g.* glyceraldehyde-3-phosphate dehydrogenase and phosphoglycerate kinase) or of the calvin cycle (*e.g.* ribulose bisphosphate carboxylase/oxygenase, phosphoribulokinase) as shown for classical Class II FBP aldolases (5, 55, 56). Because FBP aldolase is an essential constituent of glycolysis as well as gluconeogenesis, it is remarkable that the *fba* expression in both organisms *T. tenax* and *P. furiosus* is significantly higher under catabolic than under anabolic growth conditions (*T. tenax*,

glucose/CO_2; *P. furiosus*, maltose/pyruvate). An explanation might be that the higher transcript level under catabolic conditions is caused by the necessity of higher carbon flux rates through the pathway for energy conservation than required for biosynthesis.

A new family of aldolases -the archaeal type class I FBP aldolases

Despite functional similarity with the classical Class I FBP aldolases, the new family of Class I aldolases differs significantly at sequence level. These non-significant average sequence similarities as well as the absence of certain DhnA-typical motifs in classical Class I enzymes characterize this new family of Class I FBP aldolases as a very divergent, new type in addition to classical Class I aldolases. However, both types of Class I FBP aldolases like other $(\beta\alpha)_8$ (TIM) barrel proteins share, beside the predicted similar secondary structure arrangement, basic common sequence features in regions flanking the active site lysine or engaged in phosphate binding (13, 57).

Strikingly, all completed archaeal genomes contain at least one homolog of this new type of Class I FBP aldolases, with the only exception of *T. acidophilum*, which is supposed to use only the non-phosphorylative Entner-Doudoroff pathway for carbohydrate metabolism (58, 59). In contrast to Archaea, only in about 50 % of completely sequenced bacterial genomes DhnA related open reading frames have been identified and no eucaryal homolog has been assigned yet. At the moment we do not know whether this new type of Class I FBP aldolases is the only enzyme responsible for aldolase activity in Archaea. Reports of metal-dependent Class II aldolase enzyme activity in Haloarchaea (*e.g. Halobacterium halobium*) (16) suggest that additional enzymes might be present, which have not been identified yet in the sequenced genomes, due to their low sequence similarity to known Class I and II aldolases. Because of this so far obviously exclusive occurrence of this new type of aldolase, together with the absence of classical Class I and II aldolases, in Archaea and the non-significant amino acid sequence homology to classical Class I enzymes, we propose to classify this new family as archaeal type Class I FBP aldolases (Class IA) to oppose them to classical Class I aldolases only found in Eucarya and Bacteria.

Phylogenetic implications

The phylogenetic tree (Fig. 7.5) is composed of seven deeply branching lineages each bearing members of one or both prokaryotic domains, whose relationships among each other are rather poorly resolved. The presence of Class IA FBP aldolases from Bacteria and Archaea, from Euryarchaeota and Crenarchaeota (*e.g.* aldolases of Euryarchaeota in branch 1A, 2, 3, 4A; enzymes of Crenarchaeota in branch 2, 3), or even from one organism (*e.g.* enzymes of *E. coli* in branch 1B and 4B) in at least two different deeply rooting main branches suggests that early gene duplication events confer largely to the characteristic topology of the tree. Probably an early, first gene

9. Gross, W., Bayer, M. G., Schnarrenberger, C., Gebhart, U. B., Maier, T. L., and Schenk, H. E. A. (1994) Plant Physiol. 105, 1393-1398
10. Henze, K., Morrison, H. G., Sogin, M. L., and Müller, M. (1998) Gene 222, 163-168
11. Witke, C., and Götz, F. (1993) J. Bacteriol. 175 (22), 7495-7499
12. Blom, N. S., Tétreault, St., Coulombe, R. and Sygusch, J. (1996) Nature Struct. Biol. 3, 856-862
13. Copley, R. R., and Bork, P. (2000) J. Mol. Biol. 303, 627-640
14. Lang, D., Thoma, R., Henn-Sax, M., Sterner, R., and Wilmanns, M. (2000) Science 289, 1546-1550
15. Fuchs, G., Winter, H., Steiner, I., and Stupperich, E. (1983) Arch. Microbiol. 136, 160-162
16. Dhar, N. M., and Altekar, W. (1986) FEMS Microbiol. Lett. 35, 177-181
17. Krishnan, G., and Altekar, W. (1991) Eur. J. Biochem. 195, 343-350
18. Schäfer, T., and Schönheit, P. (1992) Arch. Microbiol. 158, 188-202
19. Siebers, B., and Hensel, R. (1993) FEMS Microbiol. Lett. 111, 1-8
20. Yu, J. P., Ladapo, J., and Whitman, W. B. (1994) J. Bacteriol. 176, 325-332
21. Kengen, S. W., de Bok, F. A. M., van Loo, N.-D., Dijkema, C., Stams, A. J. M., and de Vos, W. M. (1994) J. Biol. Chem. 269, 17537-17541
22. Galperin, M. Y., Aravind, L., and Koonin, E. V. (2000) FEMS Microbiol. Lett. 183, 259-264
23. Zillig, W., Stetter, K. O., Schäfer, W., Janekovic, D., Wunderl, S., Holz, I., and Palm, P. (1981) Zbl. Bakt. Hyg., I. Abt. Orig. C 2, 205-227
24. Fischer, F., Zillig, W., Stetter, K. O., and Schreiber, G. (1983) Nature 301, 511-513
25. Fiala, G., and Stetter, K. O. (1986) Arch. Microbiol. 145, 56-61
26. Siebers, B., Wendisch, V. F., and Hensel, R. (1997) Arch. Microbiol. 168, 120-127
27. Siebers, B., Klenk, H. P., and Hensel, R. (1998) J. Bacteriol. 180, 2137-2143
28. Brunner, N. A., Brinkmann, H., Siebers, B., and Hensel, R. (1998) Biochemistry 273, 6149-6156
29. Brunner, N. A., Siebers, B., and Hensel, R. (2001) in press Extremophiles
30. Schramm, A., Siebers, B., Tjaden, B., Brinkmann, H., and Hensel, R. (2000) J. Bacteriol. 182, 2001-2009
31. Kengen, S. W., Tuininga, J. E., de Bok, F. A. M., Stams, A. J. M., and de Vos, W. M. (1995) J. Biol. Chem. 270, 30453-30457
32. Tuininga, J. E., Verhees, C. H., van der Oost, J., Kengen, S. W., Stams, A. J. M., and de Vos, W. M. (1999) J. Biol. Chem. 274, 21023-21028
33. Mukund, S., and Adams, M. W. W. (1995) J. Biol. Chem. 270, 8389-8392
34. Van der Oost, J., Schut, G., Kengen, S. W., Hagen, W. R., Thomm, M., and de Vos, W. M. (1998) J. Biol. Chem. 273, 28149-28154
35. Kengen, S. W. M., Luesink, E. J., Stams, A. J. M., and Zehnder, A. J. B. (1993) Eur. J. Biochem. 213, 305-312
36. Sambrook, J., Fritsch, E. F., and Maniatis, T. (1989) Molecular Cloning: A Laboratory Manual, 2nd Ed., Cold Spring Harbor Laboratory, Cold Spring Harbor, NY
37. Bradford, M. M. (1976) Anal. Biochem. 72, 248-254
38. Higuchi, R., Krummel, B., and Saiki, R. K. (1988) Nucleic Acids Res. 16, 7351-7367
39. Stafford, W. (1992) Anal. Biochem. 203, 295-301
40. Ward, D. E., Kengen, S., van der Oost, J., and de Vos, W. M. (2000) J. Bacteriol. 182, 2559-2566
41. Thompson, J.D., Higgins, D.G., and Gibson, T. J. (1994) Nucleic Acids Res. 22, 4673-4680
42. Philippe, H. (1993) Nucleic Acids Res. 21, 5264-5272
43. Adachi, J., and Hasegawa, M. (1996) MOLPHY Version 2.3: Programs for Molecular Phylogenetics Based on Maximum Likelihood Computer Science Monographs, 28. Institute of Statistical Mathematics, Tokyo

44. Strimmer, K., and van Haeseler, A. (1996) Mol. Biol. Evol. 13, 964-969
45. Saitou, N., and Nei, M. (1987) Mol. Biol. Evol. 4, 406-425
46. Swofford, D. L. (1999) PAUP*. Phylogenetic Analysis Using Parsimony (*and Other Methods). Version 4. Sinauer Associates, Sunderland, Massachusetts.
47. Rost, B., and Sander, C. (1993) J. Mol. Biol. 232, 584-599
48. Rost, B., and Sander, C. (1994) Protein 19, 55-72
49. Condò, I., Ciammaruconi, A., Benelli, D., Ruggero, D., and Londei, P. (1999) Mol. Microbiol. 34, 377-384
50. Tolstrup, N., Sensen, C. W., Garrett, R. A., and Clausen, I. G. (2000) Extremophiles 4, 175-179
51. Soppa, J. (1999) Mol. Microbiol. 31, 1295-1305
52. Soppa, J. (1999) Mol. Microbiol. 31, 1589-1601
53. Bell, S. D., and Jackson, S. P. (2001) Current Opinion in Microbiol. 4, 208-213
54. Van der Oost, J., Ciaramella, M., Moracci, M., Pisani, F. M., Rossi, M., and de Vos, W. M. (1998) Advances in Biochemical Engineering / Biotechnology 61, 87-116
55. Gibson, J. L., Falcone, D. L., and Tabita, F. R. (1991) J. Biol. Chem. 266, 14646-14653
56. Van den Bergh, E. R. E., Baker, S. C., Raggers, R. J., Terpstra, P., Woudstra, E. C., Dijkhuizen, L., and Meijer, W. G. (1996) J. Bacteriol. 178 (3), 888-893
57. Choi, K. H., Mazurkie, A. S., Morris, A. J., Utheza, D., Tolan, D. R., and Allen, K. N. (1999) Biochemistry 38, 12655-12664
58. Budgen, N., and Danson, M. J. (1986) FEBS Lett. 196, 207-210
59. Ruepp, A., Graml, W., Santos-Martinez, M.-L., Koretke, K. K., Volker, C., Mewes, H. W., Frishman, D., Stocker, S., Lupas, A. N., and Baumeister, W. (2000) 407, 508-513

Chapter 8

Molecular and biochemical characterization of a novel type of fructose-1,6-bisphosphatase from *Pyrococcus furiosus*

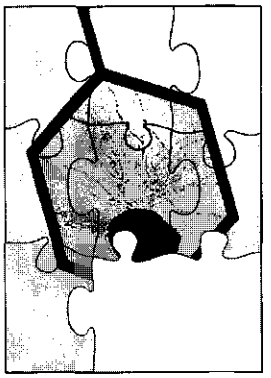

Corné H. Verhees, Jasper Akerboom, Emile schiltz, Willem M. de Vos and John van der Oost

Journal of Bacteriology, in press (2002)

Abstract

The *Pyrococcus furiosus fbpA* gene was cloned and expressed in *Escherichia coli* and the produced fructose-1,6-bisphosphatase was subsequently purified and characterized. The dimeric enzyme showed a preference for fructose-1,6-bisphosphate with a K_m of 0.32 mM and a V_{max} of 12.2 U/mg. The *P. furiosus* fructose-1,6-bisphosphatase was strongly inhibited by Li^+ (IC_{50} = 1 mM). Based on the presence of conserved sequence motifs and the specific substrate specificity of the *P. furiosus* fructose-1,6-bisphosphatase, we propose that this enzyme belongs to a new family, the class IV fructose-1,6-bisphosphatase.

The hyperthermophilic archaeon *Pyrococcus furiosus* is capable of metabolizing sugar via an Embden-Meyerhof-like pathway. A combination of physiological, biochemical and genetic studies have revealed that the pyrococcal glycolysis differs from the regular Embden-Meyerhof pathway by incorporating new conversions, novel enzymes and unique control (25) (13). Compelling examples of deviation of the canonical glycolysis are the recruitment of two unique ADP-dependent sugar kinases (23) (24) (44), a structurally distinct phosphoglucose isomerase (46), and the presence of a glyceraldehyde-3-phosphate ferredoxin oxidoreductase (30) (45). In addition, the genes encoding the homologous and distantly related fructose-1,6-bisphosphate aldolase and phospho-glycerate mutase were recently predicted, and their function was subsequently confirmed experimentally (C. Verhees, unpublished) (40). The remaining glycolytic and gluconeogenic enzymes could rather easily be identified in the genome sequence. However, no gene coding for a homolog of the gluconeogenic fructose-1,6-bisphosphatase (EC 3.1.3.11) (FBPase) could be identified in the genome sequence of *P. furiosus*. This also holds for other archaea, except for *Halobacterium sp. NRC1*, which contains a classical FBPase (31).

FBPase is an essential regulatory enzyme in the gluconeogenic pathway. It converts D-fructose-1,6-bisphosphate to D-fructose-6-phosphate, an important precursor in biosynthetic pathways. Generally, a divalent metal ion such as Mg^{2+}, Mn^{2+}, Co^{2+} or Zn^{2+} is required for catalytic activity (7) (12) (3) (43). Three-dimensional structures of several FBPases have been elucidated (49) (47) (22) (19), all containing a typical sugar phosphatase fold (http://scop.mrc-lmb.cam.ac.uk/scop) (26).

It has recently been reported that the inositol monophosphatase (I-1-Pase) (EC 3.1.3.25) from *Methanococcus jannaschii* (MJ0109) exhibits FBPase activity, and it has been suggested that this enzyme might be the missing FBPase in archaea (41). In addition MJ0109 orthologs from *Archaeoglobus fulgidus* and in *Thermotoga maritima* showed FBPase activity (41) (8). In an attempt to complete the set of glycolytic and gluconeogenic enzymes in *P. furiosus* we cloned and

expressed the MJ0109 ortholog from *P. furiosus* in *Escherichia coli*, and investigated its ability to function as a thermo-active FBPase.

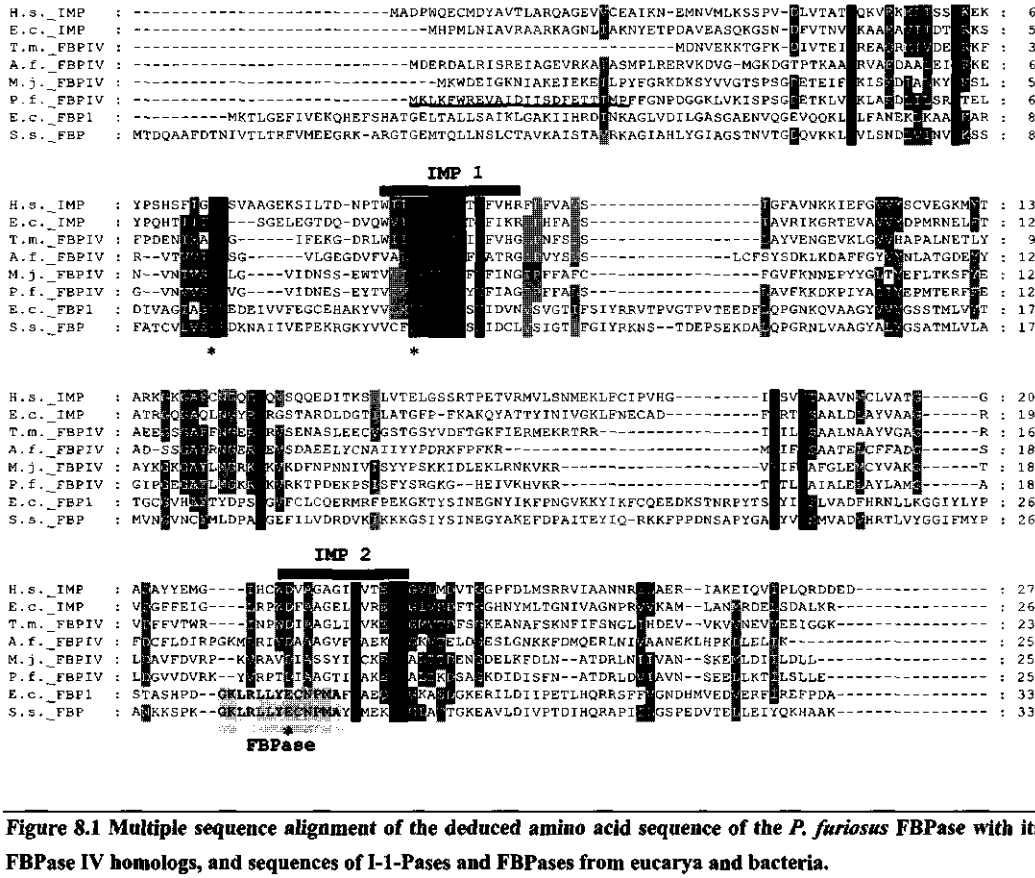

Figure 8.1 Multiple sequence alignment of the deduced amino acid sequence of the *P. furiosus* FBPase with its FBPase IV homologs, and sequences of I-1-Pases and FBPases from eucarya and bacteria.

H.s. IMP = *Homo sapiens* I-1-Pase 1 (P29218), E.c. IMP = *Escherichia coli* SuhB I-1-Pase (P22783), T.m. FBPIV = *Thermotoga maritima* TM1415 FBPase (O33832), A.f. FBPIV = *Archaeoglobus fulgidus* AF2372 FBPase (NP_071195), M.j. FBPIV = *Methanococcus jannaschii* MJ0109 FBPase (Q57573), P.f. FBPIV = *Pyrococcus furiosus* FBPase (GenBank™ accession number AF453319), E.c. FBP1 = *Escherichia coli* FBPase (P09200), S.s. FBP = *Sus scrofa* FBPase (P00636). Gaps introduced by the alignment are indicated by *hyphens*. Completely conserved regions are indicated as *black boxes*. Highly conserved regions are *shaded gray*. The IMP motifs are indicated with *black bars* above the alignment. The FBPase motif is indicated with a *gray bar* under the alignment. IMP 1 motif; [FWV]-x(0,1)-[LIVM]-D-P-[LIVM]-D-[SG]-[ST]-x(2)-[FY]-x-[HKRNSTY]; Inositol monophosphatase family signature 1 (PS00629). IMP 2 motif; [WV]-D-x-[AC]-[GSA]-[GSAPV]-x-[LIVACP]-[LIV]-[LIVAC]-x(3)-[GH]-[GA]; Inositol monophosphatase family signature 2 (PS00630). FBPase motif; [AG]-[RK]-[LI]-x(1,2)-[LIV]-[FY]-E-x(2)-P-[LIVM]-[GSA] (PS00124) (http://www.expasy.ch/ prosite). The stars (*) denote residues involved in the Li^+ binding site (47). The determined N-terminal amino acid sequence from the purified *P. furiosus* FBPase described here is *underlined*.

Transcript analysis and cloning of *fbpA*

An ortholog (*fbpA*) of MJ0109 (6) was identified in the *P. furiosus* genome database (http://www.genome.utah.edu/). This ortholog was originally annotated as an extragenic suppressor, *suhB*. The start of the *fbpA* gene was predicted based on the presence and proper spacing of a potential Shine-Dalgarno sequence and multiple alignment of the deduced amino acid sequence with those of related enzymes (Fig. 8.1). To test whether the *fbpA* gene was transcribed in *P. furiosus*, total RNA was isolated from a pyruvate-grown *P. furiosus* culture (40 mM) as described previously (48). The presence of the *fbpA* transcript was confirmed (data not shown) by using the RT-PCR System according to the instructions of the manufacture (Promega) with 1 µg of *P. furiosus* RNA, and the primers BG977 and BG978 (see below). Moreover, recent genome based microarray analysis of *P. furiosus* also revealed the expression of *fbpA* (annotated as *suhB*) (39).

The *fbpA* gene (765 bp) was PCR amplified from chromosomal DNA of *P. furiosus* as described before (44) using the primers BG977 (5'- GCGCGTCATGAAGCTTAAGTTCTGGAG-GG, sense) and BG978 (5'- GCGCGGATCCCTACTCCAGTAAGCTTAAAATTGTTTT, anti-sense), with *Bsp*HI and *Bam*HI restriction sites in bold. The PCR product was digested with *Bsp*HI/*Bam*HI, and cloned into *E. coli* XL1-Blue using a *NcoI*/*Bam*HI digested pET24d vector using established procedures and 50 µg/ml kanamycin for selection. Subsequently, the resulting plasmid pLUW558 was transformed with *E. coli* BL21(DE3).

Overexpression and purification of FBPase

An overnight culture of *E. coli* BL21(DE3) harboring pLUW558 was used as a 1% inoculum in 0.5 liter of Luria-Bertani medium with 50 µg/ml kanamycin. Gene expression was induced by adding 0.1 mM isopropyl-1-thio-α-D-galactopyranoside (IPTG) at an optical density at 600 nm of 0.5. Growth was continued for 10 h at 37 °C, and cells were harvested by centrifugation (2,200 × *g* for 20 min at 4 °C) and resuspended in 10 ml of 50 mM Tris/HCl buffer, pH 8.0. Cells were disrupted by French Press treatment (100 megapascals), and cell debris was removed by centrifugation (10,000 × *g* for 20 min at 4 °C). The resulting cell-free extract was heat-treated for 30 min at 80 °C, and precipitated proteins were removed by centrifugation (10,000 × *g* for 30 min at 4 °C). The heat-stable cell-free extract was filtered through a 0.45-µm filter and applied to a Mono-Q HR 5/5 column (1 ml, Amersham Pharmacia Biotech), equilibrated with 50 mM Tris/HCl buffer, pH 8.0. The FBPase activity eluted at 0.37 M NaCl during a linear gradient of 0.0 – 1.0 M NaCl. Active fractions were pooled and concentrated 20-fold to a final volume of 100 µl using a filter with a 10-kDa cutoff (Microsep, Pall Filtron). The concentrated pool was loaded on a Superdex 200 HR 10/30 gel filtration column (24 ml, Amersham Pharmacia Biotech), equilibrated with 50 mM Tris/HCl buffer, pH 7.8 containing 100 mM NaCl. The elution pattern (not shown) suggested the

active configuration to be a dimer (66.8 kDa) of two identical subunits of 33 kDa, in good agreement with SDS-PAGE analysis (not shown). The calculated subunit size was slightly lower, namely 27.9 kDa. The purified enzyme was desalted in 50 mM Tris/HCl buffer, pH 8.0 using a filter with a 10-kDa cutoff (Microsep, Pall Filtron). From 2.7 g cell-paste of *E. coli* BL21(DE3) containing pLUW558, a total of 27.7 mg of FBPase was purified to 95% as judged by SDS-PAGE (not shown). To ensure that the detected activity corresponds to the *P. furiosus* FBPase, the N-terminal sequence of the purified enzyme has been determined by the Edman degradation method (Met-Lys-Leu-Lys-Phe-Trp-Arg-Glu-Val-Ala-Ile-Asp-Ile-Ile-Ser-Asp-Phe-Glu-Thr-Thr-Ile-Met-Pro-Phe), revealing that the obtained amino acid sequence exactly matched the N-terminal sequence of the translated *fbpA* from *P. furiosus* (Fig. 8.1). This indicates that the *P. furiosus* FBPase had been produced and purified successfully.

Temperature dependence of the FBPase

For the determination of the temperature optimum, an appropriate amount of purified FBPase (6-30 ng) was incubated in 1-ml crimp-sealed vials containing 100 mM MOPS buffer, pH 7.4 and 10 mM $MgCl_2$. The vials were submerged in an oil bath at temperatures varying from 20 to 120 °C, preheated for 2 min, after which the enzyme reaction was initiated by injecting 15 mM fructose-1,6-bisphosphate. At different time intervals up to 15 min the reaction was stopped by transferring the vials to ice/ethanol. Aliquots were taken and the amount of fructose-6-phosphate formed was determined spectrophotometrically by measuring the reduction of $NADP^+$ (340 nm) at room temperature, in an assay with glucose-6-phosphate isomerase (EC 5.3.1.9) and glucose-6-phosphate dehydrogenase (EC 1.1.1.49), both from yeast. A linear fructose-6-phosphate production in time was observed, indicating that no *P. furiosus* FBPase was inactivated during incubation. The *P. furiosus* FBPase showed maximal activity at approximately 100 °C (data not shown).

The enzyme (18 µg/ml) lost 50% of its activity after incubating for 2 h at 100 °C in 50 mM Tris-HCl buffer, pH 8.0, according to first-order inactivation kinetics (not shown). For the determination of the melting temperature, the *P. furiosus* FBPase was dialyzed extensively against a 100 mM sodium phosphate buffer, pH 8.0, and diluted to 0.3 mg/ml in dialysis buffer. After 10 minutes of degassing, samples were analyzed in a differential scanning micro-calorimeter (VP-DSC, MicroCal) between 50-125 °C at 0.5 °C/min against the dialysis buffer. Enzyme scans were corrected using a buffer-buffer baseline. Data were analyzed with the Microcal Origin 5.0 SR2 software package. For the FBPase an apparent melting temperature of 107.5 °C was determined (not shown), which is in good agreement with the inactivation kinetics.

Catalytic properties

Kinetic parameters of the *P. furiosus* FBPase were determined discontinuously at 85 °C by varying the concentration fructose-1,6-bisphosphate (0.005-5 mM), and by the measurement of inorganic phosphate at room temperature as described before (16). The 0.2-ml assay mixture contained a 50 mM Tris/HCl buffer, pH 8.0 (room temperature), 10 mM $MgCl_2$, and 0.4 µg of purified FBPase. At this temperature the K_m and V_{max} of the *P. furiosus* FBPase with fructose-1,6-bisphosphate was 0.32 ± 0.03 mM and 12.2 ± 0.1 U/mg respectively, resulting in a catalytic efficiency (k_{cat}/K_m) of 17.7 s^{-1} mM^{-1}. The determined affinity of the purified FBPase for fructose-1,6-bisphosphate is in good agreement with the determined K_m of 0.5 mM (75 °C) in a *P. furiosus* extract (37). Kinetic parameters of the purified FBPase determined at 50 °C were as follows, a K_m of 0.31 ± 0.06 mM, a V_{max} of 0.72 ± 0.04 U/mg, and a catalytic efficiency of 1.12 s^{-1} mM^{-1}. Thus, the *P. furiosus* FBPase clearly is a thermo-active enzyme with a similar affinity for fructose-1,6-bisphosphate at 50 and 85 °C.

Table 8 1. Substrate specificity of *P. furiosus* FBPase compared to *M. jannaschii* MJ0109.

Substrate	Relative activity (%)[a]	
	P. furiosus FBPase	*M. jannaschii* MJ0109[b]
Fructose-1,6-bisphosphate	100	100
Inositol-1-phosphate	7.5	61
Glycerol-phosphate	1.7	49
Glucose-1-phosphate	2.8	42

100% activity corresponds to 12.2 and 15.2 U/mg for *P. furiosus* FBPase and MJ0109, respectively. Fructose-1-phosphate, fructose-6-phosphate, glucose-6-phosphate, phosphoenolpyruvate, 5'-AMP, 5'-ADP, and 5'-ATP could not be used as substrates by the *P. furiosus* FBPase.

[a] Enzyme assays were performed at 85 °C as described in the text.

[b] Data obtained from Stec *et al.* 2000 (41).

Specific activities of the *P. furiosus* FBPase for fructose-1,6-bisphosphate and related substrates were determined at 85 °C in the standard assay that measures release of inorganic phosphate. The 1-ml assay mixture contained 50 mM Tris/HCl buffer, pH 8.0 (room temperature), 10 mM substrate, 10 mM $MgCl_2$, and 0.02 mg of purified FBPase. Highest activity was obtained with fructose-1,6-bisphosphate (12.2 U/mg). In addition, *myo*-inositol-1-phosphate, glucose-1-phosphate, and β-glycerol phosphate could also be phosphorylated by the enzyme, although activity towards one of these substrates is relatively low (1.7-7.5%) (Table 8.1). The recently described I-1-Pase/FBPase from *M. jannaschii* (MJ0109) also phosphorylates these substrates, but with a higher relative activity (42-61%) (41) (Table 8.1). The *P. furiosus* FBPase appeared to be a rather specific phosphatase since fructose-1-phosphate, fructose-6-phosphate, glucose-6-phosphate,

phosphoenolpyruvate (PEP), 5'-AMP, 5'-ADP, and 5'-ATP could not be used as a substrate under the tested conditions.

The explanation for the low I-1-Pase activity of the *P. furiosus* FBPase might be as follows. In thermophilic archaea and bacteria several intracellular solutes are accumulated in response to osmotic and temperature stress (36) (35) (20). One of these compatible solutes is di-*myo*-inositol phosphate (DIP), a solute that accumulates at supra-optimal growth temperatures in some thermophilic species. (36) (38) (9) (34). In *P. furiosus*, temperatures above the growth optimum also lead to a significant increase of this compound (28) (33). Two different routes for DIP synthesis are known: (i) in *Methanococcos igneus* (closely related to *M. jannaschii*) I-1-Pase activity is required to form *myo*-inositol, which acts as a precursor in DIP biosynthesis (11), and (ii) in *Pyrococcus woesei* DIP is synthesized in a different way, without the *myo*-inositol forming step (38). This latter alternative pathway includes the coupling of two *myo*-inositol-1-phosphates, without a preceding I-1-Pase-mediated dephosphorylation of one of the *myo*-inositol-1-phosphate moieties. Since *P. furiosus* is closely related to *P. woesei*, it is most likely that in *P. furiosus* I-1-Pase activity is not required for DIP synthesis either, which would be in good agreement with the low activity of the *P. furiosus* FBPase on *myo*-inositol-1-phosphate.

Effectors of FBPase

The effect of inhibitors on the activity of the *P. furiosus* FBPase was investigated by adding cations and metabolites (0-100 mM) to the standard enzyme assay (85 °C) (Table 8.2). The enzyme has an absolute requirement for Mg^{2+} (data not shown). The inhibition characteristics of the *P. furiosus* FBPase clearly differ from that of characterized eukaryal and bacterial FBPases, as well as from the other presently characterized archaeal I-1-Pase/FBPase homologs. FBPase I from *E. coli* is very sensitive to AMP and PEP (1). FBPase II from *E. coli* is strongly inhibited by ATP and ADP, whereas AMP has no effect on the enzyme activity. Furthermore, FBPase II activity is enhanced in the presence of PEP (14). PEP also affects FBPase III activity, *i.e.* inhibition by AMP is reduced when PEP is present (15). The *P. furiosus* FBPase was inhibited by ADP and ATP (and to some extent AMP), but PEP did not influence the activity at all (up to 100 mM PEP). Therefore, PEP presumably is not an important metabolite in the regulation of FBPase in *P. furiosus*. In addition, glucose-6-phosphate significantly reduced *P. furiosus* FBPase activity *in vitro* (Table 8.2).

Li^+ generally is a strong inhibitor of FBPase activity (K_i ~0.3 mM) (47) (27) (42). Under the tested conditions Li^+ significantly reduced the *P. furiosus* FBPase activity (IC_{50} = 1 mM) (Table 8.2), where addition of Na^+ and K^+ showed no effect. Previously, it was shown that I-1-Pases are also strongly inhibited by Li^+ (IC_{50} ~0.3 mM) (17) (29) (18). These enzymes have a similar fold as FBPases (50), both members of the sugar phosphatase superfamily (http://scop.mrc-

lmb.cam.ac.uk/scop) (26). Inhibition of mammalian I-1-Pase by Li^+ is of particular interest, since this enzyme is being expressed in brain tissue and forms the main target in manic depression medical treatment (2) (32) (4). The mechanism of Li^+ inhibition of FBPases and IMPases is believed to be essentially the same, Li^+ binds at one of the metal binding sites, thereby retarding turnover or phosphate release (47) (9). The residues that constitute this metal binding site are conserved in lithium-sensitive I-1-Pase and in FBPase (Fig. 8.1). Remarkably, Li^+ had not such a strong effect on the *M. jannaschii* (MJ0109) and *Thermotoga maritima* (TM1415) enzymes (TM1415, IC_{50} = 100 mM, and MJ0109, IC_{50} > 250 mM), although residues constituting the Li^+ binding site are conserved (Fig. 8.1) (8) (9). Minor variations will probably distinguish in the inhibitory effect of Li^+ on the I-1-Pase and FBPase (9).

Table 8.2 Inhibitors of *P. furiosus* FBPase activity.

Effector	IC_{50} (mM)
Li^+	1
Ca^{2+}	5
AMP	30
ADP	3
ATP	4
Glucose-6-phosphate	4
Fructose-6-phosphate	25
Pyruvate	60

Enzyme assays were performed at 85 °C as described in the text (10 mM fructose-1,6-bisphosphate). IC_{50}: concentration of effector when activity of the *P. furiosus* FBPase was reduced to 50%. The addition of Na^+, K^+, glucose or PEP to the assay mixture (up to 100 mM) had no effect on FBPase activity.

Classification of FBPases

Recently, a new classification of bacterial FBPases into three groups (FBPase I, II and III) has been proposed (14). Eukaryal FBPases are orthologous to the bacterial FBPase I, both containing a typical FBPase domain (http://www.expasy.ch), and display no I-1-Pase activity (41). The typical FBPase domain is absent in the bacterial FBPase II and III (Table 8.3), suggesting that these enzymes are phylogenetically unrelated to FBPase I. Remarkably, a typical I-1-Pase domain (IMP 1) is also present in the eukaryal FBPase and the bacterial FBPase I (http://www.expasy.ch). Bacterial and eukaryal I-1-Pases contain two specific domains (IMP 1 and IMP 2), and together with the eukaryal FBPase and bacterial FBPase I, belong to the sugar phosphatase superfamily (http://scop.mrc-lmb.cam.ac.uk/scop). Comparison of the primary structure of the *P. furiosus* FBPase with the FBPase and IMP family signatures revealed that this enzyme contains both I-1-Pase domains (IMP 1 and IMP 2). No obvious FBPase domain could be detected in the *P. furiosus* sequence (Table 8.3) (Fig. 8.1). The *P. furiosus* FBPase is homologous to *M jannaschii* MJ0109, *A. fulgidus* AF2372 and *T. maritima* TM1415, all three enzymes having an IMP 1 and IMP 2 domain present in their primary structure (Fig. 8.1) and possessing dual activity (*i.e.* FBPase and I-1-Pase

activity) (41). Since these FBPases display limited sequence identity towards both eukaryal and mesophilic bacterial FBPases (FBPase I 12-16%, FBPase II and III, 11-15%), but rather seem to be significantly related to the I-1-Pases (16-35 %), we propose the *P. furiosus* FBPase and its homologs to constitute a new FBPase family based on sequence identity and substrate specificity: the type IV FBPase (FBPase IV), present in euryarchaeal and hyperthermophilic bacterial species, and potentially involved in gluconeogenesis. The presence of a conserved domain (IMP 1) in FBPase I, IV and the I-1-Pases, as well as the similar fold of these enzymes (41) (21) (5) (50) suggests that these enzymes share the same phylogenetic origin, as suggested previously (41) (50). It is tempting to speculate that the FBPase IV originally belonged to the I-1-Pase family, and subsequently evolved to convert fructose-1,6-bisphosphate efficiently to function in gluconeogenesis.

Table 8.3 Classification of Phosphatases.

	Classes of Phosphatases				
	FBPase I	FBPase II	FBPase III	FBPase IV	I-1-Pase
Taxonomic range	Eucarya, Bacteria	Bacteria	Bacteria	Archaea, HT-Bacteria	Eucarya, Bacteria
Subunit size (kDa)	~38	~36	~76	~28	~30
Oligomerization	Tetramer	Dimer	Tetramer	Dimer[a]	Dimer
Fold	Sugar phosphatase	unknown	unknown	Sugar phosphatase	Sugar phosphatase
Sequence motifs	FBPase, IMP 1	none	none	IMP 1, IMP 2	IMP 1, IMP 2

[a] The *T. maritima* enzyme is an exception having a tetrameric structure.

FBPase IV is present in the euryarchaea: *P. furiosus* (GenBank™ accession number AF453319); *P. horikoshii* (PH1897); *P. abyssi* (PAB0189); *M. jannaschii* (MJ0109); *Archaeoglobus fulgidus* (AF2372); *Methanosarcina barkeri* (MB1918); *Methanobacterium thermoautotrophicum* (MTH871), and the hyperthermophilic bacteria *Thermotoga maritima* (TM1415) and *Aquifex aeolicus* (AQ1983). Bacterial extragenic supressor proteins (SuhB) are classified within the I-1-Pase family (10), and show I-1-Pase activity but no FBPase activity (41). HT-Bacteria: Hyperthermophilic Bacteria.

We thank L. Kluskens (Wageningen University) for assistance during the DSC measurements, and Stefan Wolff (Essen University, Germany) for providing *myo*-inositol-1-phosphate. This work was supported by the Earth and Life Sciences foundation (ALW), which is subsidized by the Netherlands Organization for Scientific Research (NWO).

References

1. **Babul, J., and V. Guixe** 1983. Fructose bisphosphatase from *Escherichia coli*. Purification and characterization. Arch. Biochem. Biophys. **225:**944-949.
2. **Baraban, J. M.** 1994. Toward a crystal-clear view of lithium's site of action. Proc. Natl. Acad. Sci. U S A. **91:**5738-5749.
3. **Benkovic, S. J., and M. M. deMaine** 1982. Mechanism of action of fructose 1,6-bisphosphatase. Adv. Enzymol. Relat. Areas. Mol. Biol. **53:**45-82.
4. **Berridge, M. J., C. P. Downes, and M. R. Hanley** 1989. Neural and developmental actions of lithium: a unifying hypothesis. Cell. **59:**411-419.
5. **Bone, R., J. P. Springer, and J. R. Atack** 1992. Structure of inositol monophosphatase, the putative target of lithium therapy. Proc. Natl. Acad. Sci. U S A. 89:10031-10035.
6. **Bult, C. J., O. White, G. J. Olsen, L. Zhou, R. D. Fleischmann, G. G. Sutton, J. A. Blake, L. M. FitzGerald, R. A. Clayton, J. D. Gocayne, A. R. Kerlavage, B. A. Dougherty, J. F. Tomb, M. D. Adams, C. I. Reich, R. Overbeek, E. F. Kirkness, K. G. Weinstock, J. M. Merrick, A. Glodek, J. L. Scott, N. S. Geoghagen, and J. C. Venter** 1996. Complete genome sequence of the methanogenic archaeon, *Methanococcus jannaschii*. Science. **273:**1058-1073.
7. **Chattoraj-Bhattacharyya, S., and A. L. Majumder** 1995. Divalent cations and chelators as regulators of brain fructose-1,6- bisphosphatase. Arch. Biochem. Biophys. **316:**63-69.
8. **Chen, L., and M. F. Roberts** 1999. Characterization of a tetrameric inositol monophosphatase from the hyperthermophilic bacterium *Thermotoga maritima*. Appl. Environ. Microbiol. **65:**4559-4567.
9. **Chen, L., and M. F. Roberts** 1998. Cloning and expression of the inositol monophosphatase gene from *Methanococcus jannaschii* and characterization of the enzyme. Appl. Environ. Microbiol. **64:**2609-2615.
10. **Chen, L., and M. F. Roberts** 2000. Overexpression, purification, and analysis of complementation behavior of *E. coli* SuhB protein: comparison with bacterial and archaeal inositol monophosphatases. Biochemistry. **39:**4145-4153.
11. **Chen, L., E. T. Spiliotis, and M. F. Roberts** 1998. Biosynthesis of di-myo-inositol-1,1'-phosphate, a novel osmolyte in hyperthermophilic archaea. J. Bacteriol. **180:**3785-3792.
12. **Choe, J. Y., H. J. Fromm, and R. B. Honzatko** 2000. Crystal structures of fructose 1,6-bisphosphatase: mechanism of catalysis and allosteric inhibition revealed in product complexes. Biochemistry. **39:**8565-8574.
13. **de Vos, W. M., S. W. M. Kengen, W. G. B. Voorhost, and J. van der Oost** 1998. Sugar utilization and its control in hyperthermophiles. Extremophiles. **2:**201-205.
14. **Donahue, J. L., J. L. Bownas, W. G. Niehaus, and T. J. Larson** 2000. Purification and characterization of glpX-encoded fructose 1, 6- bisphosphatase, a new enzyme of the glycerol 3-phosphate regulon of *Escherichia coli*. J. Bacteriol. **182:**5624-5627.
15. **Fujita, Y., K. Yoshida, Y. Miwa, N. Yanai, E. Nagakawa, and Y. Kasahara** 1998. Identification and expression of the *Bacillus subtilis* fructose-1, 6- bisphosphatase gene (fbp). J. Bacteriol. **180:**4309-4313.
16. **Geladopoulos, T. P., T. G. Sotiroudis, and A. E. Evangelopoulos** 1991. A malachite green colorimetric assay for protein phosphatase activity. Anal. Biochem. **192:**112-116.
17. **Gillaspy, G. E., J. S. Keddie, K. Oda, and W. Gruissem** 1995. Plant inositol monophosphatase is a lithium-sensitive enzyme encoded by a multigene family. Plant Cell. **7:**2175-2185.
18. **Hallcher, L. M., and W. R. Sherman** 1980. The effects of lithium ion and other agents on the activity of myo-inositol-1-phosphatase from bovine brain. J. Biol. Chem. **255:**10896-10901.

19. **Johnson, K. A., L. Chen, H. Yang, M. F. Roberts, and B. Stec** 2001. Crystal structure and catalytic mechanism of the MJ0109 gene product: a bifunctional enzyme with inositol monophosphatase and fructose 1,6- bisphosphatase activities. Biochemistry. **40:**618-630.
20. **Kanodia, S., and M. F. Roberts** 1983. Methanophosphagen: a unique cyclic pyrophosphate isolated from *Methanobacterium photoautotrophicum*. Natl. Acad. Sci. USA. **80:**5217-5321.
21. **Ke, H., C. M. Thorpe, B. A. Seaton, F. Marcus, and W. N. Lipscomb** 1989. Molecular structure of fructose-1,6-bisphosphatase at 2.8-A resolution. Proc. Natl. Acad. Sci. U S A. **86:**1475-1479.
22. **Ke, H. M., Y. P. Zhang, and W. N. Lipscomb** 1990. Crystal structure of fructose-1,6-bisphosphatase complexed with fructose 6-phosphate, AMP, and magnesium. Proc. Natl. Acad. Sci. U S A. **87:**5243-5247.
23. **Kengen, S. W.M., F. A.M. de Bok, N. D. van Loo, C. Dijkema, A. J. M. Stams, and W. M. de Vos** 1994. Evidence for the operation of a novel Embden-Meyerhof pathway that involves ADP-dependent kinases during sugar fermentation by *Pyrococcus furiosus*. J. Biol. Chem. **269:**17537-17541.
24. **Kengen, S. W.M., J. E. Tuininga, F. A. M. de Bok, A. J.M. Stams, and W. M. de Vos** 1995. Purification and characterization of a novel ADP-dependent glucokinase from the hyperthermophilic archaeon *Pyrococcus furiosus*. J. Biol. Chem. **270:**30453-30457.
25. **Kengen, S. W. M., A. J. M. Stams, and W. M. de Vos** 1996. Sugar metabolism of hyperthermophiles FEMS Microbiology Reviews. **18:**119-137.
26. **Lo Conte, L., B. Ailey, T. J. Hubbard, S. E. Brenner, A. G. Murzin, and C. Chothia** 2000. SCOP: a structural classification of proteins database. Nucleic Acids Res. **28:**257-259.
27. **Marcus, F., J. Rittenhouse, T. Chatterjee, and M. M. Hosey** 1982. Fructose-1,6-bisphosphatase from rat liver Methods Enzymol. **90:**352-357.
28. **Martins, L. O., and H. Santos** 1995. Accumulation of Mannosylglycerate and Di-myo-Inositol-Phosphate by *Pyrococcus furiosus* to Salinity and Temperature. Appl. Environ. Microbiol. **61:**3299-3303.
29. **Matsuhisa, A., N. Suzuki, T. Noda, and K. Shiba** 1995. Inositol monophosphatase activity from the *Escherichia coli suhB* gene product. J. Bacteriol. **177:**200-205.
30. **Mukund, S., and M. W. W. Adams** 1995. Glyceraldehyde-3-phosphate ferredoxin oxidoreductase, a novel tungsten-containing enzyme with a potential glycolytic role in the hyperthermophilic archaeon *Pyrococcus furiosus*. J. Biol. Chem. **270:**8389-8392.
31. **Ng, W. V., S. P. Kennedy, G. G. Mahairas, B. Berquist, M. Pan, H. D. Shukla, S. R. Lasky, N. S. Baliga, V. Thorsson, J. Sbrogna, S. Swartzell, D. Weir, J. Hall, T. A. Dahl, R. Welti, Y. A. Goo, B. Leithauser, K. Keller, R. Cruz, M. J. Danson, D. W. Hough, D. G. Maddocks, P. E. Jablonski, M. P. Krebs, C. M. Angevine, H. Dale, T. A. Isenbarger, R. F. Peck, M. Pohlschroder, J. L. Spudich, K. W. Jung, M. Alam, T. Freitas, S. Hou, C. J. Daniels, P. P. Dennis, A. D. Omer, H. Ebhardt, T. M. Lowe, P. Liang, M. Riley, L. Hood, and S. DasSarma** 2000. Genome sequence of Halobacterium species NRC-1. Proc. Natl. Acad. Sci. U S A. **97:**12176-12181.
32. **Pollack, S. J., J. R. Atack, M. R. Knowles, G. McAllister, C. I. Ragan, R. Baker, S. R. Fletcher, L. L. Iversen, and H. B. Broughton** 1994. Mechanism of inositol monophosphatase, the putative target of lithium therapy. Proc. Natl. Acad. Sci. U S A. **91:**5766-5770.
33. **Ramakrishnan, V., Q. Teng, and M. W. W. Adams** 1997. Characterization of UDP amino sugars as major phosphocompounds in the hyperthermophilic archaeon *Pyrococcus furiosus*. J. Bacteriol. **179:**1505-1512.
34. **Ramakrishnan, V., F. J. M. Verhagen, and M.W.W. Adams** 1997. Characterization of Di-myo-Inositol-1,1'-Phosphate in the Hyperthermophilic Bacterium *Thermotoga maritima*. Appl. Environ. Microbiol. **63:**347-350.

35. **Ramos, A., N. D. H. Raven, R. J. Sharp, S. Barolucci, M. Rossi, R. Cannio, J. Lebbink, J. van der Oost, W. M. de Vos, and H. Santos** 1997. Stabilization of enzymes against thermal stress and freeze-drying by mannosylglycerate. Appl. Environ. Microbiol. **63:**4020-4025.

36. **Santos, H., and M. S. da Costa** 2001. Organic solutes from thermophiles and hyperthermophiles. Methods Enzymol. **334:**302-315.

37. **Schäfer, T., and P. Schönheit** 1993. Gluconeogenesis from pyruvate in the hyperthermophilic archaeon *Pyrococcus furiosus*: involvement of reactions of the Embden-Meyerhof pathway. Arch. Microbiol. **159:**359-363.

38. **Scholz, S., S. Wolff, and R. Hensel** 1998. The biosynthesis pathway of di-myo-inositol-1,1'-phosphate in *Pyrococcus woesei*. FEMS Microbiol. Lett. **168:**37-42.

39. **Schut, G. J., J. Zhou, and M. W.W. Adams** 2001. DNA Microarray Analysis of the Hyperthermophilic Archaeon *Pyrococcus furiosus*: Evidence for a new type of sulfur-reducing enzyme complex. J. Bacteriol. **183:**7027-7036.

40. **Siebers, B., H. Brinkmann, C. Dorr, B. Tjaden, H. Lilie, J. van der Oost, and C. H. Verhees** 2001. Archaeal fructose-1,6-bisphosphate aldolases constitute a new family of archaeal type class I aldolase. J. Biol. Chem. **276:**28710-28718.

41. **Stec, B., H. Yang, K. A. Johnson, L. Chen, and M. F. Roberts** 2000. MJ0109 is an enzyme that is both an inositol monophosphatase and the 'missing' archaeal fructose-1,6-bisphosphatase. Nat. Struct. Biol. **7:**1046-1050.

42. **Storey, K. B.** 1982. Fructose-1,6-bisphosphatase from bumblebee flight muscle. Methods Enzymol. **90:**366-371.

43. **Tejwani, G. A.** 1983. Regulation of fructose-bisphosphatase activity. Adv. Enzymol. Relat. Areas. Mol. Biol. **54:**121-194.

44. **Tuininga, J. E., C. H. Verhees, J. van der Oost, S. W.M. Kengen, A. J. M. Stams, and W. M. de Vos** 1999. Molecular and biochemical characterization of the ADP-dependent phosphofructokinase from the hyperthermophilic archaeon *Pyrococcus furiosus*. J. Biol. Chem. **274:**21023-21028.

45. **van der Oost, J., G. Schut, S. W. M. Kengen, W. R. Hagen, M. Thomm, and W. M. de Vos** 1998. The ferredoxin-dependent conversion of glyceraldehyde-3-phosphate in the hyperthermophilic archaeon *Pyrococcus furiosus* represents a novel site of glycolytic regulation. J. Biol. Chem. **273:**28149-28154.

46. **Verhees, C. H., M. A. Huynen, D. E. Ward, E. Schiltz, W. M. de Vos, and J. van der Oost** 2001. The phosphoglucose isomerase from the hyperthermophilic archaeon *Pyrococcus furiosus* is a unique glycolytic enzyme that belongs to the cupin superfamily. J. Biol. Chem. **276:**40926-40932.

47. **Villeret, V., S. Huang, Y. Zhang, Y. Xue, and W. N. Lipscomb** 1995. Crystal structure of spinach chloroplast fructose-1,6-bisphosphatase at 2.8 A resolution. Biochemistry. **34:**4299-4306.

48. **Ward, D. E., S. W. M. Kengen, J. van der Oost, and W. M. de Vos** 2000. Purification and characterization of the alanine aminotransferase from the hyperthermophilic Archaeon *Pyrococcus furiosus* and its role in alanine production. J. Bacteriol. **182:**2559-2566.

49. **Weeks, C. M., A. W. Roszak, M. Erman, R. Kaiser, H. Jornvall, and D. Ghosh** 1999. Structure of rabbit liver fructose 1,6-bisphosphatase at 2.3 A resolution. Acta. Crystallogr. D Biol. Crystallogr. **55:**93-102.

50. **Zhang, Y., J. Y. Liang, and W.N. Lipscomb** 1993. Structural Similarities between Fructose-1,6-bisphosphatase and Inositol Monophosphatase Biochemical and Biophysical Research Communications.**190:**1080-1083.

Chapter 9

Promoter architecture of genes encoding glycolytic enzymes in *Pyrococcus furiosus*

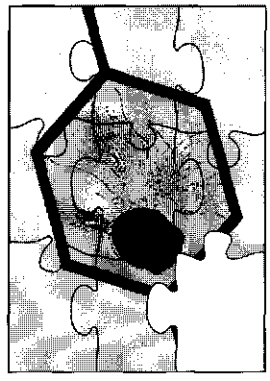

Corné H. Verhees, Jasper Akerboom, John van der Oost and Willem M. de Vos

A modified version of this chapter will be submitted for publication

Abstract

The glycolytic pathway of the hyperthermophilic archaeon *Pyrococcus furiosus* differs significantly from the canonical Embden-Meyerhof pathway because it consists of novel enzymes and is subjected to a unique control. Recently, the complete set of genes encoding glycolytic enzymes from *P. furiosus* has been identified, and the enzymes have been studied in detail. However, little is known about transcriptional regulation and promoter structure of the archaeal glycolytic genes. In this study the transcription initiation sites of pyrococcal genes encoding glycolytic enzymes have been identified. Their promoter sequences have been compared with other promoter sequences from *P. furiosus*, and consensus sequences for the TATA box (NTTWWWWA) and the BRE element (RAAAAN) are proposed for this hyperthermophilic archaeon. Remarkably, an inverted repeat ($ATCACN_5GTGAT$) was identified in *P. furiosus* promoter sequences of genes encoding glycolytic and other sugar metabolic proteins. It is discussed that this inverted repeat may be involved in the common regulation of these genes.

Introduction

Pyrococcus furiosus uses a modified Embden-Meyerhof pathway during growth on sugars (1). All of the genes that encode the glycolytic enzymes have been identified, either by homology searching of its genome or by reversed genetics. A combination of metabolic, biochemical and genetic approaches has established that the pyrococcal glycolysis differs from the Embden-Meyerhof pathway because of new conversions, novel enzymes and unique control (1) (2) (3) (4) (5) (6) (7).

In the classical Embden-Meyerhof pathway the irreversible phosphorylation reactions catalyzed by hexokinase, phosphofructokinase and pyruvate kinase are allosterically regulated control sites. However, the ADP-dependent glucokinase and ADP-dependent phosphofructokinase of the euryarchaeon *P. furiosus* are not allosterically controlled by any of the usual effector compounds (C. Verhees, unpublished) (5). Furthermore, the pyruvate kinase of the crenarchaeon *Thermoproteus tenax* is not allosterically regulated neither (8). Thus these enzymes do not act as the major control points similar to that in the classical glycolysis. Alternatively, the novel glyceraldehyde-3-phosphate ferredoxin oxidoreductase could be an important enzyme in control of the *Pyrococcus* glycolysis. The enzyme catalyzes the irreversible oxidation of glyeralde-3-phosphate and the expression of its gene is strongly induced by growth on sugars (4). Recent studies have shown that a number of pyrococcal glycolytic enzymes are regulated at transcription level as well (6) (7) (9). Therefore, regulation of the glycolytic flux in *P. furiosus* might involve modulation of gene expression rather than allosteric regulation of enzyme activities.

In bacteria and eucarya transcriptional control of glycolysis can be positively or negatively regulated. In gram-positive bacteria, the catabolite control protein (CcpA) was found to be a transcriptional activator of glycolytic operons including genes encoding phosphofructokinase, pyruvate kinase and lactate dehydrogenase (10) (11). In gram-negative bacteria, the fructose repressor protein (FruR) negatively regulates transcription of genes encoding glycolytic enzymes, and positively regulates transcription of genes encoding gluconeogenic enzymes (12). In yeast, a DNA-binding protein (GRC1) was found to strongly reduce the transcription levels of most glycolytic enzyme encoding genes (13) (14). No homologs of these regulators could however be identified to be encoded by the genome of *P. furiosus* or other archaea.

A small number of archaeal transcriptional regulators have identified and studied experimentally (15) (16) (17) (18) (19). A homolog of the leucine-responsive regulatory protein (LRP) from *P. furiosus* has been studied in detail and was found to autoregulate its own promoter (16). LRPs from bacteria are either global or specific regulators involved in control of amino acid metabolism. However, no target genes have thus far been identified for the *P. furiosus* LRP. In addition, no regulators are yet known that are responsible for the modulated gene expression of the pyrococcal glycolytic enzymes.

In this study, transcription initiation sites of some of the glycolytic genes are determined, promoter structures are compared, and functionally important elements are identified. The results reveal details of the promoter architecture in *P. furiosus* and allowed for the identification of a conserved inverted repeat in the promoter sequences of genes encoding glycolytic enzymes. Analysis of the complete *P. furiosus* genome reveals that this inverted repeat, termed PSR -for *Pyrococcus* Specific Repeat- is present in the promoter sequences of glycolytic genes and those encoding proteins involved in α-linked sugar degradation. A putative function of PSR in transcription regulation is discussed.

Experimental procedures

Organism and growth condition

P. furiosus (DSM 3638) was grown in chemically defined medium as described previously (20) with the only exception that yeast extract was omitted and substituted by the individual amino acids (0.25 mM final concentration). Maltose (10 mM) or pyruvate (40 mM) was added as the primary carbon source.

Transcript analyses

RNA was isolated from maltose and pyruvate grown *P. furiosus* cells as described previously (21). The transcription starts were determined with fluorescence (IRD800)-labeled antisense oligonucleotides (Table 9.1). Primer extension reactions were performed using the Reverse Transcription System (Promega) according to the instructions of the manufacturer with following modifications. Hybridization of total RNA (15 µg) and oligonucleotide (5 pmol) was performed for 10 min at 68 °C before allowing to cool to room temperature. The reaction (20 µl final volume) was started by addition of dNTPs (1 mM), $MgCl_2$ (5 mM), RNAsin (20 U), and avian myeloblastosis virus-reverse transcriptase (22.5 U). After incubation for 30 min at 45 °C the reaction volume was diluted to 50 µl with 10 mM Tris/HCl (pH 8.5), 1 µl of RNase A (5 mg/ml) was added and the sample was incubated for 10 min at 37 °C. cDNA was precipitated with ethanol, dissolved in 3 µl loading buffer and 1 µl was applied to a sequencing gel in parallel with the sequencing reactions obtained with the same oligonucleotide.

Table 9.1 5'-(IRD800)-labeled antisense oligonucleotides.

Gene	Nucleotide sequence	Target residues[1]
glk	5'-TGTCCAAGTATTTTATAGCGTCG-3'	102-124
pgi	5'-CTTTCCATGCCCTTTCATCAAC-3'	103-124
pfk	5'-ATTTTATCGGGACCAAATTCC-3'	102-122
fba	5'-CAAAGTCCGTAGGGCCGTGC-3'	99-118
tpi	5'-AATTGTTACACCTGTTTCTTTGTAC-3'	102-126
gor	5'-ATGTCCTTAGTTCATTGTGTCTC-3'	102-124
pyk	5'-ATTCTTGCAACATTCATCCCCG-3'	89-110
pps	5'-TGGTGGAACTGGAATTCCAGC-3'	97-117

[1]The numbers indicate the position of the nucleotides downstream the translation start site.

Results and discussion

Genomic organization

The genes encoding the enzymes of the modified Embden-Meyerhof pathway in *Pyrococcus* have been identified directly by homology or by determination of the N-termini of the purified enzymes (5) (7) (6) (C. Verhees, in prep.) (22) (3) (4). Their location on the genomes of the three sequenced pyrococcal strains (*P. furiosus*, *P. horikoshii* and *P. abyssi*) indicates that the genes are scattered over the complete genome and not located in operon structures with any of the other glycolytic genes (Fig. 9.1). In bacteria, glycolytic genes are often distributed over the complete genome as well. However, sometimes genes are clustered, *e.g.* glyceraldehyde-3-phosphate dehydrogenase is often clustered with 3-phosphoglycerate kinase and sometimes with triose-phosphate isomerase or fructose-1,6-bisphosphate aldolase. The latter can also be co-transcribed with phosphoglycerate kinase (23) (24) (25). Moreover, in the hyperthermophilic archaeon

Thermoproteus tenax the fructose-1,6-bisphosphate aldolase gene is co-transcribed with the phosphofructokinase gene, both encoding reversible enzymes (6). The different location and direction of the genes on the three *Pyrococcus* genomes reflects the highly flexibility of these genomes as noted before (26) (27).

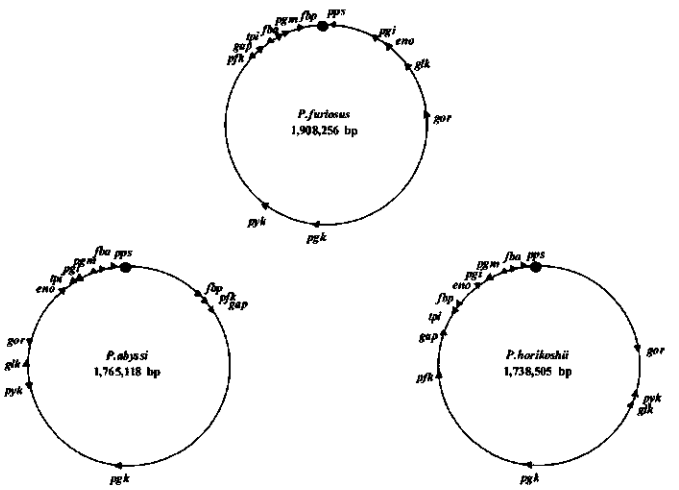

Figure 9.1 Genomic organization of genes encoding glycolytic and gluconeogenic enzymes in *P. furiosus*, *P. horikoshii* and *P. abyssi*.

glk = ADP-dependent glucokinase (AF127910); *pgi* = phosphoglucose isomerase (AF381250); *pfk* = ADP-dependent phosphofructokinase (AF127909); *fbp* = fructose-1,6-bisphosphatase (pf1862791); *fba* = fructose-1,6-bisphosphate aldolase (AF368256); *tpi* = triose-phosphate isomerase (pf1771224), *gor* = glyceraldehyde-3-phosphate ferredoxin oxidoreductase (AAC70892); *gap* = glyceraldehyde-3-phosphate dehydrogenase (pf1729229); *pgk* = 3-phosphoglycerate kinase (pf1012695); *pgm* = phosphoglycerate mutase (pf1810133); *eno* = enolase (pf232621); *pyk* = pyruvate kinase (pf1135494); *pps* = phospho*enol*pyruvate synthase (P42850). *Filled circles* denote origin of replication (27). Direction of the genes is indicated by *arrows*.

Mapping transcription start sites and promoter elements

Transcription initiation sites of *P. furiosus* glycolytic genes were determined by primer extension analyses (Fig. 9.2). Remarkably, the transcription start sites of the *glk*, *fba* and *tpi* genes were identified at the guanosine residue of a putative ribosomal binding site (GGTGAT), located 10-11 nucleotides upstream of the ATG start codon. All investigated transcription start sites of the euryarchaeon *P. furiosus* genes were found to be located at the first position of or immediately upstream of a putative ribosomal binding sites. This contrasts to a considerable number of identified transcription initiation sites in the crenarchaeon *Sulfolobus solfataricus*, that are all located downstream of the initiation codon (28).

A comparison of pyrococcal promoter sequences (Fig. 9.2) reveals two conserved sequence elements positioned around -26/-27 and –33/-34, that most likely correspond to the TATA box and transcription factor B recognition element (BRE), respectively (29) (30). The archaeal TATA binding protein TBP is known to bind to the TATA box, which is generally centered at position -26/-27. However, some flexibility exist in the spacing between the TATA box and the transcription start site, *i.e.* a divergence from the ideal distance by 1 or 2 nucleotides appears to be compatible with faithful start site selection (31) (29). A consensus for TATA box sequences has been proposed for several archaeal groups (Table 9.2). Based on the comparison of investigated *P. furiosus* promoter regions, the following TATA box consensus is proposed -30NTTWWWWA-23 (Table 9.2) This consensus resembles strongly that reported recently for halophiles (29). It is likely that this sequence is recognized by the known *Pyrococcus* TBP, since another dedicated protein can be excluded, based on the absence of homologs in the genome of *P. furiosus* and the faithful *in vitro* transcription of the glutamate dehydrogenase (32) and glyceraldehyde ferredoxin oxidoreductase genes (4). A consensus sequence has been proposed for the 6-nucleotide BRE immediately upstream of the TATA box for *Sulfolobus* (Table 9.2) (30). The key role for the archaeal BRE is to direct the oriented assembly of the archaeal pre-initiation complex upon binding of transcription factor B (30). Two nucleotides, positioned 3 and 6 upstream of the TATA box, are the strongest specificity determinants of the archaeal BRE (30). These nucleotides are apparently conserved in the *P. furiosus* promoter sequences and a BRE consensus for *P. furiosus* is proposed, -36RAAAAN-31 (Table 9.2), which is highly similar to that of the *Sulfolobus* consensus.

Table 9.2 Consensus sequences of archaeal promoter elements.

Archaeal groups	TATA box[1]	BRE site[1]	Reference
Halophiles	-29(T-T-T-W-W-W)-24	-[2]	(29)
Methanogens	-30(Y-T-T-A-T-A-T-A)-23	-	(29)
Sulfolobus	-30(Y-T-T-T-T-A-A-A)-23	-36(R-N-W-A-A-W)-31	(29) (30)
Pyrococcus	-30(N-T-T-W-W-W-W-A)-23	-36(R-A-A-A-A-N)-31	This study

[1]The numbers indicate the position of the nucleotides upstream the transcription start site. [2]No consensus described.

Remarkably, considerable nucleotide symmetry was observed in a variety of promoter sequences (Fig 9.2). A specific repeated sequence appears to be conserved in the promoter sequences of all but one (*pyk*; see below) genes encoding glycolytic enzymes. It consists of a conserved pentanucleotide inverted repeat spaced by 5 nucleotides with the consensus $ATCACN_5GTGAT$. However, this 15-nucleotide sequence is extended by 2-8 nucleotides in several of these promoter sequences, that further contribute to the perfect inverted repeat.

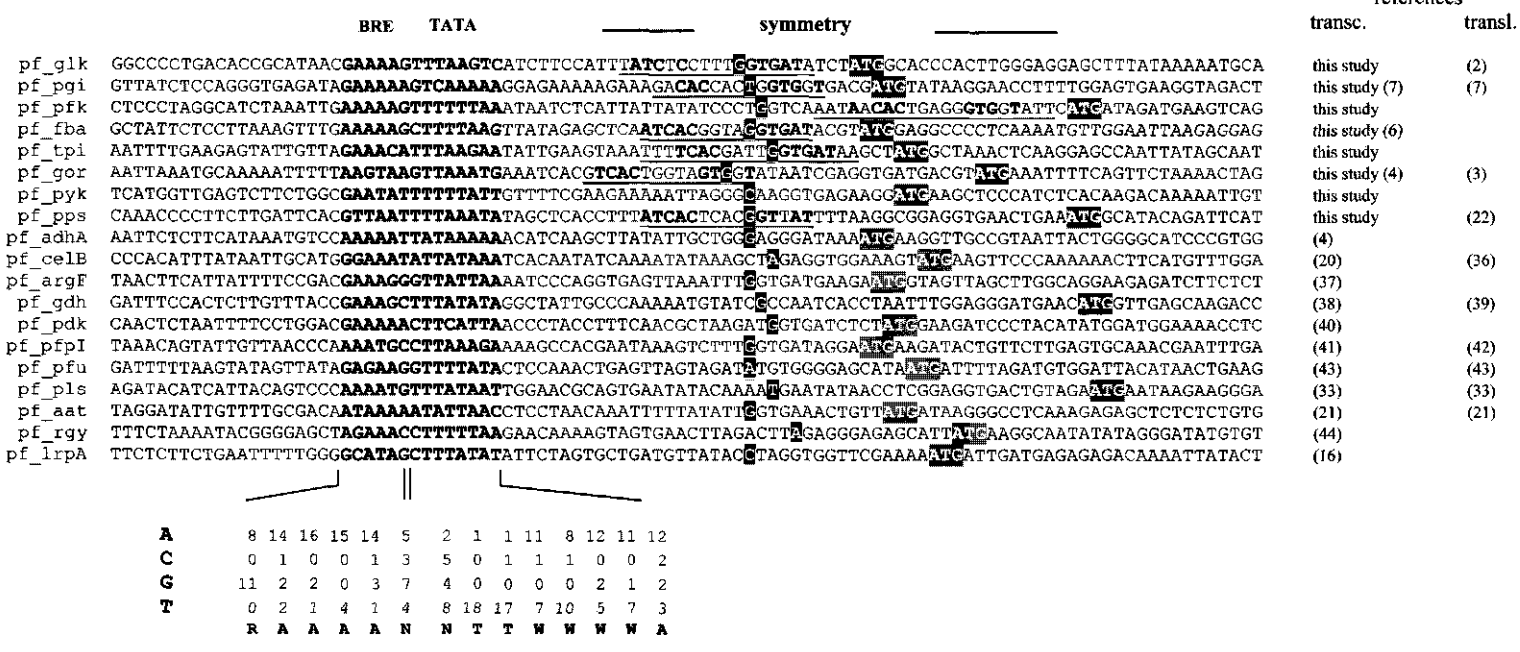

Figure 9.2 Multiple sequence alignment of promoter sequences from *P. furiosus*. Putative promoter elements are indicated in *bold*. The BRE and TATA boxes are indicated above the alignment and consensus sequences are presented under the alignment. Symmetric elements are *underlined*. Determined transcription start sites are indicated in *black boxes*. Translation start sites are indicated in *grey boxes*. References of experimentally determined transcription (transc.) and translation (transl.) start sites are included. pf = *P. furiosus*. pf_adhA = alcohol dehydrogenase (AAC25556); pf_celB = β-glucosidase (AAC25555); pf_argF = ornithine carbamoyltransferase (Q51742); pf_gdh = glutamate dehydrogenase (JN0854); pf_pdk = prolyl endopeptidase (JC4084); pf_pfpI = protease (Q51732); pf_pfu = DNA polymerase (P80061); pf_pls = pyrolysin (T28159); pf_aat = alanine aminotransferase (AF65616); pf_rgy = reverse gyrase (AAB49283); pf_lrpA = leucine-responsive regulatory protein (AAD20389).

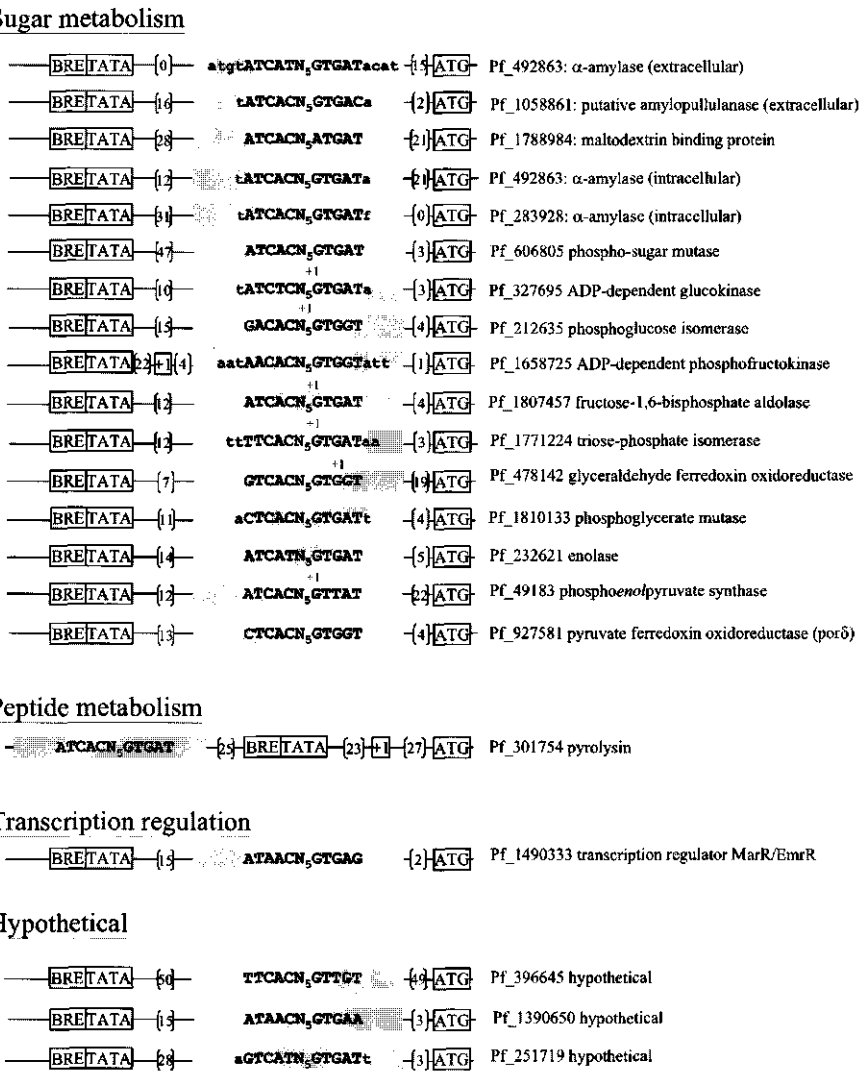

Figure 9.3 Occurrence of PSR-elements in the *P. furiosus* genome.

BRE, TATA box and translation start sites are indicated in *transparent boxes*. PSR-elements are indicated in *grey boxes*. Transcription initiation sites are indicated as +1 The nucleotide distance between the boxes are indicated between *brackets*. The complete *P. furiosus* genomic sequence is available at http://www.utah.edu.

Based on imperfect variants in the promoter sequences, the complete genome of *P. furiosus* was screened. Motifs identified downstream and more than 100 bp upstream of predicted translation start sites were omitted. In total, this inverted repeat was identified 21 times in putative and characterized promoter sequences in the 2.0 Mb genome of *P. furiosus* (http://www.utah.edu). The majority [a total of 16] of these, are in front of genes that encode proteins involved in starch and glucose metabolism. In addition, this inverted repeat appears to be present in promoter sequences of 5 other genes encoding pyrolysin, a putative transcription regulator, and three hypothetical proteins (Fig 9.3). This inverted repeat has been termed *Pyrococcus*-Specific Repeat (PSR). The PSR-element is exclusively found in promoter sequences encoding proteins involved in α-linked sugar degradation and uptake. All these genes appear to be transcribed as monocistronic messengers based on experimental data (4) (33) (7) (6) and/or the architecture of the sequences located upstream the translation start and downstream the translation termination site. *MalE* is the first gene of a gene cluster including *malF*, *malG* and an α-amylase, but these genes are suggested to be transcribed separately (S. Koning, pers. comm).

Interestingly, PSR is absent in promoter sequences of *fbp*, *gap* and *pgk* genes, encoding enzymes that solely act in gluconeogenesis, and also in promoter sequences of genes involved in the catabolism of β-linked glucose poly-/oligo-saccharides, like β-glucosidase and the cellobiose transporter. Remarkably, it is also absent in the sequences upstream the *pyk* gene, but present in the *pps* gene. Although it has been suggested before that phospho*enol*pyruvate synthase rather than pyruvate kinase might be operating in glycolytic direction in this archaeon (34), this is still a matter of debate (22) (J. Tuininga, pers. comm.).

The position of PSR, located downstream the TATA box suggests that it may be involved in the negative control of gene expression, by binding a transcriptional regulator or trans-acting protein. Similarly, the location, 25 nucleotides upstream the BRE site of the mapped pyrolysin (*pls*) promoter (33) indicates that it may be involved in transcription activation of this gene. A specific form of catabolite repression could be the anticipated mechanism involved. In the presence of peptides, α-sugar utilization would then thus be repressed in *P. furiosus*. It has indeed been shown that growth on tryptone inhibits glycolysis in the closely related *Thermococcus zilligii*, even after addition of glucose (35). However, experimental data are obviously required to confirm this hypothesis. The presence of PRS in promoter regions of genes encoding many sugar-converting enzymes, including the complete glycolysis, would indicate that it might represent a specific site for regulation of the *P. furiosus* glycolytic pathway. Unexpectedly, this site is not present in promoter sequences of homologous genes in *P. horikoshii* and *P. abyssi*. This might reflect the evolution of a more sophisticated regulatory system after divergence of the *Pyrococcus* species. This would be in agreement with the recent gain of some saccharolytic enzymes by *P. furiosus*, such as the ones involved in β-glucan degradation (26).

Acknowledgment

This research was supported by the Earth and Life Sciences Foundation (ALW), which is subsidized by the Netherlands Organization for Scientific Research (NWO). We thank Arjen Brinkman (Wageningen University) for providing some of the promoter sequences and Thijs Ettema (Wageningen University) for computer assistance.

References

1. Kengen, S. W., de Bok, F. A., van Loo, N. D., Dijkema, C., Stams, A. J., and de Vos, W. M. (1994) *J. Biol. Chem.* 269, 17537-17541.
2. Kengen, S. W., Tuininga, J. E., de Bok, F. A., Stams, A. J., and de Vos, W. M. (1995) *J. Biol. Chem.* 270, 30453-30457.
3. Mukund, S., and Adams, M. W. (1995) *J. Biol. Chem.* 270, 8389-8392.
4. van der Oost, J., Schut, G., Kengen, S. W., Hagen, W. R., Thomm, M., and de Vos, W. M. (1998) *J. Biol. Chem.* 273, 28149-28154.
5. Tuininga, J. E., Verhees, C. H., van der Oost, J., Kengen, S. W., Stams, A. J., and de Vos, W. M. (1999) *J. Biol. Chem.* 274, 21023-21028.
6. Siebers, B., Brinkmann, H., Dorr, C., Tjaden, B., Lilie, H., van der Oost, J., and Verhees, C. H. (2001) *J. Biol. Chem.* 276, 28710-28718.
7. Verhees, C. H., Huynen, M. A., Ward, D. E., Schiltz, E., de Vos, W. M., and van der Oost, J. (2001) *J. Biol. Chem.* 276, 40926-40932.
8. Schramm, A., Siebers, B., Tjaden, B., Brinkmann, H., and Hensel, R. (2000) *J. Bacteriol.* 182, 2001-2009.
9. Schut, G. J., Zhou, J., and Adams, M. W. (2001) *J. Bacteriol.* 183, 7027-7036.
10. Luesink, E. J., van Herpen, R. E., Grossiord, B. P., Kuipers, O. P., and de Vos, W. M. (1998) *Mol. Microbiol.* 30, 789-798.
11. van den Bogaard, P. T., Kleerebezem, M., Kuipers, O. P., and de Vos, W. M. (2000) *J. Bacteriol.* 182, 5982-5989.
12. Ramseier, T. M., Bledig, S., Michotey, V., Feghali, R., and Saier, M. H., Jr. (1995) *Mol. Microbiol.* 16, 1157-1169.
13. Baker, H. V. (1986) *Molecular and Cellular Biology* 6, 3774-3784.
14. Baker, H. V. (1991) *Proc. Natl. Acad. Sci. U. S. A.* 88, 9443-9447.
15. Napoli, A., van der Oost, J., Sensen, C. W., Charlebois, R. L., Rossi, M., and Ciaramella, M. (1999) *J. Bacteriol.* 181, 1474-1480.
16. Brinkman, A. B., Dahlke, I., Tuininga, J. E., Lammers, T., Dumay, V., de Heus, E., Lebbink, J. H., Thomm, M., de Vos, W. M., and van Der Oost, J. (2000) *J. Biol. Chem.* 275, 38160-38169.
17. Enoru-Eta, J., Gigot, D., Thia-Toong, T. L., Glansdorff, N., and Charlier, D. (2000) J. *Bacteriol.* 182, 3661-3672.
18. Hochheimer, A., Hedderich, R., and Thauer, R. K. (1999) *Mol. Microbiol.* 31, 641-650.
19. Bell, S. D., and Jackson, S. P. (2000) *J. Biol. Chem.* 275, 31624-31629.
20. Kengen, S. W., Luesink, E. J., Stams, A. J., and Zehnder, A. J. (1993) *Eur. J. Biochem.* 213, 305-312.
21. Ward, D. E., Kengen, S. W., van Der Oost, J., and de Vos, W. M. (2000) *J. Bacteriol.* 182, 2559-2566.

22. Hutchins, A. M., Holden, J. F., and Adams, M. W. (2001) *J. Bacteriol.* 183, 709-715.
23. Plaumann, M., Pelzer-Reith, B., Martin, W. F., and Schnarrenberger, C. (1997) *Curr. Genet.* 31, 430-438.
24. Gibson, J. L., Falcone, D. L., and Tabita, F. R. (1991) *J. Biol. Chem.* 266, 14646-14653.
25. van den Bergh, E. R., Baker, S. C., Raggers, R. J., Terpstra, P., Woudstra, E. C., Dijkhuizen, L., and Meijer, W. G. (1996) *J. Bacteriol.* 178, 888-893.
26. Ettema, T., van der Oost, J., and Huynen, M. (2001) *Trends Genet.* 17, 485-487.
27. Myllykallio, H., Lopez, P., Lopez-Garcia, P., Heilig, R., Saurin, W., Zivanovic, Y., Philippe, H., and Forterre, P. (2000) *Science* 288, 2212-2215.
28. Tolstrup, N., Sensen, C. W., Garrett, R. A., and Clausen, I. G. (2000) *Extremophiles* 4, 175-179.
29. Soppa, J. (1999) *Mol. Microbiol.* 31, 1295-1305.
30. Bell, S. D., Kosa, P. L., Sigler, P. B., and Jackson, S. P. (1999) *Proc. Natl. Acad. Sci. U. S. A.* 96, 13662-13667.
31. Soppa, J. (1999) *Mol. Microbiol.* 31, 1589-1592.
32. Hethke, C., Geerling, A. C., Hausner, W., de Vos, W. M., and Thomm, M. (1996) *Nucleic Acids Res.* 24, 2369-2376.
33. Voorhorst, W. G., Eggen, R. I., Geerling, A. C., Platteeuw, C., Siezen, R. J., and Vos, W. M. (1996) *J. Biol. Chem.* 271, 20426-20431.
34. Sakuraba, H., Utsumi, E., Kujo, C., and Ohshima, T. (1999) *Arch. Biochem. Biophys.* 364, 125-128.
35. Xavier, K. B., da Costa, M. S., and Santos, H. (2000) *J. Bacteriol.* 182, 4632-4636.
36. Voorhorst, W. G., Eggen, R. I., Luesink, E. J., and de Vos, W. M. (1995) *J. Bacteriol.* 177, 7105-7111.
37. Roovers, M., Hethke, C., Legrain, C., Thomm, M., and Glansdorff, N. (1997) *Eur. J. Biochem.* 247, 1038-1045.
38. Eggen, R. I., Geerling, A. C., Waldkotter, K., Antranikian, G., and de Vos, W. M. (1993) *Gene* 132, 143-148.
39. Ohshima, T., and Nishida, N. (1993) *Biosci. Biotechnol. Biochem.* 57, 945-951.
40. Robinson, K. A., Bartley, D. A., Robb, F. T., and Schreier, H. J. (1995) *Gene* 152, 103-106.
41. Halio, S. B., Blumentals, II, Short, S. A., Merrill, B. M., and Kelly, R. M. (1996) *J. Bacteriol.* 178, 2605-2612.
42. Blumentals, II, Robinson, A. S., and Kelly, R. M. (1990) *Appl. Environ. Microbiol.* 56, 1992-1998.
43. Uemori, T., Ishino, Y., Toh, H., Asada, K., and Kato, I. (1993) *Nucleic Acids Res.* 21, 259-265.
44. Borges, K. M., Bergerat, A., Bogert, A. M., DiRuggiero, J., Forterre, P., and Robb, F. T. (1997) *J. Bacteriol.* 179, 1721-1726.

Chapter 10

Summary and concluding remarks

In the last few decades microorganisms have been isolated from rather unknown and hostile locations, such as those with high salt concentrations, an extreme pH, or low or high temperatures. Microorganisms isolated from these environments are referred to as extremophiles (1). The most extensively studied group of these extremophiles are the hyperthermophiles, microorganisms that have an optimum temperature for growth above 80 °C (2). Except for two bacterial genera, the *Thermotageles* and *Aquifex*, all hyperthermophiles isolated to date belong to the domain of the archaea. The archaea compose together with the bacteria and eucarya the three domains of life (3).

Pyrococcus furiosus is a hyperthermophilic archaeon, with an optimal growth temperature of 100 °C that grows heterotrophically on a variety of substrates including peptides and saccharides. For its growth on saccharides it uses a modified version of the Embden-Meyerhof pathway, that involves novel enzymes and unique control mechanisms. The research described in this thesis has mainly focussed on the molecular and biochemical characterization of enzymes involved in the upper part of glycolysis in *P. furiosus* and related organisms (Fig. 10.1).

A brief outline of this study is giving in **Chapter 1**. In **Chapter 2** sugar metabolism in archaea is reviewed. Recent studies on various modifications in the Entner-Doudoroff and Embden-Meyerhof pathways are discussed, and potential scenarios on the evolution of sugar metabolism are proposed.

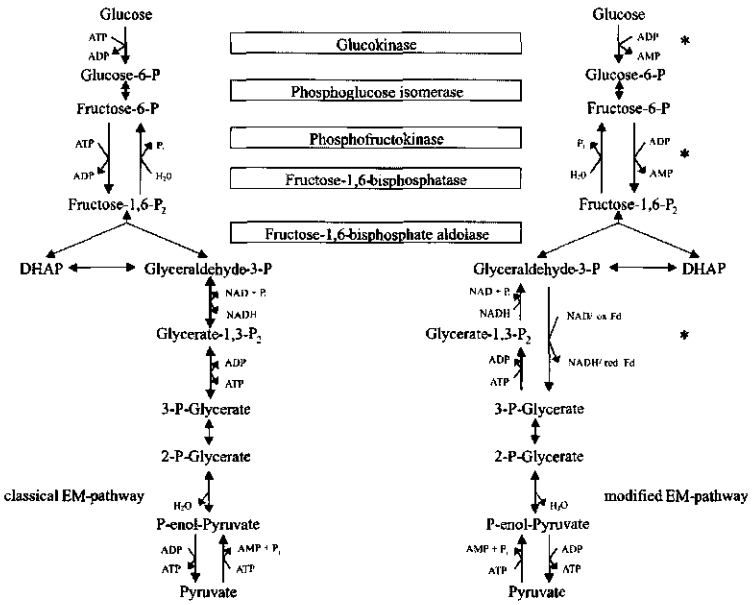

Figure 10.1 Classical Embden-Meyerhof (EM) pathway *vs* modified EM-pathway.
Classical EM-pathway is operative in bacteria and eucarya. Modifications (*) in the EM-pathway are found in archaea. Enzymes that were under investigation in this thesis are indicated in *blocks*.

Chapter 3 describes the first characterization of an ADP-dependent phosphofructokinase (ADP-PFK). Attempts to purify the ADP-PFK from *P. furiosus* cell extracts were not successful, because of the difficult purification procedure of this enzyme, which tends to stick to other proteins. Alternative approaches based on anticipated homology with the ADP-dependent glucokinase (ADP-GLK) have resulted in the identification of the gene encoding the ADP-PFK on the *P. furiosus* genome. The gene encoding the ADP-PFK was functionally expressed in *Escherichia coli* using a well-established expression system. The production of the ADP-PFK in the mesophilic *E. coli* allowed for a simple purification procedure consisting of a heat-treatment of the cell extract followed by a single chromatographic step. The purified enzyme was able to phosphorylate fructose-6-phosphate into fructose-1,6-bisphosphate with ADP as phosphoryl group donor. Classical PFKs use ATP or PP_i as potential phosphoryl group donor, indicating that the *P. furiosus* enzyme differs from its canonical counterparts. The enzyme was not regulated by any of the known allosteric modulators of ATP-PFKs, implying that the *P. furiosus* glycolysis does not possess a typical site of regulation.

Sequence analysis on the primary structure of the ADP-PFKs showed no significant sequence similarity with the classical monophyletic PFKs (PFKA). However, high similarity (21% identity) was observed with the ADP-dependent glucokinase (ADP-GLK) from *P. furiosus*, suggesting that both ADP-dependent sugar kinases are phylogenetically related, and belong to the same enzyme family. Orthologs of the ADP-PFK were identified in genome databases of the closely related *P. horikoshii* and *P. abyssi*. Also the paralogous ADP-GLK was present in these Pyrococci. Furthermore, orthologs of the ADP-PFK were identified in the hyperthermophilic methanogen *Methanococcus jannaschii* and the mesophilic methanogen *Methanosarcina mazei* (**Chapter 4**). Based on a combination of genomic comparison and activity measurements it is concluded that ADP-PFKs are not restricted to the *Thermococcales*, but are present in mesophilic methanogens as well. Interestingly, uncharacterized homologs (presumably ADP-dependent) of this unusual kinase are present in several higher eucarya, including human, mouse and fly. The gene encoding the ADP-PFK from *M. jannaschii* was expressed in *E. coli*, and the enzyme was subsequently purified. The biochemical characteristics of the first ADP-PFK from a chemolithoautotrophic archaeon were compared to those of the ADP-PFK from the heterotrophic archaea *P. furiosus* and *Thermococcus zilligii* (**Chapter 4**).

In **Chapter 5** an ATP-dependent galactokinase (catalyzing the first step of the Leloir pathway) from *P. furiosus* is described. Therefore, both ADP-dependent sugar kinases and an ATP-dependent sugar kinase appear co-exist in this hyperthermophile. The three dimensional structure of the *P. furiosus* galactokinase has recently been solved in close collaboration with the group of Prof. David Rice (Sheffield, England). Despite the ADP-dependent sugar kinases, the ATP-dependent galactokinase shares two conserved motifs and a high degree of overall similarity (± 32 % identity)

to the canonical galactokinases. The galactokinase and the ADP-GLK from *P. furiosus* were produced in *E. coli*, and their characteristics were compared to each other and to their canonical counterparts. The kinetic and physical parameters of the heterologously produced ADP-GLK were in good agreement with those of the native ADP-GLK, indicating that the enzyme was successfully produced and folded in *E. coli*. The affinity for ATP of the galactokinase was extremely high at 90 °C (K_m for ATP of 0.008 mM) compared to the classical galactokinase from mesophiles. However, the affinity for galactose was comparable to that of the canonical enzymes. It was suggested that the extremely high affinity of the galactokinase for ATP might reflect an adaptation to a relative low intracellular ATP concentration in *P. furiosus*. This might also explain the presence of the ADP-dependent sugar kinases in *P. furiosus*. Both the ATP-dependent galactokinase and the ADP-GLK showed a high catalytic efficiency for their phosphoryl group donor at 90 °C, compared to their mesophilic counterparts.

Chapter 6 describes the purification of a unique phosphoglucose isomerase from *P. furiosus*, its characterization, isolation of the corresponding gene, and prediction of the structure of the enzyme. The phosphoglucose isomerase was purified from a *P. furiosus* extract. The N-terminal sequence of the purified enzyme was determined, and the gene, named *pgiA*, could be identified on the *P. furiosus* genome. Subsequent expression in *E. coli* revealed that the gene indeed encoded a phosphoglucose isomerase. The *pgiA* gene was transcribed as a mono-cistronic messenger, and the transcription start site was mapped. Despite similar substrate specificity and kinetic parameters, no significant sequence similarity was obtained with classical phosphoglucose isomerases. In contrast, the enzyme shares similarity with the CUPIN superfamily (double-stranded beta-helices) that consists of a variety of proteins that are generally involved in sugar binding or protein interaction. This is the first example of a phosphoglucose isomerase that belongs to the CUPIN superfamily, and it is the first characterization of an archaeal phosphoglucose isomerase to date. The novel phosphoglucose isomerase and the two ADP-dependent sugar kinases are examples of an excessive replacement of enzymes in glycolysis, and are a compelling example of convergent evolution.

Chapter 7 focuses on two archaeal fructose-1,6-bisphosphate aldolases, *i.e* fructose-1,6-bisphosphate aldolase from the crenarchaeon *Thermoproteus tenax* and from the euryarchaeon *P. furiosus*. The genes encoding these enzymes were identified in the genomes based on sequence similarity with a novel fructose-1,6-bisphosphate aldolase from *E. coli*. Transcript analyses reveal that the *in vivo* expression of both genes is induced during sugar fermentation. Subsequently, the genes were expressed in *E. coli*, and the encoded proteins were purified to homogeneity. Both the archaeal enzymes use a Schiff base mechanism for catalysis similar to the Class I aldolases, in contrast to the Class II aldolases that use metal ions for catalyses. As revealed by phylogenetic analyses, orthologs of the *T. tenax* and *P. furiosus* enzyme appear to be present in almost all sequenced archaeal genomes, as well as in some bacterial genomes, strongly suggesting that this

new enzyme family represents the typical archaeal fructose-1,6-bisphosphate aldolase. Because this family shows no overall sequence similarity to classical Class I and II enzymes, a new name is proposed, archaeal type Class I fructose-1,6-bisphosphate aldolase (Class IA). Despite to low sequence similarity between the archaeal type Class I fructose-1,6-bisphosphate aldolases and the classical Class I and Class II aldolases, sequence signatures could be identified resembling the active site region (Lys-191) and the phosphate-binding motif of classical Class I fructose-1,6-bisphosphate aldolases and other members of the $(\beta\alpha)_8$ barrel superfamilies. This suggests that the archaeal type Class I enzymes are distantly related to the classical Class I fructose-1,6-bisphosphate aldolases, and that they share the same ancestral origin.

In **Chapter 8** the *P. furiosus* gluconeogenic fructose-1,6-bisphosphatase is described. The gene was identified in the genome based on the sequence similarity with the recently described *Methanococcus jannaschii* bi-functional inositol-monophosphatase/fructose-1,6-bisphosphatse. The gene was functionally expressed in *E. coli*, and the enzyme was subsequently purified to homogeneity. Biochemical characteristics were compared with the homologous gene product from *M. jannaschii* (MJ0109), revealing distinct characteristics in substrate specificity and inhibitors. The *M. jannaschii* enzyme is a bi-functional enzyme with high activity on inositol-1-phosphosphate and fructose-1,6-bisphosphate. The *P. furiosus* enzyme has a more specific substrate specificity with a clear preference for fructose-1,6-bisphosphate. Therefore, the enzyme can be regarded as a true fructose-1,6-bisphosphatase. Sequence analysis of the *P. furiosus* fructose-1,6-bisphosphatase reveals the enzyme to be more similar to inositol monophosphatases than to fructose-1,6-bisphosphatases (type I), both belonging to the sugar phosphatase superfamily, with similar folding and sequence motifs. Because of the higher similarity of the *P. furiosus* enzyme to the inositol monophosphatases, and because of its specific preference for fructose-1,6-bisphosphate, the enzyme was proposed to belong to a new sub-family: the euryarchaeal fructose-1,6-bisphosphatase (type IV). This new sub-family shows limited sequence similarity to classical fructose-1,6-bisphosphatase from bacteria and eucarya (type I), and no significant sequence similarity to the bacterial fructose-1,6-bisphosphatases (type II and III).

Preliminary results in promoter architecture of genes encoding glycolytic enzymes are described in **Chapter 9**. Promoter elements were identified, and a putative glycolytic regulator binding site (ATCACNNNNNGTGAT, where N are random nucleotides) is observed specifically in *P. furiosus* promoter sequences of glycolytic-enzyme encoding genes. Complete analysis of the *P. furiosus* genome revealed that this motif is present in 21 promoter sequences. The majority of the genes encode enzymes involved in sugar metabolism. Further research is needed to reveal the function of this putative binding site.

In conclusion, this project has resulted in the identification of unique genes encoding novel enzymes of modified glycolytic pathways in archaea. Key enzymes of the pyrococcal glycolytic

pathway were shown to be modified in enzyme catalysis, evolution and regulation. In close collaboration with the group of Prof. David Rice (Sheffield, England) significant progress has been made in crystallization of the ADP-PFK and galactokinase from *Pyrococcus*. Finally, it is postulated that regulation of the glycolytic flux in *P.furiosus* might involve modulation of gene expression rather than allosteric regulation of enzyme activities. High throughput screening by transcriptomic and proteomic approaches like DNA micro-arrays and 2D-gelelectrophoresis, and generation of knock-out mutants in Pyrococcus will provide more insight in the actual significance of regulation of gene expression in archaeal central metabolism in the near future.

References

1. Horikoshi, K. (1997) *Extremophiles*

2. Stetter, K.O. (1996) *FEMS Microbiol. Rev.* **18**: 149-158

3. Woese, C.R., Kandler, O., Wheelis, M.L. (1990) *Proc. Natl. Acad. Sci.* **87**: 4576-4579

Chapter 11

Nederlandse samenvatting

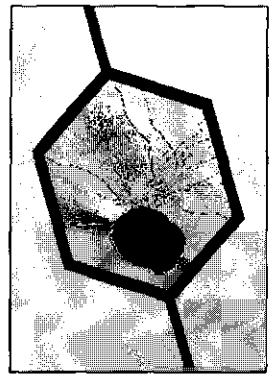

Gedurende de afgelopen vier jaar is me vaak door niet-onderzoekers gevraagd waar ik nu eigenlijk mee bezig was. Het even uitleggen was er vaak niet bij, mede door de vele vaktermen die doorgaans in het lab gebruikt worden. Deze samenvatting is juist bedoeld voor die mensen die interesse hebben getoond in mijn onderzoek, maar geen idee hadden wat ik nu precies aan het doen was.

Met het onderzoek dat in dit proefschrift is beschreven hebben we getracht suikeromzettingen in ons model-organisme beter te begrijpen. Het onderzoek is uitgevoerd binnen het Laboratorium voor Microbiologie en is gefinancierd door ALW-NWO.

Het organisme (oftewel het beestje)

Overal om ons heen is leven. Mensen, dieren en planten zijn hier het zichtbare bewijs van. Maar er is nog meer leven, hoewel niet zichtbaar voor het blote oog. Dit zijn de bacteriën. Deze minuscuul kleine organismen (vaak kleiner dan 0,003 mm) kom je overal tegen. Op je huid zitten al miljarden van deze bacteriën. Van sommige bacteriën kun je ziek worden, maar andere heb je juist nodig om te overleven. Archaea hebben uiterlijke kenmerken van bacteriën, maar onderscheiden zich door te kunnen overleven onder vaak extreme condities. Archaea die onder zeer extreme condities leven, zoals bijvoorbeeld bij temperaturen rond het kookpunt van water worden hyperthermofielen genoemd. Je vindt deze hyperthermofiele archaea onder vulkanische omstandigheden zowel op het land als in de zee. Het organisme dat in dit boekje beschreven is heet *Pyrococcus furiosus* alias "de ziedende vuurbal" en is dus zo'n archaeon dat leeft bij extreem hoge temperatuur. *Pyrococcus* is ontdekt in 1986 nabij het strand van het eiland Vulcano in Italië (Fig.11.1). Hij voelt zich het prettigst in een zoute omgeving en bij een temperatuur van 100°C. Mede door zijn leefomstandigheid en grote verscheidenheid aan eetgewoonten is dit een interessant organisme om te bestuderen. In dit boekje is de vertering van suikers onder de loep genomen (Fig. 11.2).

Figure 11.1 ***Pyrococcus furiosus.***
Bron: http://www.uniregensburg.de/Mikrobio/Stetter/Bilderhtml/pyrococcus.html

De route

Zoals een mens onder normale omstandigheden moet eten om in leven te blijven, zo moet *Pyrococcus* dit ook. Een belangrijke voedselbron voor zowel de mens als *Pyrococcus* is suiker, waaruit energie wordt gehaald en vele bouwstoffen worden gemaakt. Er zijn veel stappen nodig om van suiker de gewenste eindproducten te maken. De route waarvan wij, maar ook *Pyrococcus* gebruik maakt om suiker af te breken heet de glycolyse. Het woord glycolyse komt van het griekse woord glycos, wat suiker betekent en lysis, wat oplossen betekent. Dus glycolyse betekent eigenlijk het oplossen van suiker.

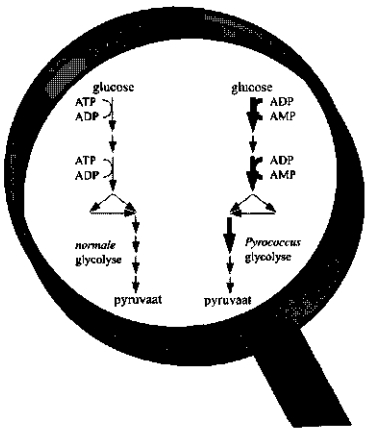

Fig. 11.2 De glycolyse onder de loep genomen.
De normale glycolyse bestaat uit 10 stappen die door 10 verschillende enzymen worden uitgevoerd. De glycolyse van *Pyrococcus* bestaat echter maar uit 9 stappen, die door 9 verschillende enzymen worden uitgevoerd. *Pyrococcus* heeft dus een enzym dat 2 stappen in slechts 1 stap kan doen. Een ander groot verschil tussen de beide routes is het gebruik van het hulpcomponent ADP i.p.v. ATP. De belangrijkste verschillende stappen in de *Pyrococcus* glycolyse zijn aangeven met dikke zwarte pijlen.

De enzymen

Je zou de glycolyse kunnen zien als een zwarte doos waarin suiker (glucose) wordt omgezet in een eindproduct (pyruvaat) (Fig. 11.3). Maar wij gaan hierin verder! Verschillende stappen zijn nodig om glucose in pyruvaat om te zetten via deze glycolyse (Fig 11.2). In iedere stap wordt een kleine verandering aangebracht wat uiteindelijk ertoe leidt dat glucose volledig is omgezet in pyruvaat. Het gereedschap dat nodig is om deze kleine verandering te doen worden enzymen genoemd. Dit zijn eiwitten die je kunt vergelijken met kleine fabriekjes die component X in component Y omzetten. Voor elke verandering is een ander enzym nodig. Dus deze enzymen zijn ook nog eens heel specifiek. De naamgeving van de enzymen heeft te maken met de verandering die ze aanbrengen. Zo zetten enzymen met de naam kinasen een energierijke verbinding (P) aan een

component (A) (A → A-P). Verschillende enzymen uit de *Pyrococcus*-glycolyse zijn in dit proefschrift beschreven en er is gekeken naar welke verandering ze teweegbrengen en hoe goed ze dit doen. Hieruit is naar voren gekomen dat *Pyrococcus* enzymen heeft die unieke omzettingen kunnen doen, welke nog niet eerder in detail bestudeerd waren. Vervolgens is gekeken of de betreffende enzymen uit *Pyrococcus* verwant zijn aan enzymen in andere organismen. Dit is uitgezet in een stamboom, waarbij de onderlinge verwantschap bekeken is. Het is nu gebleken dat *Pyrococcus* gebruik maakt van een variant van de glycolyse waarbij een aantal stappen tussen het beginpunt glucose en eindpunt pyruvaat afwijken van de bestaande glycolyse in bacteriën en de mens. *Pyrococcus* maakt hier gebruik van andere, niet verwante enzymen, die soms net een andere omzetting doen waardoor ze uniek te noemen zijn.

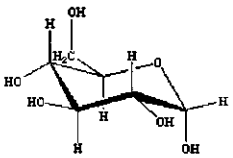

Glucose
$C_6H_{12}O_6$

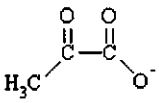

Pyruvaat
$C_3H_3O_3$

Figure 11.3 Structuurformules van glucose en pyruvaat.

Het zoeken naar enzymen

Allemaal leuk en aardig zul je denken, maar hoe krijg je nu deze enzymen in handen om ze vervolgens te kunnen bestuderen. Hiervoor hebben we een tweetal strategieën gebruikt. In de eerste strategie hebben we het voor ons interessante enzym uit *Pyrococcus* gevist, dit heet het zuiveren van een enzym. Dit zou je kunnen vergelijken met het zoeken naar een speld in een hooiberg. Maar door slim te werk te gaan kun je heel gericht zoeken. In *Pyrococcus* zitten wel honderden verschillende enzymen. Al deze enzymen hebben specifieke eigenschappen. Door nu gebruik te maken van deze verschillende specifieke eigenschappen, zoals bijvoorbeeld grootte en lading, kun je de enzymen van elkaar scheiden. Zo kun je een scheiding op basis van grootte vergelijken met de werking van een zeef. Afhankelijk van de grootte van de mazen kan iets door de zeef gaan of er juist in achter blijven. Waar je enzym zich bevindt na elke stap kun je controleren door de omzetting te meten die specifiek is voor dat enzym (bijvoorbeeld A → A-P). Na 5 tot 6 verschillende van dit soort technieken toegepast te hebben houd je meestal je gezuiverd enzym waar naar je op zoek was over en kun je beginnen met dit enzym eens grondig te gaan bestuderen.

In een tweede strategie maken we in eerste instantie gebruik van de computer. Van heel veel enzymen is al bekend wat ze doen en hoe ze eruit zien. Van deze enzymeigenschappen zijn profielen gemaakt en deze zijn systematisch geordend. Door geavanceerde computerprogramma's te gebruiken kunnen we als het ware zoeken in *Pyrococcus* naar overeenkomsten met die bestaande enzymprofielen (de tak van sport die hierin gespecialiseerd is wordt ook wel bioinformatica genoemd). Om dit te kunnen doen moeten natuurlijk gegevens van *Pyrococcus* ook beschikbaar zijn in het computerbestand (zie erfelijk materiaal). Hierna kunnen we met onze trucjesdoos, waar heel wat gepipetteer bij komt kijken het enzym laten maken door een bacterie die we daarvoor getraind hebben. Vervolgens kunnen we op een relatief makkelijke manier via 1 à 2 stappen (strategie 1) het enzym zuiveren.

Het erfelijk materiaal

Erfelijke eigenschappen bevinden zich bij bacteriën en archaea op een enkel groot molecuul, het chromosoom. Echter bij de mens zijn er 46 van deze chromosomen. Een chromosoom is gemaakt van DNA (de veel gebruikte afkorting voor de chemische naam van het erfelijk materiaal). De samenstelling van het complete DNA van verschillende bacteriën, archaea en ook de mens is nu bekend. Zo kunnen we nu dus ook alle DNA van *Pyrococcus* in kaart brengen. Alleen dit DNA zegt natuurlijk nog niets. Wat we willen weten is wat het DNA betekent, we willen het als het ware kunnen lezen. Een gen is nu een bepaalde volgorde van het DNA en bevat de informatie die nodig is om een eiwit, of de enzymen die in dit proefschrift zijn besproken, te produceren. Deze genen worden van generatie op generatie doorgegeven middels overerving (of celdeling bij bacteriën en archaea), maar kunnen ook direct tussen (niet) verwante organismen worden overgebracht (horizontale overdracht). Op deze manier ontstaat er evolutie van het gen. Door het vergelijken van de samenstelling van een gen met dat van soortgenoten en andere organismen hebben we ontdekt dat genen (die coderen voor de glycolyse-enzymen) zich ook op verschillende manieren geëvolueerd hebben, zowel door celdeling als horizontale genoverdracht.

In de startblokken

Hoe wordt nu de met informatie die op een gen ligt een enzym gemaakt? Een gen bevat alle informatie (DNA) welke nodig is om een enzym te maken. De speciale code die op het gen ligt geeft heel precies de bouwstenen en hun volgorde aan zoals ze in het enzym komen te zitten. Het gen is dus een soort blauwdruk voor het enzym. Maar hoe gaat die vertaling van DNA naar enzym nu eigenlijk in zijn werk? Allereerst wordt het DNA via een speciale machinerie vertaald in boodschapper RNA (mRNA). Dit wordt wel eens vergeleken met een racebaan (Fig. 11.4). De

machinerie is de raceauto en het gen is het parcours. De pitstop van waaruit de raceauto vertrekt is erg belangrijk, dit is een stukje DNA dat voor het gen ligt (dit wordt de promoter genoemd). De raceauto wordt hier klaargemaakt en alle onderdelen worden bevestigd. Op het moment dat het stoplicht op groen springt scheurt de raceauto het parcours (gen) op. Na een rondje over het parcours is het DNA vertaald in mRNA. De raceauto krijgt alleen het groene licht als er op dat moment behoefte is aan de specifieke eigenschappen die het gen bezit, dus als er behoefte is aan het enzym. Zo zal voor de glycolyse gelden: als er suiker aanwezig is dan wordt er druk gereden om alle benodigde enzymen aan te maken. Maar met het mRNA zijn we er nog niet. Dit mRNA is de boodschapper die vertrekt naar de ribosomen (de eiwitsynthese-fabrieken) waar het enzym gemaakt wordt. Dus om een enzym te maken dient het DNA eerst vertaald te worden in mRNA, dat vervolgens weer als boodschapper dient voor de ribosomen waar het enzym dan daadwerkelijk gemaakt wordt (Fig. 11.4).

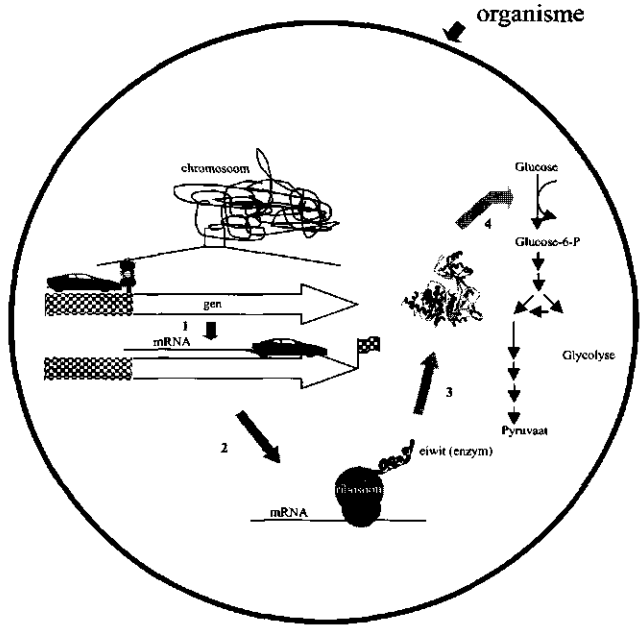

Fig. 11.4 Van gen tot enzym.

Schematische weergave hoe een enzym aangemaakt wordt in een organisme. 1. Het coderende gen wordt vertaald in boodschapper RNA (transcriptie). 2. Dit boodschapper RNA wordt gelezen door de ribosomen en het enzym wordt primair aangemaakt (translatie). 3. Het enzym vouwt zich in een actieve vorm. 4. Uiteindelijk doet het enzym de specifieke omzetting waar het voor gemaakt is, bijvoorbeeld de eerste stap in de glycolyse.

Wat weten we nu?

De aangegeven strategieën hebben ertoe geleid dat we alle genen die coderen voor enzymen uit de glycolyse van *Pyrococcus* hebben kunnen lokaliseren op het chromosoom. Je kunt dit vergelijken met een puzzel, de zogenaamde glycolyse-puzzel. Omdat we de complete DNA-volgorde van *Pyrococcus* al wisten hadden we eigenlijk al veel informatie in handen (puzzelstukjes). Maar omdat de genen zoveel afwijken van bekende genen waren we nog niet in staat om van ieder mogelijk glycolyse-gen de functie te voorspellen (waar moeten de puzzelstukjes komen te liggen in de glycolyse-puzzel?). Daarom hebben we de coderende enzymen gezuiverd uit *Pyrococcus* en hebben we de enzymen laten maken door getrainde bacteriën op basis van het *Pyrococcus* erfelijk materiaal. Dit heeft ertoe geleid dat we tot dusver onbekende glycolyse-enzymen hebben kunnen bestuderen welke geen of geringe verwantschap vertonen met enzymen uit andere organismen die een vergelijkbare omzetting kunnen doen. Vervolgens hebben we alle puzzelstukjes van glycolyse-enzymen op de juiste plaats in de glycolyse kunnen neerleggen. Hieruit kwam naar voren dat de grootste variatie, d.w.z. de aanwezigheid van unieke enzymen, zich bevindt in het bovenste deel van de glycolyse. Het onderste gedeelte van de glycolyse bleek weinig te variëren tussen *Pyrococcus* en andere organismen. Het idee is dat het onderste deel van de route origineel een functie had in de synthese van celcomponenten (anabool) en dat vervolgens met het verkrijgen van het bovenste gedeelte er in *Pyrococcus* een volledige glycolyse is ontstaan die het mogelijk maakte suikers om te zetten en erop te groeien (katabool).

Tot slot is een eerste aanzet gegeven in de regulatie van de glycolyse, d.w.z. wanneer mag de raceauto gaan rijden en wanneer niet. Het blijkt namelijk dat er in de promoters van deze genen (pitstop) een signaal aanwezig is dat het stoplicht aan of uit zou kunnen zetten en zodoende de race kan laten verlopen of juist stil zetten.

Curriculum vitae

Cornelis Hubertus Verhees werd geboren op de koude winterdag van 19 december 1972 in Oisterwijk. Hij kwam te wereld als het derde kind in het gezin van Anton en Henriëtte Verhees-Meijnckens. In zijn geboortedorp doorliep Corné vervolgens de kleuterschool, basisschool en middelbare school. In 1990 slaagde hij voor zijn H.A.V.O.-eindexamen op de R.K. scholengemeenschap Durendael. Hierna werd hij een fanatieke NS-reiziger die elke dag op en neer reisde van Oisterwijk naar Etten-Leur, alwaar hij in 1990 begon aan de studie medische-biotechnologie aan Hogeschool West-Brabant. Zijn stage- en afstudeervak deed hij bij Gist-brocades te Delft. Onder begeleiding van ir. Bert Geraats bestudeerde hij de lipase-productie door *Pseudomonas alcaligenes*. Toen in 1994 het H.L.O-diploma behaald was stond de jonge ingenieur voor de keuze in dienst te gaan of verder te gaan studeren. Zonder er lang over hoeven na te denken koos hij bewust voor het laatste. De studie bioprocestechnologie aan de toenmalig Landbouw Universiteit Wageningen was een logische en snel gemaakte keuze. Na een gewenningsperiode door de omschakeling van een HBO naar een academische manier van studeren verliep de studie redelijk vlotjes. Een afstudeervak Bacteriële Genetica aan de vakgroep Microbiologie werd gevolgd onder begeleiding van dr. John van der Oost en prof. dr. Willem M. de Vos. In september 1997 studeerde hij af en begon Corné als onderzoeker in opleiding bij de vakgroep Microbiologie aan de toenmalig Landbouw Universiteit Wageningen. In zijn onderzoek bestudeerde hij de glycolyse van het thermofiele archaeon *Pyrococcus furiosus*. De uitkomsten van deze studie staan weergegeven in dit proefschrift. Sinds 1 december 2001 is hij in dienst als postdoc binnen dezelfde vakgroep. In deze nieuwe functie onderzoekt Corné de potenties van *P. furiosus* als producent van fijnchemicaliën.

List of publications

Tuininga, J.E., Verhees, C.H., van der Oost, J., Kengen, S.W.M., Stams, A.J.M., de Vos, W.M. (1999) Molecular and biochemical characterization of the ADP-dependent phosphofructokinase from the hyperthermophilic archaeon *Pyrococcus furiosus*. *J.Biol.Chem.* 274: 21023-21028.

Kaper, T., Verhees, C.H., Lebbink, J.H.G., van Lieshout, J.F.T., Kluskens, L.D., Ward, D.E., Kengen, S.W.M., Beerthuyzen, M.M., de Vos, W.M., van der Oost, J. (2000) Characterization of β-glycosyl hydrolases from *Pyrococcus furiosus*. *Methods Enzymol.* 330: 329-346.

Kengen, S.W.M., Tuininga, J.E., Verhees, C.H., van der Oost, J., Stams, A.J.M., de Vos, W.M. (2000) ADP-dependent glucokinase and phosphofructokinase in *Pyrococcus furiosus*. *Methods Enzymol.* 331: 41-53.

Siebers, B., Brinkmann, H., Dörr, C., Tjaden, B., Lilie, H., van der Oost, J., Verhees, C.H. (2001) Archaeal fructose-1,6-bisphosphate aldolases constitute a new family of archaeal type class I aldolase. *J. Biol. Chem.* 276: 28710-28718.

Verhees, C.H., Huynen, M.A., Ward, D.E., de Vos, W.M., van der Oost, J. (2001) The phosphoglucose isomerase from the hyperthermophilic archaeon *Pyrococcus furiosus* is a unique glycolytic enzyme that belongs to the cupin superfamily. *J. Biol. Chem.* 276: 40926-40932.

Verhees, C.H., Tuininga, J.E., Kengen, S.W.M., Stams, A.J.M., van der Oost, J., de Vos, W.M. (2001) ADP-dependent phosphofructokinases in mesophilic and thermophilic methanogenic archaea. *J. Bacteriol.* 183: 7145-7153.

Verhees, C.H., Koot D., Ettema, T.J.G., de Vos, W.M., van der Oost, J. (2002) Biochemical adaptations of two sugar kinases from the hyperthermophilic archaeon *Pyrococcus furiosus*. *Biochem. J. In press.*

Verhees, C.H., Akerboom, J., Schiltz, E., de Vos, W.M., van der Oost, J. (2002) Molecular and biochemical characterization of a novel type of fructose-1,6-bisphosphatase from *Pyrococcus furiosus*. *J. Bacteriol. In press.*

Verhees, C.H., van der Oost, J., de Vos, W.M. (2002) Unraveling glycolysis in archaea- unique adaptations in central metabolic routes. *Manuscript in preparation.*

Verhees, C.H., Akerboom, J., van der Oost, J., de Vos, W.M. (2001) Promoter architecture of genes encoding glycolytic enzymes in *Pyrococcus furiosus. Manuscript in preparation.*

Van Lieshout. J.F.T., Verhees, C.H., Ettema, T.J.G., van der Sar, S, de Vos, W.M., van der Oost, J. (2002) Characterization and site-directed mutagenesis of a novel and extremely thermostable α-galactosidase from *Pyrococcus furiosus. Manuscript in preparation.*

Awards

M&T 3rd Progress Report Meeting, June 7 1999, Winner of 1999 "Best Presentation Award", theme 2: Biotransformation